UNIVERSITY OF CALIFORNIA SAN DIEGO

Sonogenetics: Developing Tools for Ultrasound Mediated Neuromodulation

A Dissertation submitted in partial satisfaction of the requirements
for the degree Doctor of Philosophy

in

Neurosciences

by

Uri Magaram

Committee in charge:

Professor Sreekanth Chalasani, Chair
Professor Shelley Halpain, Co-chair
Professor Matthew Banghart
Professor Ed Callaway
Professor James Friend

2022

The Dissertation of Uri Magaram is approved, and it is acceptable in quality and form for publication on microfilm and electronically.

University of California San Diego

2022

DEDICATION

To my mom, Zhanna Magaram.

TABLE OF CONTENTS

LIST OF FIGURES

ACKNOWLEDGEMENTS

First and foremost, I would like to acknowledge and thank Dr. Sreekanth Chalasani. Shrek took a chance on me as a graduate student, was kind enough to let me join his lab, and trusted me with an extremely important and challenging project. Nothing would be possible without his endless patience, generous funding, and thoughtful guidance through numerous ups and countless downs. I am also grateful to my committee members, Dr. Ed Callaway, Dr. Shelley Halpain, Dr. Matthew Banghart, and Dr. James Friend, for their feedback and suggestions.

I would like to thank all of my colleagues in the Chalasani lab, particularly those with whom I worked closely on these projects. I especially am indebted to the research assistants who provided their time and energy well beyond the call of duty. A special thank you to Rani Shiao, Connor Weiss, and Janki Patel; I will always be grateful. Thank you to Drs. Dan Gibbs and Terri Grider for providing so many materials that kicked off this project, as well as Drs. Ed Callaway and Kirstie Salinas for resources and crucial help with two-photon imaging experiments.

The lab of Dr. James Friend was integral to this work, and I am thankful for their collaborative efforts, especially those of fellow graduate student Aditya Vasan who never shied away from risky experiments.

Additionally, I am thankful for the Neurosciences Graduate Program at UC San Diego and the Salk Institute for providing so many valuable resources.

Thank you to Drs. Indira Raman and David McLean – without whom I would not have learned the ins and outs of doing laboratory neuroscience research, and who sparked my desire to pursue it further.

Finally, I would like to deeply thank my family, friends, and Dill who have provided unwavering support during this challenging time; I hope to make it all worth it.

Chapter 1, in full, is a reprint of the material as it appears in: U. Magaram, C. Weiss, A. Vasan, K. C. Reddy, J. Friend and S. H. Chalasani. (2022) Two pathways are required for ultrasound-evoked behavioral changes in Caenorhabditis elegans. *PLOS ONE* 2022 Vol. 17 Issue 5 Pages e0267698. The dissertation author was the primary investigator and co-author of this paper.

VITA

2011 Bachelor of Arts/Science in Integrated Science, Mathematics, Northwestern University

2022 Doctor of Philosophy in Neurosciences, University of California San Diego

PUBLICATIONS

Magaram, U., Weiss, C., Vasan, A., Reddy, K. C., Friend, J., & Chalasani, S. H. (2022). Two pathways are required for ultrasound-evoked behavioral changes in Caenorhabditis elegans. *PloS one*, *17*(5), e0267698.

Duque, M., Lee-Kubli, C. A., Tufail, Y., Magaram, U., Patel, J., Chakraborty, A., Mendoza Lopez, J., Edsinger, E., Vasan, A., Shiao, R., Weiss, C., Friend, J., & Chalasani, S. H. (2022). Sonogenetic control of mammalian cells using exogenous Transient Receptor Potential A1 channels. *Nature communications*, *13*(1), 600.

Vasan, A., Orosco, J., Magaram, U., Duque, M., Weiss, C., Tufail, Y., Chalasani, S. H., & Friend, J. (2022). Ultrasound Mediated Cellular Deflection Results in Cellular Depolarization. *Advanced science (Weinheim, Baden-Wurttemberg, Germany)*, *9*(2), e2101950.

Mei, J., Vasan, A., Magaram, U., Takemura, K., Chalasani, S. H., & Friend, J. (2022). Well-free agglomeration and on-demand three-dimensional cell cluster formation using guided surface acoustic waves through a couplant layer. *Biomedical microdevices*, *24*(2), 18.

ABSTRACT OF THE DISSERTATION

Sonogenetics: Developing Tools for Ultrasound Mediated Neuromodulation

by

Uri Magaram

Doctor of Philosophy in Neurosciences

University of California San Diego, 2022

Sreekanth Chalasani, Chair

Neuromodulatory tools are important for understanding how the brain functions in health and disease and for treating disorders whose pathology is primarily neurological. Clinical techniques such as deep brain stimulation (DBS), transcranial magnetic stimulation (TMS), and pharmacological interventions have all been used thus far to neuromodulate various pathologies.

Each has benefits and drawbacks—TMS is minimally invasive but DBS gives more precise targeting, while pharmacology is non-invasive but hard to control temporally. Genetic techniques such as optogenetics and chemogenetics offer more targeted control, but are not yet used clinically, and optogenetics will likely require implantation of a fiber optic cannula to deliver light to target tissue. To overcome these limitations, ultrasound-based neuromodulation is being explored to non-invasively control specific populations of neurons in a spatially and temporally precise way. Ultrasound transducers can be focused to millimeter resolution, and research in several animal models including human studies have shown neuromodulatory effects of transcranial ultrasound stimulation. While these studies are promising, they do not account for the heterogeneity of neuronal subtypes in the brain. Additionally, the mechanisms of ultrasound-based neuromodulation are speculated but not fully understood—these include thermal effects, cavitation effects, membrane permeabilization, and mechanosensitive protein channel-mediated effects.

To make ultrasound a more reliable and useful neuromodulatory tool, a sonogenetics approach is proposed to sensitize ultrasound-insensitive neurons by expressing mechanosensitive proteins in populations of interest and targeting them with ultrasound. This approach requires a biological component, the candidate mechanosensitive protein channels, and a technological component, the ultrasound transducers capable of delivering the neuromodulatory stimulus. Each of these components is explored in this dissertation: Chapter 1 focuses on ultrasound mechanosensitivity in the nematode *C. elegans*, elucidating novel findings about multiple ultrasound-sensitive pathways and their underlying protein channels. Chapter 2 explores the development of a novel transducer that is small enough to be worn by an awake, freely moving mouse yet powerful enough to trigger endogenous neuronal activity measured by fiber photometry.

Together, these findings advance the quest to build a single-component sonogenetics toolbox capable of dissecting neural circuitry and ultimately treating neurological disorders by precisely controlling neuronal activity with ultrasound.

INTRODUCTION

Organisms must maintain internal homeostasis in the face of ever-changing environmental stimuli to survive. In almost all multicellular organisms, a nervous system coordinates this response to external environmental factors by receiving sensory inputs and coordinating motor actions in communication with the rest of the body. The nerve cells that transmit these signals are one of the most ancient specialized cell types, having evolved approximately 600 million years ago from motile pro- and eukaryotic action potentials [1].

Although they vary in size across phyla from hundreds to billions of cells [2], nervous systems comprise neurons which organize themselves into a network and communicate via ionochemical electrical signals to process relevant ethological information. Neuroscientists seek to understand how these systems work in health and disease on genetic, molecular, cellular, circuit and systems levels using a variety of tools and techniques.

Recording or observing neuronal activity using electrical, optical, or other techniques provides valuable insights into how the neural code can or should look in a functional system. However, conclusions made from recording neural activity during different physiological states can only be correlative, since other hidden variables could be facilitating both observations. In order to make causal conclusions about the function of a particular neuron or its components, one must be able to precisely manipulate and change neural activity using neuromodulatory tools.

Neuromodulation has two principle uses, depending on context: (i) Endogenously, neuromodulation occurs when molecules other than canonical neurotransmitters modify the electrical properties of neuronal circuits [3], and (ii) Neuromodulation describes the manipulation of nervous system activity using an external tool. The latter definition is the one referred to herein.

At the intersection of biology and technology, neuromodulatory tools come in different flavors – electrical, magnetic, optical, thermal, mechanical – with corresponding benefits and drawbacks regarding their ability to modify neuronal activity with varying spatial and temporal control, as well as considerations about their levels of invasiveness and ability to overcome the heterogeneous nature of neuronal subtypes in the brain. For ultrasound to become a widely used part of this neuromodulatory toolkit would both expand understanding of mechanobiology and facilitate new methods of dissecting neural circuitry in a minimally invasive way.

I. Considerations of Neuromodulation

Temporal Specificity

External stimuli are received, processed, and integrated within the brain on widely varying timescales [4-7]. Thus, to perturb circuitry and probe the function of brain regions, researchers need methods that are capable of disrupting neuronal activity anywhere from milliseconds to hours.

Depending on their ion channel composition and function, different neurons can discharge action potentials at different rates. Fast-spiking interneurons in cortical areas can spike as fast as ~600 Hz, with individual action potentials lasting only milliseconds [8]. As the understanding of the neural code produced by neurons expands, so will the need to be able to generate an individual action potential in an individual neuron. Long term potentiation (LTP), which strengthens connections between neurons and is one of the principal proposed mechanisms underlying learning and memory [9], can be evoked in the hippocampus by electrical pulses that last only a few seconds but result in more efficient synaptic transmission and increased neuronal excitability that can last minutes, hours or more [10]. Furthermore, the precise timing between a presynaptic input and

postsynaptic action potential, which can vary by just milliseconds, can determine whether that synapse is strengthened by LTP or weakened by long term depression (LTD) [9].

On longer timescales, neuromodulatory treatment of neurological disorders may require tools that alter brain activity for periods ranging from months to years to minimize the frequency of therapeutic surgery or medical evaluation. To diagnose and follow progression of brain disorders, medical professionals often rely on electroencephalography (EEG) and magnetoencephalography (MEG) to survey electrical and magnetic activity patterns throughout the brain, respectively [11]. Slowed or otherwise abnormal EEG/MEG recordings are classic hallmarks of many diseases including Parkinson's and Alzheimer's diseases, autism, and epilepsy [12-14]. Thus, treatments for these diseases may involve techniques that permanently return neuronal firing to healthy baseline levels.

Patients with schizophrenia also report disruptions in regular sleep-wake cycles and are at increased risk of insomnia [15]. Treatment of these complications may require permanent modulation of the suprachiasmatic nucleus or circadian timekeeping genes such as CLOCK, CRY1, and PER2 [16].

Because of the variable timescales of brain activity and long-term nature of many neurological conditions, neuromodulatory tools must be adapted to activate or inhibit neuronal firing anywhere from single millisecond-long transients to the minutes- or hours-long timing necessary for perception and cognition.

Spatial Specificity

Combined with variable timescales of activity, the brain is also spatially complex with components whose structures span orders of magnitude in size. The approximate volume of the

average human brain is on the order of ~1300 cm^3 [17]; axons such as the sciatic nerve can be a few microns in diameter and project over a meter [18]. Though the number of "brain regions" is constantly evolving as new research uncovers sub-structures of existing ones, smaller regions such as the locus coeruleus, the brain's primary norepinephrine source, span about 15 mm [19] while cerebral cortex makes up roughly 80% of all the mass of the brain and ~20% of its neurons [20].

Individual neurons also vary in size, with soma ranging from 5 to 100 μm in diameter, and although the number of neurons (as well as their glial counterparts) per volume can vary, one cubic centimeter of human brain can have 1.5 x 10^6 neurons and 10,000 times as many synapses [21]. Synaptic clefts where pre- and post-synaptic neurons exchange chemical and electrical information are even smaller, ranging from 20-30 nm in central nervous system and 50 nm at the neuromuscular junction [22].

Neuromodulatory tools may seek to change the neuronal activity of large brain volumes, such as electrical stimulation targeted to change the oscillation patterns in loci of epileptic seizures [23]. However, tools used to dissect neurocircuitry on a more refined level would need to be able to distinguish between even individual synapses. These spatial ranges present challenges for designing versatile neuromodulatory tools.

Heterogeneity of cell types

In the late 1800s Ramon y Cajal pioneered neuroanatomical illustration of the variety of neurons in the nervous system and their exquisite arborizations [24]. Since that time, neuroscientists have been classifying neurons by their locations, connections, structures, and functions. Decades after Cajal's work, neurotransmitters such as glutamate [25] and GABA [26] were identified and extensively studied for their generally excitatory and inhibitory functions,

respectively, in the brain. Immunoreactivity to particular molecules revealed that neurons are not all identical and can express a variety of proteins and molecules, suggesting that morphological identification is insufficient to characterize and classify neurons [27].

Examining just a small portion of cortical tissue reveals many different neuronal cell types within a small volume organized into layers, from excitatory pyramidal neurons to local inhibitory interneurons [28]. These classifications can change over time as improved technologies such as single-cell RNA sequencing reveals more refined differences between cells and their functions [29] on a genetic level.

Powerful neuromodulatory tools would be able to distinguish between such dense and immense heterogeneity in neuronal structure and function, and likely would require a genetic component paired with an activating modality.

Invasiveness

In the context of *in vivo* application, the invasiveness of a neuromodulatory technique will depend on the modality of activation as well as the distance from which a neuron or brain region can be targeted. Tools that produce large electric fields such as those used in transcranial electrical stimulation can reach neurons in the brain without the need for lesions of any kind [30]. Similarly, the magnetic fields produced by transcranial magnetic stimulation coils seem capable of reaching neurons centimeters deep in the brain through intact skull as measured by fMRI studies [31]. As related to temporal, special, and neuronal heterogeneity these techniques trade specificity for minimal invasiveness. Chemical neuromodulatory techniques such as pharmacological agents are also considered non-invasive since they do not produce lesion-like tissue damage, but they cannot be turned on and off on a millisecond timescale once in the body.

Deep brain stimulation (DBS) has shown efficacy in treating Parkinson's symptoms by targeting specific brain regions with electrical stimulation that can be tuned by the patient and overseeing doctor, but requires cranial surgery for electrode implantation [32]. Optogenetics, a light-based neuromodulation tool, offers high spatial and temporal specificity but for those proteins activated by light in the visible spectrum, fiber optic cannula are required to deliver light to deeper brain regions due to the absorption of light by biological tissue [33]. Despite electrodes and fibers decreasing in size, tissue damage around the implantation persists. And, although deeper brain structures in mice have been targeted with optogenetics tools using infrared-shifted light, more advances would be required to target the significantly larger human brain.

II. Established Neuromodulatory Techniques

Deep Brain Stimulation

Some neuromodulatory tools affect neuronal electrical activity without first changing their molecular composition. Since the principal signaling mechanism of neurons involves rapid, biochemical electrical signals, any electromagnetic interference in their vicinity should have an effect on their activity. Deep brain stimulation (DBS), first approved for human use by the Food and Drug Administration (FDA) in 1997, relies on electrode implants into the brain to send electrical pulses to modify the activity of the surrounding neurons [34]. Diseases such as Parkinson's, dystonia, obsessive-compulsive disorder, and epilepsy have all been treated using DBS with varying degrees of efficacy [34].

For Parkinson's treatment, the most established application thus far, a thin lead with multiple electrodes is implanted into either the subthalamic nucleus (STN) or internal segment of the globus pallidus (GPi), two regions linked to Parkinson's tremors by lesion studies [35].

Although the success rates of GPi-DBS in alleviating dyskinesia has been reported as high as 89% [36], variability in the substructures of the GPi targeted [37] can contribute to off-target effects, such as tonic muscle contractions, dysphagia, and mood changes [37]. While the stimulation protocol can be tuned to achieve best results for the patient both in frequency (120-180 Hz) and amplitude (1-5 V) [38], these parameters are generally determined by trial and error, indicating that the underlying problem is that the mechanism of DBS is unknown. Ideas vary between the "inhibition hypothesis" (elements proximal to the electrode are inhibited by depolarization block, inactivation of voltage-gated currents, inhibitory afferent activation), "excitation hypothesis" (local elements and afferent axons are excited by stimulation) and even "disruption hypothesis" (information flow, including aberrant information, is blocked through the GPi) [39] suggesting the need for a unified mechanistic understanding of DBS.

This disputed mechanistic understanding could contribute to the spatial and temporal variability between the application and effects of DBS in both human patients and animal models. Electrophysiology studies reveal that 3 V pulses can target neurons as far away as 1.5 mm [40], but the heterogeneity of neuronal subtypes in the targeted area makes it difficult to isolate and exploit desired neuromodulatory effects. This, combined with the invasive nature of the procedure, motivates the search for more precise and less invasive neuromodulatory tools.

Transcranial Magnetic Stimulation

Transcranial magnetic stimulation (TMS) is a noninvasive form of neuromodulation which, similarly to DBS, exploits the electrical properties of neurons without modifying their molecular components, but by using electromagnetic induction rather than direct electrical stimulation. An electric current is applied to a magnetic coil, and the resulting magnetic field

generated around the coil is placed over the patient's scalp to induce inverted electric charge in the adjacent brain region. Varying results have been reported on the efficacy of TMS in both psychiatric applications such as anxiety, obsessive-compulsive, and post-traumatic stress disorders as well as neurological conditions like Alzheimer's disease and epilepsy [41].

Limitations in the intensity of the magnetic field capable of being generated by the TMS coil restricts its targeting to mostly cortical regions in humans, with significant reductions in magnetic induction at distances greater than 5 cm from the coil, and safety problems after 6 cm [42]. Novel coil technologies suggest it may be possible to stimulate deeper brain regions without increasing the intensity of stimulation to unsafe levels [43, 44], an important consideration given that TMS recipients may experience auditory threshold changes, facial twitching, and, albeit rarely, seizures during TMS treatment [45]. These adverse effects suggest that TMS is indeed capable of modulating neural activity, although the nature of these effects is under debate, including both long-term potentiation and long-term depression [46]. Some studies have shown that lower frequencies (< 1 Hz) have inhibitory while higher ones (5-25 Hz) have excitatory effects in cortex [47].

These variable effects, combined with the heterogeneous populations of neurons that are targeted without genetic specificity, could contribute to the mixed results reported in successfully treating psychiatric and neurological disorders, particularly since the mechanisms of these disorders themselves are complex and under investigation. As TMS technology and targeting improves, so too might its success rate and applications.

II.i. Genetic Techniques for Neuromodulation

The heterogeneity of neuronal subtypes and functions in the brain is vast and dense. As a result, targeting brain regions rather than circuit components could result, for example, in excitatory effects when inhibitory ones are desired, vice versa, or both where excitatory neurons are locally interconnected with inhibitory ones [48, 49]. Genetic techniques address this problem by genetically expressing molecular "actuators", usually proteins, on target neurons and then selectively activating or silencing these neurons with modalities such as light, chemicals, heat, magnetic induction, or acoustics [50].

Optogenetics

Optogenetics has become almost a ubiquitous neuroscience research tool since its *in vitro* validation by Boyden et al. [51]. In particular, optogenetics' wide adoption was facilitated by the "single-component" technique; a single gene delivered to target cells or tissues renders them sensitive to stimulation by light illumination. Researchers expressed Channelrhodopsin-2 (ChR2), a rapidly activatable cation channel used by the algae *Chlamydomonas reinhardtii* for phototaxis in cultured hippocampal neurons. Electrophysiology recordings demonstrated that light-activated depolarizing transient currents generated action potentials in response to even high frequency pulses (30 Hz), and consistently reproducible spike trains at lower ones (5 Hz).

Since 2005, the number of publications that have used or studied optogenetics itself has grown exponentially. Perhaps one of the biggest drivers of this is the speed and temporal precision with which neurons can be manipulated using optogenetics. Since the first experiments which peaked at 40 Hz stimulation [51], mutations made to rhodopsin channels have generated accelerated on-off kinetics, allowing researchers to elicit even 400 Hz spike trains in fast-spiking

parvalbumin interneurons and 100 Hz in hippocampal neurons [52]. These manipulations demonstrate the temporally precise optogenetic control conferred to target neurons, even if such high frequencies are above their natural occurring spike rates, up to 200 Hz bursts for fast spiking interneurons [53] and 60 Hz for hippocampal neurons [54]. Similarly, the fidelity of optogenetic stimulation – how frequently a light pulse generates extra action potentials or none at all, has also improved significantly with channels such as ChETA via rational mutagenesis, reducing spike doublets and eliminating the plateau potential altogether [54].

Combining clever genetic, viral, and light delivery methods also confers high specificity to optogenetic manipulations. Two-photon illumination, rather than fiber optic placement, has been used to optogenetically stimulate an individual neuron in cortex to map synaptic connectivity to its neighbors [55]. Neurons that project to multiple regions can be stimulated at their soma to evoke their overall contribution to circuits and behaviors, while implanting the fiber optic cannula and stimulating at specific synaptic terminals reveals nuanced contributions of specific efferent fibers [56-59].

Inhibitory optogenetics channels have also been discovered and developed. Archeorhodopsin, a light-activatable proton pump, and halorhodopsin, a light gated chloride channel, are activatable by red (655 nm) or yellow (570 nm) light, respectively, and hyperpolarize their constituent neurons [60, 61]. In fact, both inhibitory and excitatory optogenetic manipulations have been achieved simultaneously in the same neurons by using opsins with non-overlapping excitation spectra [62]. All of these tools together offer unprecedent levels of control over neurons and circuits, giving researchers the ability to make causal conclusions about their contributions to physiology.

Whether optogenetics is approved in humans remains to be seen; blue light has been shown to cause inherent damage/activation in naïve nervous tissue [63, 64] and the limitations of light penetration through tissue means fiber optic implantation will likely remain necessary to target deeper structures. Additionally, the prevalence of fluorescence based optical imaging techniques for observing neural physiology introduces challenges when also using fluorescence as a stimulation tool, suggesting the need for additional modalities to provide orthogonality between precise neuromodulation and simultaneous recording. Still, the ever-increasing fidelity combined with wavelength-shifted optogenetic channels make it a powerful and transformative technique.

Chemogenetics

Pharmacological interventions for neuromodulations are intertwined with human history, beginning with ingestion of naturally occurring compounds (e.g. caffeine, tobacco, alcohol) and developing into isolated and synthesized molecules [65]. Much of pharmacological history is based on activating or inactivating proteins native to neurons and their components (morphine, SSRI, amphetamines), and current treatments of diseases and disorders are based on this concept. However, pharmacologically activating or inactivating any specific population of neurons and only that population required the invention of a non-native protein that could be activated by an exogenous ligand that would not be found in the native tissue. Receptors activated solely by synthetic ligands (RASSLs) and their improved counterparts, designer receptors exclusively activated by designer drugs (DREADDs) have filled this role since 1998 [66].

In 1998, RASSLs first appeared in the literature [66] as a "G protein-coupled peptide receptor engineered to respond to synthetic small molecules, rather than their natural ligands." Coward et al. modified the k opioid receptor with substitutions from mu and delta opioid receptors,

specifically in the extracellular loop 2 domains. This chimeric protein showed significantly decreased binding affinity to k-specific *endogenous* peptides, while retaining its ability to bind *exogenous* drugs [66]. Thus, they had created a G protein-coupled receptor that did not exist natively in mammalian cells, nor did it bind anything native to mammalian cells, allowing them to selectively trigger calcium-based activity cascades with the receptor via drug application. Coward et al. were not the first group to engineer and modify G protein-coupled receptors towards chemogenetic tools [67], nor did they specifically discuss their invention in the context of neuroscience research. As the first iteration, RASSLs ligands had some binding affinity issues [66] and conformational instability problems at high concentrations [68].

Directed evolution, rather than rational design, offers a robust solution to improving protein function by exploiting randomness and volume [69]. In the late 2000s, several publications used directed evolution to randomly mutagenize muscarinic receptors in yeast, generating what are now known as DREADDs [70-72]. This family of chemogenetic receptors are activated by clozapine-N-oxide, an inert but bioavailable compound. Expression in hippocampal neurons of hM4D, an inhibitory DREADD, induced hyperpolarization and neuronal silencing [72], suggesting that these tools could be expressed elsewhere in the nervous system and used to study the function of different neurons by modulating their activity.

The spatial and temporal precision of DREADD manipulations depends on the experimental methods used. Since the activating molecule clozapine-n-oxide (CNO) is injected into the animal subject and spreads throughout the body, expression of DREADDS must be limited to the target region or neurons of interest. Targets as large as pre-frontal cortex injected with microliters of viral vectors can be activated at once [73] or expression can be limited to highly specific subtypes with multiplexed intersectional CreFlp systems [74]. Unlike optogenetics, which

gives control over individual neurons at millisecond-scale precision, chemogenetics works on much longer time-scales due to drug diffusion and binding kinetics. *In vivo* onset of activation can take as long as 5-10 minutes and persist for as long as an hour after application [72, 75]. While CNO-driven activation can happen in milliseconds *in vitro*, the unbinding kinetics during washout suggest that the effects of the drug persist long after [76].

Clinical DREADD applications are exciting to imagine as they would require no implants of any kind and could circumvent off-target effects of canonical drugs. However, some studies suggest that CNO itself has effects *in vivo* even in the absence of DREADD expression [77, 78], suggesting the need for further development of proteins and protein-specific ligands.

III. Use of Ultrasound in Biomedical Applications

The efficacy and safety of ultrasound (US) as an imaging, diagnostic, and therapeutic tool has been established for decades [79]. First identified in bat echolocation [80] as well as other species including porpoise [81] and mouse [82], ultrasound was harnessed as a tool with the discovery of piezoelectric materials which convert mechanical to electrical energy and vice versa [83-85].

In simplified terms, US propagates through its medium of transmission as a longitudinal wave of alternating compression and rarefaction zones, which means the energy of the wave is carried by local oscillations in the medium itself while the medium as a whole stays in place. The physical properties of ultrasound, defined as sound waves whose frequency is above the 20 KHz threshold of human hearing, make it an attractive tool for applications in both engineering and medicine; relationships between the physical properties of mechanical waves determine the parameters and tradeoffs needed for certain applications.

The speed of US propagation is determined by the medium—soft tissues like organs transmit at speeds similar to water, ~1500 m/s [86, 87] while stiffer media such as bone transmit faster at 2770 m/s [88]. At constant speed, the wavelength scales inversely with the frequency, thus higher US frequencies yield shorter wavelengths and better resolution for imaging: above 15-20 MHz, ultrasound imaging systems can resolve structures less than 100 μm on the perpendicular axis of the beam [89]. While this can be useful for resolving structures near the surface of the medium, higher ultrasound frequencies are absorbed as heat and attenuate more quickly in tissue than lower ones, so that higher resolution means less depth of penetration [90]. Since higher frequency waves also carry more energy than lower frequency waves at the same amplitude, considerations must be made when using ultrasound in biological tissue to avoid permanent damage [91].

Thermal effects resulting from ultrasound exposure and absorption must be carefully considered in any biological US application. While brief or low-amplitude changes in temperature can result in reversible effects such as upregulation of heat shock proteins [92] or rapid heat dissipation, sustained or high-amplitude temperature changes in tissue can result in apoptosis [93] and teratogenesis, the malformation of an embryo or fetus [94]. The nature of US induced temperature change depends not only on both the intensity and duration of US exposure, but also on the absorption coefficient of specific tissues. For example, the absorption coefficient of bone (20 dB/cm•MHz) is roughly 40 times that of brain (0.6 dB/cm•MHz) [95], increasing the risk of thermal damage to bone and any tissue adjacent to it. The thermal index (TI) of an ultrasound device is designated as the ratio of total acoustic power to acoustic power necessary to raise tissue temperature by 1°C anywhere along the beam [96], and is used by the FDA to set safety guidelines

for ultrasound imaging. For example, when TI = 3, exposure time of embryo or fetus must be limited to no more than one minute, whereas TI up to 1.0 is restricted to one hour exposure [97].

While thermal effects generated by oscillating molecules can confound US applications, strictly mechanical effects are also generated during US exposure which can cause potential safety issues. Acoustic cavitation occurs when microbubbles in the transmission medium expand and contract in an ultrasound field, and can generate secondary effects including shock waves, micro-jets, extreme instantaneous temperatures and shear-forces [98]. Even in the absence of bubbles, dissolved gas can be drawn out of solution in tissue under high negative pressures exerted by ultrasound [91]. While this phenomenon can be used for targeted applications such as microbubble-mediated high-focus-ultrasound driven blood brain barrier opening [99] and sonoporation-induced drug delivery [100], unstable cavitation can lead to damage and apoptosis in off-target tissue.

Additionally, acoustic streaming forces capable of displacing ions and small molecules produce movements around the surfaces of cells not necessarily in the direction of incidence of the ultrasound wave [101]. Both phenomena have been shown to have effects on cells *in vitro* including membrane disruption [100-102] and increased protein synthesis [103], and, while it is hypothesized that the more dangerous events are not triggered by diagnostic ultrasound [104], the FDA still sets a safety boundary on the Mechanical Index (MI), defined as peak rarefaction pressure divided by center frequency of ultrasound wave in MHz [105]. At the moment, the FDA approved MI limit is 1.9 [106] although some research shows microbubble interactions at lower MI *in vivo* [107].

Despite the risks of excessive US exposure for biological tissues, under the safety guidelines established for medical US applications, it has flourished as a useful method for

imaging, diagnosing, and even treating certain medical conditions. Perhaps nowhere is this more evident than in obstetrics, where fetal sonograms are currently almost ubiquitous. Doppler ultrasound used to track fluid flow, which operates at 1000x intensity compared to B-mode ultrasound, has been shown to have bioeffects in fetal chicks [108] and has been recommended to be avoided for early human fetuses [109]. However, most attempts at finding bioeffects in human fetuses of lower intensity, B-mode sonogram US have been inconclusive at best, particularly when epidemiological analysis is attempted [110].

As a diagnostic tool, ultrasonography is capable of imaging tissues in the human body including tendons, muscles, joints, vessels, and internal organs. Deeper structures such as liver, kidneys, and pancreas are imaged using 3 MHz US to account for absorption and refraction through the body, while more superficial structures such as the neck, breasts, and pelvis are imaged using 5 and sometimes 7 MHz frequencies for better resolution [111]. Even 10 and 20 MHz probes have been used for ultrasonography in the eye [112]. Since US echoes occur as a result of differences in US impedance ($I = pc$, where p is density of medium and c is speed of sound in medium), tendon injuries [113], bone stress injuries [114], and tumors in soft tissues [115] can all be visualized with the right US probe, parameters, and expertise.

Although imaging and diagnostic applications of US imaging use parameters minimize thermal and mechanical effects in tissue, these "dangerous" effects can be useful in other applications including lithotripsy and tumor ablation. Shock wave lithotripsy uses repeated, high intensity ultrasound pulses on the order of 60 MPa and only 1 μs in a targeted way to destroy renal or ureteric stones [116]. These pulses produce the same cavitation events that diagnostic and imaging US applications seek to avoid. Similarly, high intensity focused ultrasound (HIFU) has been used as a non-invasive method to treat malignant tumors in pancreas, liver, breast, and

prostate by using intensities of 100-10000 W/cm^2 and compression pressures up to 70 MPa [117] to destroy tumorous tissue via thermal and mechanical effects. These intensities are several orders higher than those used in imaging (B-mode, pulsed, Doppler) and can damage neighboring tissue if the targeting is not precise enough, but the destructive nature of such US is also harnessed for therapeutic purposes in this case [117].

Taken together, the mechanical properties, non-invasiveness of the probes, and established uses of ultrasound in biological applications, as well as even the "undesirable" thermal and mechanical effects make it a potential tool for neuromodulation when targeted at brain tissue. Indeed, dozens of studies have shown modified neuronal activity during and after ultrasound exposure.

IV. Ultrasound as a Means of Neuromodulation

The following section will review studies into ultrasound-mediated neuromodulation in model organisms from *C. elegans* to *H. sapiens*, specifically those which did not use exogenous ultrasound-sensitive agents such as microbubbles [118].

Early explorations into US neuromodulatory effects date back as early as 1928, when Edmund Newton Harvey showed that US can trigger muscle contractions by acting on nerves [119, 120]. Several decades later, William Fry and colleagues directly measured electrical activity from crayfish ventral nerve cord exposed to ~35 w/cm^2 US over the course of 50 seconds. Interestingly, they found that the rate of spikes first increased, then decreased, then disappeared altogether before reappearing 25 seconds after US was turned off [121]. Importantly, these changes could not be explained by temperature changes alone, since the maximal temperature change was 1°C and changing the temperature without US exposure did not reproduce the effects [121]. Around the same time Young and Hanneman also showed differential effects of US exposure in mammalian

nerves by exposing cat saphenous nerve bundles to a range of US parameters. 20 500 ms pulses abolished action potentials in C fibers while leaving alpha and delta signals intact [122].

Although Fry and others had been pioneering high-intensity US as a tool to lesion brain tissues in humans in the late 1950's [123, 124], reports of US effects on intact brain and skull early on were sparse and mixed. Fry and colleagues reported inhibition of light-evoked cortical signals during US irradiation of lateral geniculate nucleus [125], while Foster and Wiederhold reported activation of auditory-nerve responses during intense 30 W/cm^2, 5 MHz US pulses as short as 70 μs [126].

Other preparations have revealed US-driven modulation of neuronal activity. In slice preparations, 150kHz PRF, 6μs, center frequency 750 KHz US pulses significantly decreased the dendritic field potential in hippocampal CA1 [127]. Similarly, 500 KHz ultrasound pulses focused on dentate gyrus had a reversibly inhibitory effect on presynaptic fiber volley and dendritic field potentials [128]. These studies were careful to avoid thermal effects as well as intensities that could produce cavitation; later experiments showed sodium and calcium transients in hippocampal CA1 pyramidal neurons stimulated by 440 KHz US that were abolished in the presence of tetrodotoxin (TTX) with no indications of cavitation events [129].

In vivo experiments also reveal neuromodulatory effects of US stimulation in mammals. In mice, transcranial US stimulation (25-50 KHz, 0.16-0.57 ms, 1.2-3.0 KHz) evoked increased cortical spiking in primary motor cortex (M1) measured by increased local field potential (LFP) that was attenuated by TTX [130]. Immobilized and anesthetized mice exposed to increasing durations of 300, 400, 500 and 600 KHz continuous ultrasound pulses displayed EMG signals whose frequency correlated both with intensity and duration of US pulses [131, 132], as well as

some responses at 1.4 and 2.9 MHz [132]. In more ventral regions like hippocampus, increases in spike frequency were also recorded during transcranial US stimulation at 25 KHz [130].

Ultrasound stimulation in humans has shown neuromodulatory in both the peripheral and central nervous systems. Stimulation protocols designed to evoke either a mechanical or a thermal sensation through fingertips exposed to US showed distinct signals in both EEG and fMRI imaging of human subjects, as well as reports of sensation on a scale of 1-10 [133]. Similarly, volunteers reported cooling, warming, vibrotactile sensations, and mild nociception when exposed to pulsed focused ultrasound to the skin of the fingers for 10 s using 350 or 650 KHz pulses [134] although no temperature change was recorded at the skin. The studies used different intensities (11.8-54.8 W/cm2 and 3-100 mW/cm2, respectively) of US stimulation, but also different frequencies and waveforms suggesting more research needs to be done on the relationship between US parameters and neuronal stimulation. In transcranial US studies, direct stimulation of thalamus in human subjects evoked somatosensory potentials recorded via EEG and significantly altered subjects' discrimination in a two point discrimination task [135], while simultaneous transcranial US during intra-cortical facilitation TMS exposure decreased the motor evoked potentials (MEP), suggesting an inhibitory effect [136]. Remarkably, US targeting of the thalamus was successful despite a mean distance of 57 mm from the scalp, illustrating the ability of US to target deeper brain structures without the need for implantation or surgery [135].

The mechanisms underlying US neuromodulation continue to be subjects of investigation and are of particular interest in order to inform more targeted and intelligent US stimulation parameter design for desired excitatory or inhibitory effects. Early hypotheses revolved around thermal and cavitation effects [137], since changes in temperature are known to change neuronal activity [138] and cavitation could lead to various mechanical stress-induced changes [139].

However, in both earlier and recent studies, researchers are mindful of these possibilities and take precautions to avoid confounding mechanical effects with thermal ones by calculating [140] and sometimes measuring temperature changes directly to avoid large changes, as well as by keeping the MI of their stimulation parameters below those known to cause cavitation.

In the absence of cavitation, more subtle mechanical effects are hypothesized to explain neuromodulatory phenomena driven by US stimulation. One hypothesis is that as brain tissue expands and contracts on a microscopic level, synapses between neurons lose contact either through depletion of synaptic vesicle clusters or temporarily increasing the distance between the pre- and post-synaptic terminals [141]. Another hypothesis supported by both experimentation [142] and modeling [143] suggests that the properties of neuronal membranes are altered during exposure to US radiation forces, including their area and capacitance. Recent studies have also suggested that *in vivo* effects observed in guinea pigs and mice are mediated by cochlear and auditory pathways (at 220 KHz and 500 KHz, respectively) rather than direct mechanical effects [144, 145], although these lower frequencies do not exclude direct mechanical effects at higher frequencies.

Another hypothesis is that radiation forces from US change neuronal activity through the action of mechanosensitive protein channels. This force-sensing class of channels is implicated in organisms' ability to respond to external cues such as shear force, touch, and gravity, as well as internal forces such as turgor pressure and membrane deformation [146]. Several types of mechanosensitive channels have been identified and cloned - Piezo1 and Piezo2 are found throughout mammalian tissues [147-149], the mechanosensitive channels of large (MscL) and small (MscS) conductance help bacteria regulate osmotic pressure [150-152], and the transient receptor potential (TRP) family of proteins which responds to a variety of stimuli contains TRPN,

a mechanosensitive channel in invertebrates [153-155]. Other mammalian protein channels, such as voltage gated potassium (Kv), sodium (Nav), and calcium (Cav) channels, also show some mechanosensitivity [156, 157] and could potentially transduce acoustic radiation force by virtue of their tight interaction with the membranes of neurons.

V. SONOGENETICS PROJECT RATIONALE

The studies described thus far are promising steps towards development of widespread ultrasound-based neuromodulation. The extensive use of ultrasound in diagnostics, imaging, and therapy has generated a large body of literature on the safety of US propagation in biological tissue [91], the FDA sets guidelines regarding medical applications [158], and many studies have documented the safety of ultrasound specifically in transcranial stimulation [137]. US technologies capable of non-invasively transcranially targeting brain regions with high spatial specificity can focus on a 1 mm-diameter focal spot with 740 KHz and even 5 MHz [159, 160], as compared to 10 cm^2 within half-maximum power for transcranial electrical stimulation [161] and 10 cm^2 spread at a depth of 1.5 cm for transcranial magnetic stimulation [162].

Still, a 1 mm^3 volume can contain as many as 9.2 x 10^4 neurons and 7.2 x 10^8 synapses in 1 mm^3 of mouse brain [163], with variable functions and genetic distinctions. Furthermore, while microsecond-scale ultrasound at sufficient intensity is capable of evoking single action potentials in some preparations [164], there is not yet an optogenetics-like 1-to-1 mapping of ultrasound stimulation to action potential discharge. As well, most *in vivo* studies in mice used anesthetized or otherwise immobilized mice, suggesting the need for ultrasound transducer technology that can be used in awake, behaving animals for dissecting physiologically-relevant neural circuitry.

The purpose of this thesis is to describe steps taken towards better understanding of mechanosensitive channels and new technologies that could facilitate sonogenetic neuromodulation.

CHAPTER 1

Two pathways are required for ultrasound-evoked behavioral changes in Caenorhabditis elegans

Abstract

Ultrasound has been shown to affect the function of both neurons and non-neuronal cells, but, the underlying molecular machinery has been poorly understood. Here, we show that at least two mechanosensitive proteins act together to generate *C. elegans* behavioral responses to ultrasound stimuli. We first show that these animals generate reversals in response to a single 10 msec pulse from a 2.25 MHz ultrasound transducer. Next, we show that the pore-forming subunit of the mechanosensitive channel TRP-4, and a DEG/ENaC/ASIC ion channel MEC-4, are both required for this ultrasound-evoked reversal response. Further, the *trp-4;mec-4* double mutant shows a stronger behavioral deficit compared to either single mutant. Finally, overexpressing TRP-4 in specific chemosensory neurons can rescue the ultrasound-triggered behavioral deficit in the *mec-4* null mutant, suggesting that both TRP-4 and MEC-4 act together in affecting behavior. Together, we demonstrate that multiple mechanosensitive proteins likely cooperate to transform ultrasound stimuli into behavioral changes.

Introduction

Ultrasound has been shown to modify neuronal activity in number of animal models including humans [165, 166]. However, the direction of this action is somewhat controversial with some reporting activation [129, 167-170], while others demonstrate inhibition [166, 171-173]. Moreover, the underlying mechanisms for ultrasound action on neuronal membranes have been suggested to include thermal [174-176], mechanical (direct or via cavitation [177-179]) or a combination of two [180]. Additionally, ultrasound neuromodulation has also been shown to include astrocyte signals *in vitro* [181] and auditory signals *in vivo* [182, 183]. To identify the underlying molecular mechanisms, we and others have been examining how ultrasound affects neurons in tractable invertebrate systems [179, 184-186] or mammalian cell [187, 188] and slice cultures [129, 189].

The nematode, *C. elegans* with just 302 neurons connected by identified chemical and electrical synapses generating robust behaviors with powerful genetic tools is ideally suited to probe the molecular effects of ultrasound on neuronal membranes [190-192]. We previously showed that the pore-forming subunit of the mechanosensitive ion channel TRP-4 is required to generate behavioral responses mediated by microbubbles activated by a single 10 ms pulse of ultrasound generated from a 2.25 MHz focused transducer [184]. This channel is specifically expressed in few dopaminergic (CEPs, and ADE) and interneurons (DVA and PVC) in *C. elegans*, where it has been shown to be involved in regulating the head movement and locomotion [155, 193]. Surprisingly, we found that ectopically expressing this TRP-4 in a neuron rendered that neuron sensitive to ultrasound stimuli, confirming ultrasound-triggered, microbubble-mediated control [184]. Moreover, a second mechanosensitive protein, a DEG/ENaC/ASIC ion channel MEC-4 was also shown to be required for behavioral responses to a 300 ms duration, 1 KHz pulse

repetition frequency at 50% duty cycle generated from a 10 MHz focused ultrasound transducer [185]. These two studies confirm that ultrasound effects on *C. elegans* behavior is likely mediated by mechanosensitive proteins.

In this study, we used genetic tools in *C. elegans* to test whether TRP-4 and MEC-4 are both required to mediate the behavioral effects of ultrasound stimuli. We generated a *trp-4 mec-4* double mutant and compared its ultrasound responses to both single mutants. Also, we found that ectopically expressing TRP-4 in specific chemosensory neurons can rescue the behavioral deficits in both *trp-4* and *mec-4* null mutants, confirming that these genes act together to drive ultrasound-evoked behavior. Our study demonstrates that multiple mechanosensory pathways act in concert to generate behavioral responses to ultrasound stimuli.

Materials & Methods

Ultrasound Imaging Assay

A schematic of the system for imaging ultrasound-triggered behavior appears in Figure 1A. An immersible 2.25 MHz central frequency point focused transducer (V305-SU-F1.00IN-PTF, Olympus NDT, Waltham, MA) was positioned in a water bath below a 60 mm 2% agar-filled petri dish, and connected via waterproof connector cable (BCU-58-6W, Olympus). A single 10ms pulse was generated using a TTL pulse to trigger a multi-channel function generator (MFG-2230M, GWINSTEK, New Taipei City, Taiwan); the amplitude of the signal was adjusted through a 300-W amplifier (VTC2057574, Vox Technologies, Richardson, TX) to achieve desired pressures. *C. elegans* behavior was captured through a high speed sCMOS camera (Prime BSI, Photometrics, Tuscon, AZ) and a 4x objective (MRH00041, Nikon, Chicago, IL). Worm movement was compensated via a custom joystick-movable cantilever stage (LVP, San Diego, CA) controlled by Prior Box (ProScanIII, Prior, Cambridge, UK). All components were integrated via custom MetaMorph software (Molecular Devices, San Jose, CA). A goose-neck lamp (LED-8WD, AmScope, Irvine, CA) at ~45° provided oblique white light illumination.

The ultrasound transducer was focused in the Z-plane to the focal plane of the camera, allowing for X-Y motion of the stage and petri dish using the joystick-movable stage all in the focal plane of both the ultrasound transducer and camera. The petri dish was coupled to the ultrasound transducer via degassed water in the water bath.

For 10 MHz experiments, the 2.25 MHz transducer was replaced with a 10 MHz line-focused transducer (A327S-SU-CF1.00IN-PTF, Olympus) coupled via plastic 20 mL syringe and degassed water as previously described [185]. The plastic portion of the petri dish was removed to

couple the transducer directly to the agar slab, and a 2x objective (MRD00025, Nikon) replaced the 4x objective to allow for full imaging of the larger focal area of the transducer.

Behavioral Assays

For experiments with microbubbles, polydisperse microbubbles (PMB, Advanced Microbubbles, Newark, CA) were diluted to a concentration of ~$4x10^7$ and added to an empty 2% agar plate 20 minutes before imaging to allow for absorption/evaporation of the solvent media, leaving microbubbles on the surface of the agar. A dry filter paper with a 1 cm hole previously soaked with 200 mM copper sulfate solution was placed around the microbubble lawn, and a young adult *C. elegans* was moved from a home plate to the imaging plate using an eyelash. The agar plate was moved around using the motorized stage to place the worm into the focal zone of the transducer where it was stimulated with a single ultrasound pulse of appropriate amplitude. Videos were recorded for 10 seconds at 10 frames/second, with ultrasound stimulation (described above, via TTL pulse) occurring at 1.5 seconds.

Reversals with more than two head bends were characterized as large reversals, those with fewer than two head bends were characterized as small reversals, and omega bends were those which led to a high-angled turn that lead to a substantial change in direction of movement [184]. Wildtype animals were tested daily to monitor and maintain a baseline level of reversal behavior, and comparisons between strains were made for animals recorded within same days of testing. Where possible, wildtype, mutants and rescue animals were tested on the same day. For 10 MHz ultrasound stimulation, all deviations from the baseline are plotted in Supplementary Figure S3C. Behavioral data were collected over at least three days to confirm reproducibility, the data were then pooled for final statistical analysis, shown in relevant figures.

C. elegans

Wildtype *C. elegans* – CGC N2; VC1141 *trp-4(ok1605);* GN716 *trp-4(ok1605)* outcrossed four times [185]; TU253 *mec-4(u253)*[185]; IV903 *trp-4(ok1605); mec-4(u253),* made by crossing GN716 and TU253.

ASH rescues: IV133 *ueEx71 [Psra-6::trp-4; Pelt-2::GFP]* made by injecting N2 with 50ng/μL *Psra-6::trp-4*, 10ng/μL *elt-2::gfp* for ASH overexpression of *trp-4*. IV160 *trp-4(ok1605) I; ueEx88 [Psra-6::trp4; Pelt-2::GFP]* made by injecting VC1141 with 50ng/μL *Psra-6::trp-4*, 10ng/μL *elt-2::gfp* for ASH rescue of *trp-4*. IV840 *mec-4(u253) X; ueEx71 [Psra-6::trp-4; Pelt-2::GFP]* made by crossing IV133 and TU253.

AWC rescues: IV157 *ueEx85 [Podr-3::trp-4; Pelt-2::GFP]* made by injecting N2 with 50ng/μL *Podr-3::trp4*, 10ng/μL *elt-2::gfp* for AWC overexpression of *trp-4*. IV162 *trp-4(ok1605) I; ueEx89 [Podr-3::trp-4; Pelt-2::GFP]* made by injecting VC1141 with 50ng/μL *Podr-3::trp-4*, 10ng/μL *elt-2::gfp* for AWC rescue of *trp-4*. IV839 *mec-4(u253) X; ueEx85 [Podr-3::trp-4; Pelt-2::GFP]* made by crossing IV157 and TU253.

Behavioral Ultrasound Pressure and Temperature Measurements

Pressure and temperature measurements were collected through 2% agar plates using a Precision Acoustics Fiber-Optic Hydrophone connected to a 1052B Oscilloscope (Tektronix, Beaverton, OR). The hydrophone probe was moved sub-mm distances using the same stage used for animal recordings while the petri dish was held in place using a three-prong clamp. The noise floor for this instrument is 10 kPa [194], and the uncertainty of the instrument is 10% in the frequency range used in this study [195], allows us to adequately measure pressures used in this study (>500 kPa). The full width at half maximum (FWHM) reported was determined by

interpolating the perpendicular distances at which half of the maximum pressure was measured using the fiberoptic hydrophone, and averaging over the amplifier gains used to achieve various pressures.

Statistical Analysis

Data were analyzed by combining several days' recordings within several days' experimental sessions, with sample sizes chosen to reflect those described previously [184]. All behavioral data were plotted as proportion of response plus/minus standard error of the proportion. For significance tests, two-proportion z-tests were used with Bonferroni corrections for multiple comparisons. All sample sizes were >30, and animals were chosen at random from their broader population. The observer was not blind to the genotype of the group being tested. Animals were excluded from the study if they showed visible signs of injury upon transfer to the assay.

Results

To test the behavioral responses of *C. elegans* to various ultrasound stimuli, we aligned a transducer with a holder that positioned agar plates at the water level in a tank (**Fig 1.1A**). Animal responses were captured using a camera and analyzed (**Fig 1.1B, 1.1E**, See Methods for more details). Next, we evaluated both pressure and temperature changes at the agar surface for a single 10 ms pulse of ultrasound stimuli of different intensities. We assessed the area on the agar surface which was ensonified by the ultrasound stimuli and found that our system delivered mechanical, but not temperature changes (**Fig 1.1C, 1.1D**). We found that ultrasound stimuli delivering peak negative pressures greater than 0.75 MPa amplified by 1-10 μm-sized gas filled microbubbles generated robust responses in wild-type (WT) animals. We analyzed these responses and found that animals generated robust increases in their large reversals (events where the head bends twice or more), but not omega bends or small reversals (where the head bends only once) (**Figure 1.2, Fig 1.4**). These data are consistent with previous studies showing that *C. elegans* generates dose-dependent responses to ultrasound stimuli [184, 185].

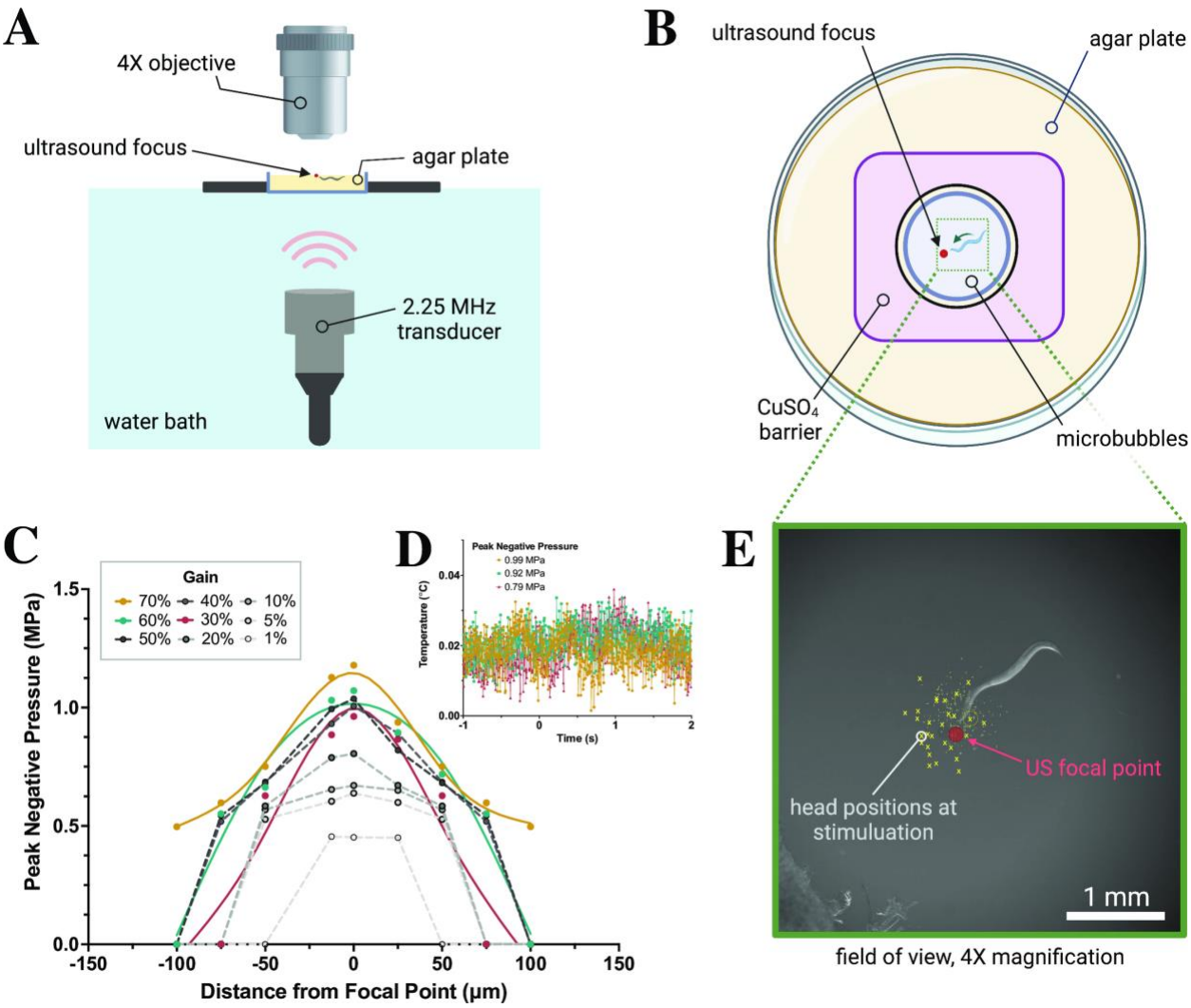

Figure 1.1 | **Recording *C. elegans* behavior in response to ultrasound at 2.25 MHz**. (**A**) Schematic of 2.25 MHz ultrasound imaging system with transducer, water bath, and 4x objective over agar plate. (**B**) Top view of agar plate with animals corralled by copper sulfate barrier (1.5 cm in diameter) on agar plate with polydisperse microbubbles. (**C**) Fiberoptic hydrophone measurements at perpendicular distance from focal point of transducer show peak negative pressures ~1 MPa, with (**D**) negligible temperature changes at 10ms ultrasound pulses at t=0. Individual points connected via spline fit. (**E**) Relative head positions (yellow dots) of each animal at time of stimulation, some example points highlighted for visibility.

We then analyzed the behavioral responses of null mutants in both the TRP-4 and MEC-4 channels to ultrasound. We found that *trp-4(ok1605)* and *mec-4(u253)* mutants are both defective in their ultrasound-evoked large reversal behavior both with and without gas-filled microbubbles (**Fig 1.2A**, **1.2B**). Also, we observe that *mec-4(u253)* null mutants have significant defects at higher (>0.92 MPa), but not lower pressures generated from a 2.25 MHz ultrasound transducer (**Fig. 1.2A, 1.2B**). Similarly, we also found that an outcrossed allele of *trp-4(ok1605 4X)* was also defective in its response to ultrasound stimuli at higher pressures (**Fig 1.2A, 1.2B**). This result is consistent with our previous study, which identified a critical role for *trp-4* in mediating ultrasound-evoked behavioral responses [184]. Additionally, we found that *C. elegans* can also respond to ultrasound stimuli even in the absence of gas-filled microbubbles, consistent with a previous study [185]. Moreover, we find that at least at lower ultrasound pressures (0.79 MPa), the probability of *C. elegans'* responses are increased in the presence of microbubbles (**Fig 1.2A, 1.2B**). Importantly, we found that at high pressure, the *trp-4(ok1605 4X); mec-4(u253)* double mutant had a stronger defect in ultrasound-trigged large reversal responses compared to either single mutant (**Fig 1.2C, 1.2D**), both with and without microbubbles (**Fig. 1.2C, 1.2D**), suggesting that these genes likely act together. Moreover, we do not observe any consistent change in small reversals, however changes in omega bends were similar to what we found with large reversals (**Fig 1.4**). These data are consistent with previous studies showing that omega bends often occur together with large reversals [196, 197]. Collectively, these data indicate that MEC-4 and TRP-*4* channel proteins might be acting together to mediate *C. elegans* behavioral responses to ultrasound stimuli.

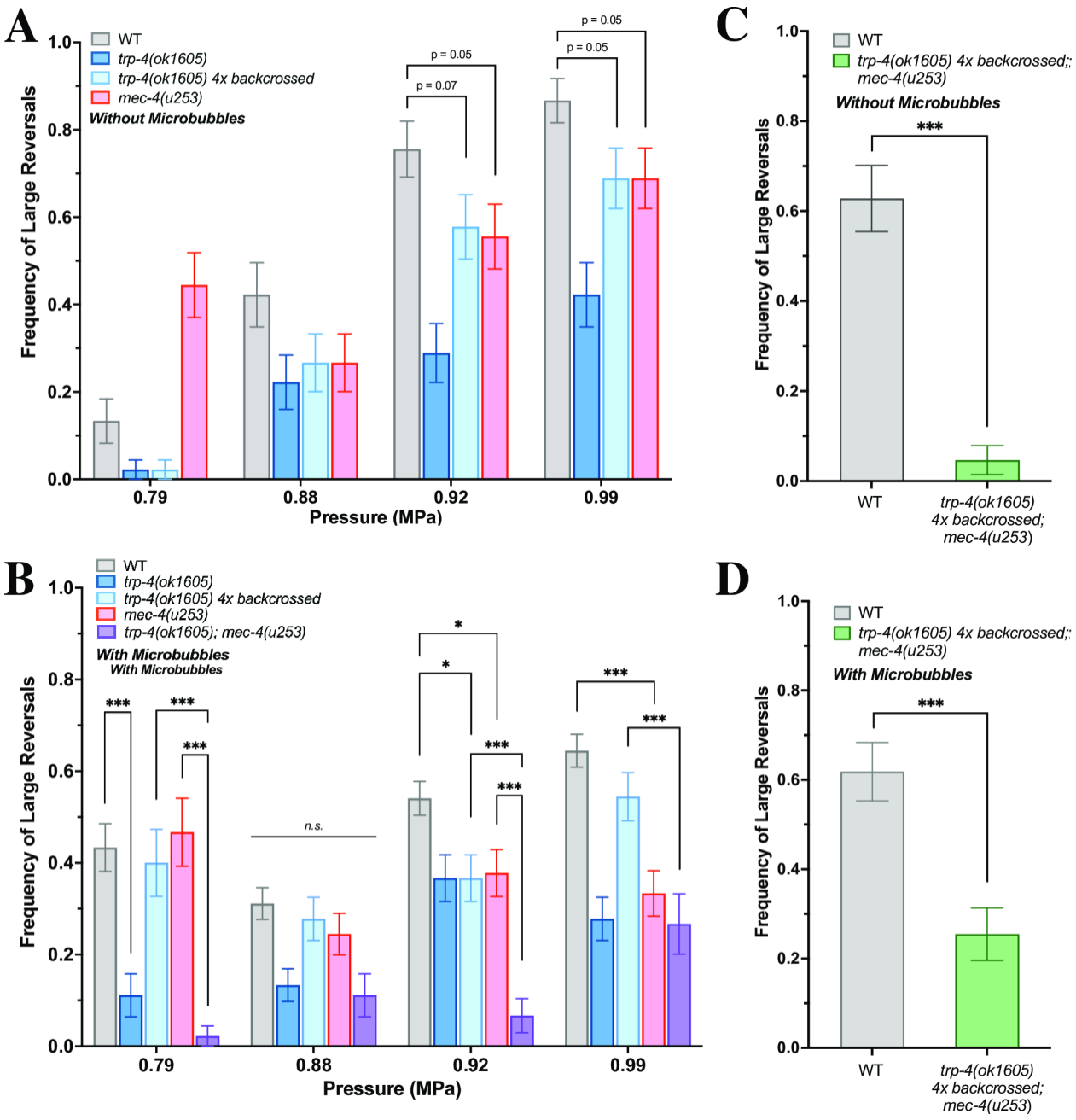

Figure 1.2 | **Mutants in mechanosensitive proteins are defective in their responses to ultrasound**. Frequency of large reversals (more than two head bends) with and without microbubbles. Large reversal frequency (**A**) without microbubbles and (**B**) with microbubbles at various peak negative pressures are quantified. n = 90-135 for each condition, n = 45 for double mutant strains. At certain pressures, the double mutant *trp-4;mec4* responds significantly less than each of the individual mutants, which respond less than WT animals. At 0.99 MPa, the outcrossed double mutant *trp-4 4x;mec-4* shows a significant defect in large reversals both without (**C**, n = 43) and with (**D**, n = 55) microbubbles. Proportion of animals responding with standard error of the proportion are shown. ***p < .001, **p < .01, *p < .05 by two-proportion z-test with Bonferroni correction for multiple comparisons, with c = 2 for **2A**, c = 5 for **2B**.

To confirm whether these two mechanosensitive proteins are acting together, we tested combinations of transgenic animals ectopically expressing TRP-4 in various null mutant backgrounds. We expressed TRP-4 under ASH and AWC-chemosensory neuron selective promoters and analyzed the ultrasound responses of the resulting transgenics [184]. Neither ASH nor AWC expression of TRP-4 in wildtype animals altered its ultrasound-behavior (**Fig 1.3A, 1.3B**). However, at lower pressures (0.79 MPa) TRP-4 expression in AWC chemosensory neurons was able to partially rescue large reversals in both *trp-4(ok1605)* and *mec-4(u253)* mutants (**Fig 1.3A).** In contrast, we found that ASH expression of TRP-4 was able to partially rescue behavioral deficits in both the *trp-4(ok1605)* and *mec-4(u253)* null mutants only at higher pressures (> 0.92 MPa) (**Fig 1.3B**). These data suggest that TRP-4 protein likely functions in different neurons to affect ultrasound-evoked large reversals: AWC for lower pressures and ASH at higher pressures (**Fig 1.3A, 1.3B**). While AWC neurons are known to have an expanded fan-shaped cilia, ASH neurons have a rod shaped cilia [198]. We suggest that this difference in the shape of the cilia might result in AWC and ASH neurons having a different sensitivity to ultrasound-evoked stimuli. In addition, we found that AWC and ASH-selective expression of *trp-4* was able to rescue the behavioral deficits observed in the *trp-4(ok1605 4x)* outcrossed strain (**Fig. 1.3C**) confirming that TRP-4 likely functions in these two chemosensory neurons to drive ultrasound-evoked large reversal behaviors. Also, while small reversals were not consistent, omega bends often matched large reversals (**Fig 1.5**). Collectively, these data suggest that TRP-4 and MEC-4 likely act together to generate large reversals in response to ultrasound stimuli.

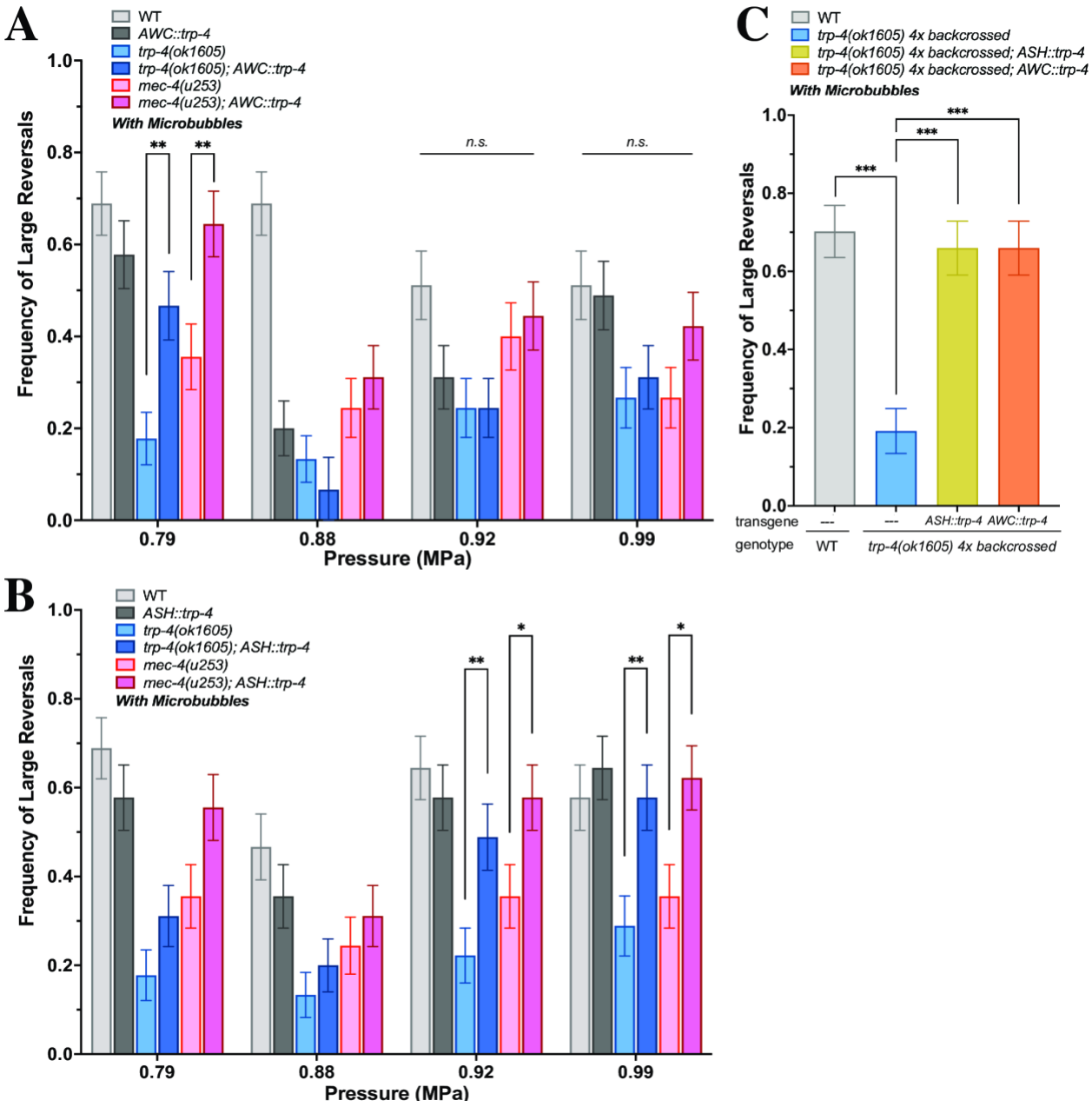

Figure 1.3 | ***MEC-4* and *TRP-4* act in parallel to mediate ultrasound-evoked behavioral changes**. Frequency of large reversals (more than two head bends) in strains ectopically expressing TRP-4. Large reversal frequency with (**A**) *AWC::trp-4* and (**B**) *ASH::trp-4* in different backgrounds at different peak negative pressures are quantified. At certain conditions, trp-4 expression significantly increases large reversal frequency in both *trp-4* knockout and *mec-4* knockout animals. (**C**) At 0.99 MPa, TRP-4 expression in both ASH and AWC rescues large reversal behavior in the outcrossed *trp-4(ok1605)4x* mutant. n = 45 for each condition. Proportion of animals responding with standard error of the proportion are shown. *** $p < .001$, ** $p < .01$, * $p < .05$ by two-proportion z-test.

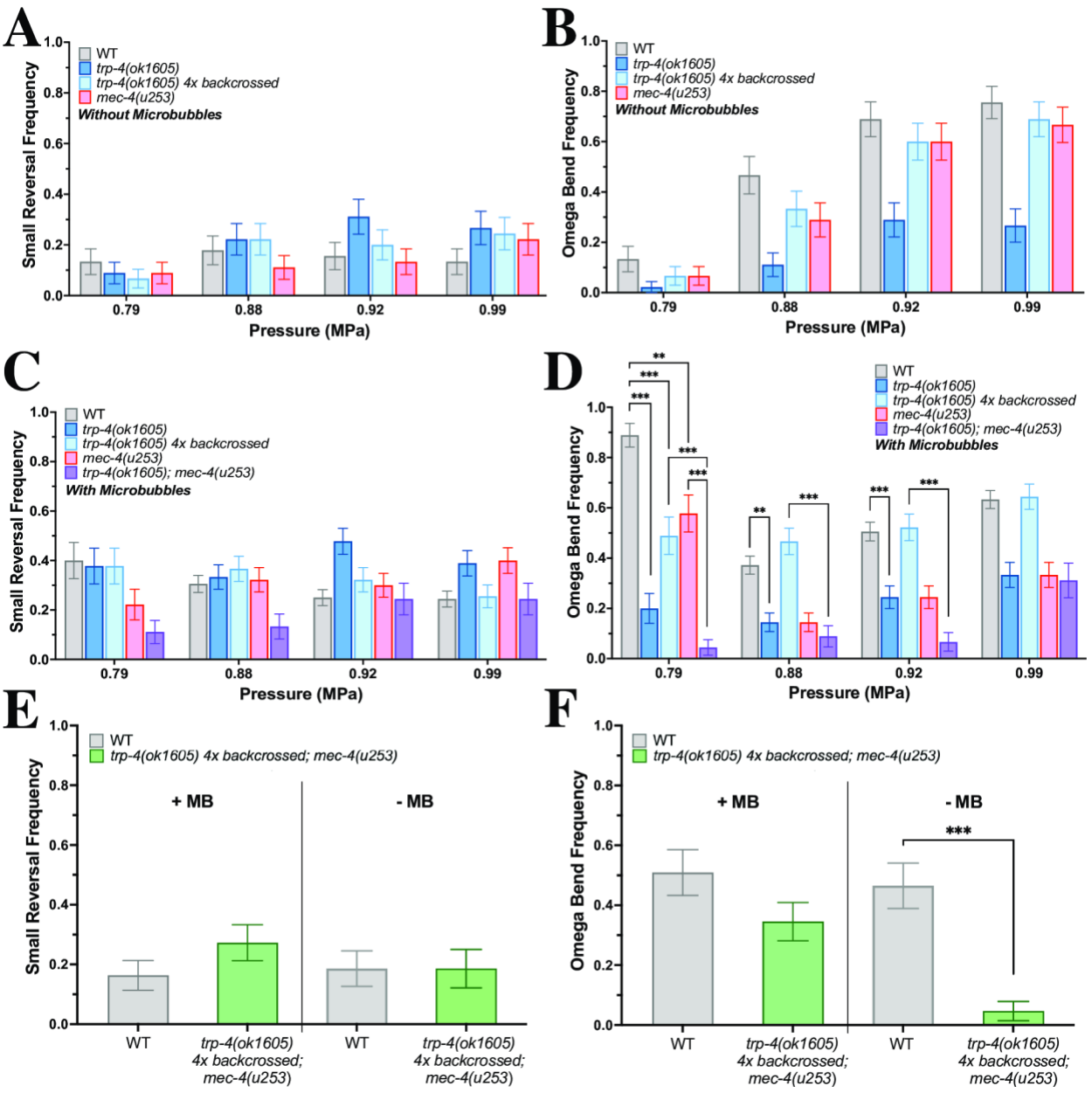

Figure 1.4 | Mutants in mechanosensitive proteins are not defective in their small reversals or omega bends. Frequency of small reversals, defined as fewer than two head bends, and omega bends in different strains at different peak negative pressures. (**A**, **C**, **E**) Small reversals and (**B**, **D**, **F**) omega bends from Figure 2 recordings. n = 45 for each condition (n = 90-135 in c-d single mutants). Proportion of animals responding with standard error of the proportion are shown. *** $p < .001$, ** $p < .01$, * $p < .05$ by two-proportion z-test with Bonferroni correction (c = 5) for multiple comparisons.

Figure 1.5 | ***MEC-4 and TRP-4*** **expression does not change small reversal frequency.** Frequency of small reversals, defined as fewer than two head bends, and omega bends in different strains at different peak negative pressures. (**A**, **C**, **E**) Small reversals and (**B**, **D**, **F**) omega bends from Figure 3 recordings. n = 45 for each condition, Proportion of animals responding with standard error of the proportion are shown. *** $p < .001$, ** $p < .01$, * $p < .05$ by two-proportion z-test with Bonferroni correction (c = 3) for multiple comparisons.

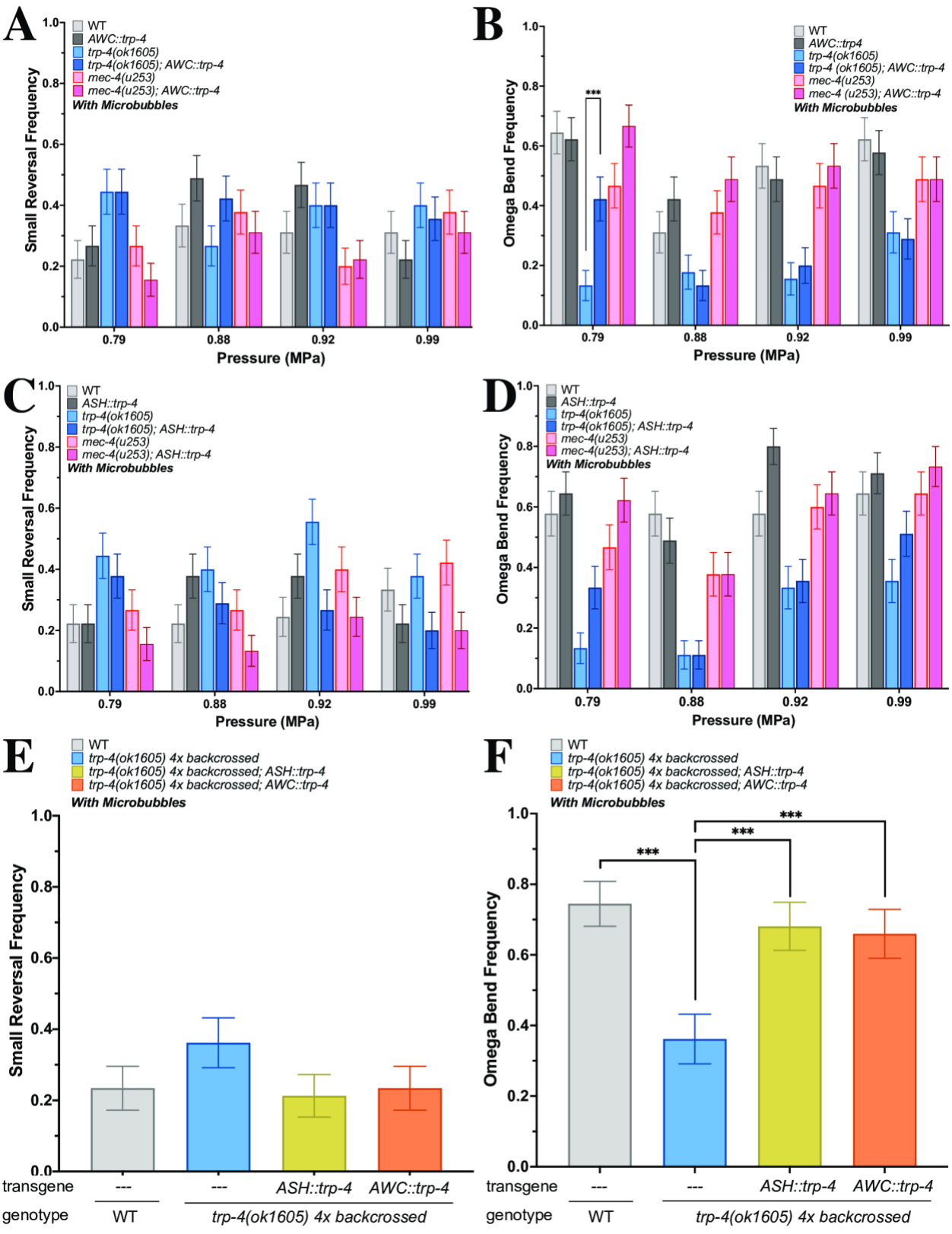
A
WT
AWC::trp-4
trp-4(ok1605)
trp-4(ok1605); AWC::trp-4
mec-4(u253)
mec-4(u253); AWC::trp-4
With Microbubbles
Small Reversal Frequency
Pressure (MPa)
B
WT
AWC::trp4
trp-4(ok1605)
trp-4 (ok1605); AWC::trp-4
mec-4(u253)
mec-4 (u253); AWC::trp-4
With Microbubbles
***
Omega Bend Frequency
Pressure (MPa)
C
WT
ASH::trp-4
trp-4(ok1605)
trp-4(ok1605); ASH::trp-4
mec-4(u253)
mec-4(u253); ASH::trp-4
With Microbubbles
Small Reversal Frequency
Pressure (MPa)
D
WT
ASH::trp-4
trp-4(ok1605)
trp-4(ok1605); ASH::trp-4
mec-4(u253)
mec-4(u253); ASH::trp-4
With Microbubbles
Omega Bend Frequency
Pressure (MPa)
E
WT
trp-4(ok1605) 4x backcrossed
trp-4(ok1605) 4x backcrossed; ASH::trp-4
trp-4(ok1605) 4x backcrossed; AWC::trp-4
With Microbubbles
Small Reversal Frequency
transgene
genotype
WT
trp-4(ok1605) 4x backcrossed
ASH::trp-4
AWC::trp-4
F
WT
trp-4(ok1605) 4x backcrossed
trp-4(ok1605) 4x backcrossed; ASH::trp-4
trp-4(ok1605) 4x backcrossed; AWC::trp-4
With Microbubbles
***
Omega Bend Frequency
transgene
genotype
WT
trp-4(ok1605) 4x backcrossed
ASH::trp-4
AWC::trp-4

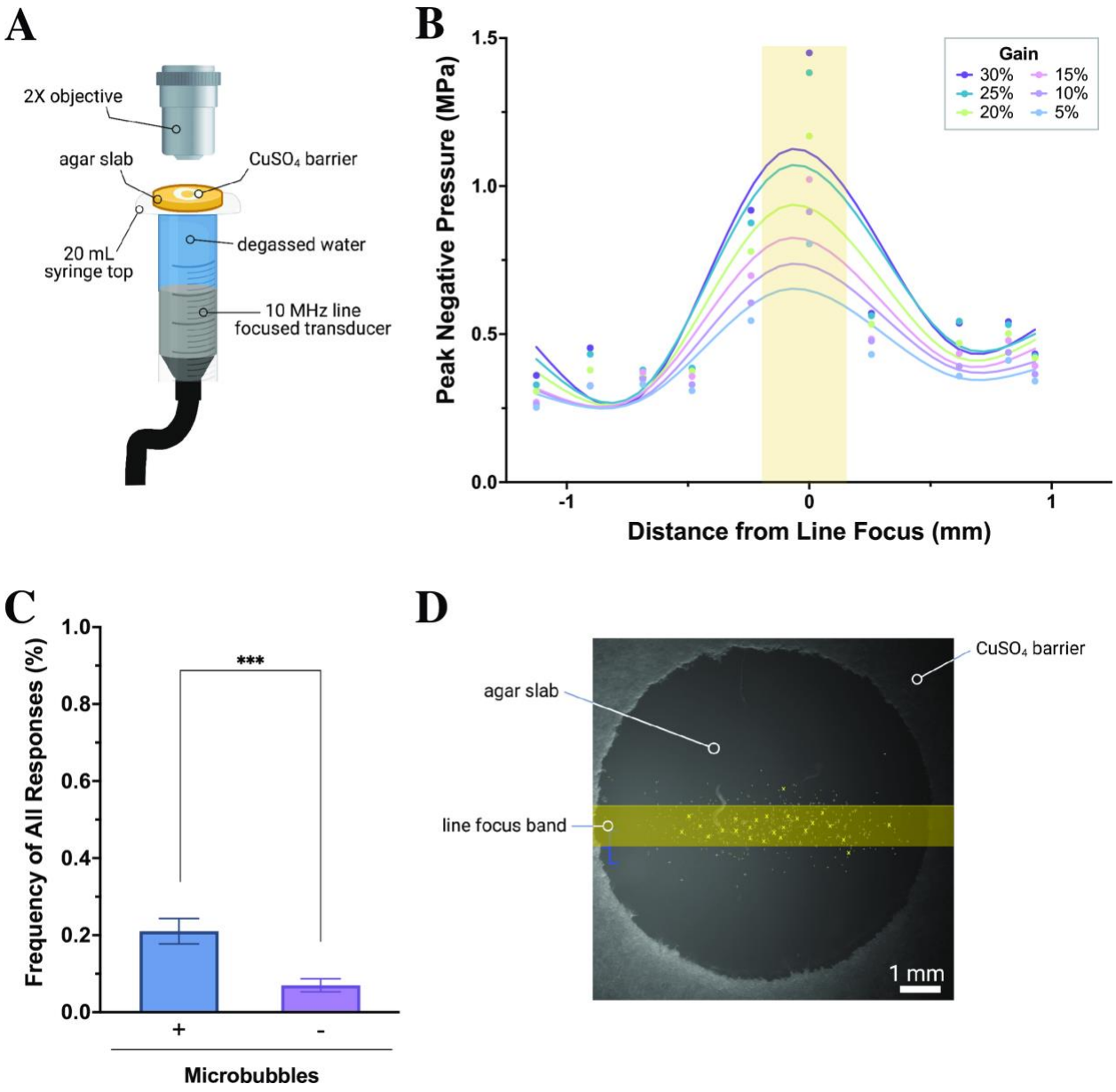

Figure 1.6 | Schematic of 10 MHz behavioral imaging setup, modified from Kubanek et al., 2018 [185]. (**A**) Experimental setup has agar slab with C. elegans corralled by a copper sulfate barrier resting on top of a 20 mL syringe. Degassed water couples the piezoelectric line-focused transducer (10 MHz) to the agar slab. (**B**) Hydrophone measurements at different perpendicular positions relative to the transducer line focus, with peak negative pressures reaching 1 MPa at highest amplifier settings. Yellow bar represents line focus of highest pressure, points connected via spline fit, FWHM ~ 0.52mm. (**C**) C. elegans exhibits minimal behavioral responses to 10 MHz ultrasound stimuli, although these are significantly enhanced in the presence of microbubbles. (**D**) Example image of C. elegans on agar slab approaching ultrasound focal line. Yellow dots (some highlighted for visibility) represent head positions of each of n = 224 worms, indicating a significant proportion of ultrasound stimulations occurred when the head was positioned within the high-pressure band (yellow).

Discussion

We showed that a double mutant that deleted both MEC-4 and TRP-4 channels had stronger behavioral deficits compared to either single mutant alone. Additionally, we showed that AWC and ASH-specific expression of TRP-4 could partially rescue the deficit in both *mec-4(u253)* and *trp-4(ok1604 4x)* single mutants confirming that these two pathways act together to drive ultrasound-evoked changes in large reversals. We suggest that expression of TRP-4 channel in AWC and ASH neurons renders them sensitive to ultrasound stimuli. Activating these neurons has been previously shown to generate reversal behavior [199, 200]. We speculate that the ultrasound-driven activation of ASH and AWC neurons mediated by TRP-4 channels acts independent of the MEC-4 pathway to generate reversal behavior.

The nematode *C elegans* has provided insights into our understanding of how ultrasound affects animal behavior. We previously showed that ultrasound evoked behavioral changes required the pore-forming subunit of the TRP-4 mechanosensitive channel [184]. This protein is selectively expressed in a few dopaminergic and interneurons and is likely involved in generating head movement and coordinating locomotory behaviors. We suggested that delivering ultrasound to the head of the animal likely activates this channel resulting in reversal behavior [184]. Moreover, a second mechanosensitive channel, MEC-4 (DEG/ENaC/ASIC) has been shown to be required for ultrasound-evoked behavioral responses in *C. elegans* [185]. MEC-4 is a key component of the touch sensitive mechanosensitive ion channel and is expressed in the ALM, PLM, AVM, PVM, FLP and other touch-activated neurons [201, 202]. This study indicated that ultrasound delivered to the head of the animal would also generate a reversal response [185]. While we find that *mec-4(u253)* and *trp-4(ok1605 4X)* mutants are indeed defective under our stimulus conditions and likely act together to generate ultrasound-evoked behavioral changes, we are unable

to observe ultrasound-evoked behavioral changes to 10 MHz ultrasound stimuli (**Fig 1.6**). Although we were unable to achieve the magnitude of behavior reported in [22], we observed that, consistent with our other findings, introducing microbubbles to the assay did significantly increase worm responses to ultrasound stimuli **(Fig 1.6C).** Perhaps, differences in ultrasound delivery and stimulus parameters might explain the discrepancy between our study and previous studies, which have reported *C. elegans* responses to 10 MHz and ~28 MHz [185, 203, 204]. Additionally, while previous studies have shown that *mec-4(u253)* are defective to a broad range of ultrasound pressures delivered from 10 MHz transducer [185], we observe that these *mec-4(u253)* mutants are only defective at pressures greater than 0.92 MPa delivered from a 2.25 MHz transducer. These data might imply that distinct molecular machinery might sense ultrasound stimuli at different frequencies. Furthermore, we find that *trp-4(ok1605 4x)* has similar behavioral deficits compared to *mec-4(u253)* animals confirming that these two genes might act together to affect ultrasound-evoked behaviors.

Ultrasound has been used to non-invasively manipulate both neuronal and non-neuronal cells in a number of animals including humans. We show that animals missing two mechanosensitive proteins are defective in their responses to ultrasound stimuli, confirming a role for mechanosensation in mediating the biological effects of this modality. This is also consistent with multiple studies identifying other mechanosensitive proteins that can confer ultrasound sensitivity to mammalian cells *in vitro* and *in vivo* [187-189, 205-207]. This is particularly relevant to the method of using ultrasound to selectively and non-invasively manipulate cells within an animal ("Sonogenetics"). Furthermore, our study implies that ultrasound might affect at least two mechanosensitive ion channels to affect animal behavior. Identifying downstream signaling

pathways of these and other ultrasound-sensitive mechanosensitive channels would provide a framework to decode ultrasound neuromodulation and enhance sonogenetic control.

Acknowledgements

Chapter 1, in full, is a reprint of the material as it appears in: U. Magaram, C. Weiss, A. Vasan, K. C. Reddy, J. Friend and S. H. Chalasani. (2022) Two pathways are required for ultrasound-evoked behavioral changes in Caenorhabditis elegans. *PLOS ONE* 2022 Vol. 17 Issue 5 Pages e0267698. The dissertation author was the primary investigator and co-author of this paper.

CHAPTER 2

Simultaneous ultrasound-mediated neuromodulation and fiber photometry in an awake, freely-moving mouse

Abstract

Transcranial neuronal ultrasound stimulation has been shown to have an effect on the activity of neurons with a number of proposed mechanisms including thermal effects, cavitation effects, microstreaming effects, membrane permeabilization, and mediation via mechanosensitive channels. However, the majority of *in vivo* studies in mammals have used lower frequency ultrasound (< 1 MHz) due to its high transmissibility through intact skull, and immobilized or anesthetized animals to facilitate use of bulky lead zirconate transducers. The following experiments show that transcranial endogenous neuronal activation can be achieved with higher frequency ultrasound (~7 MHz) that can ultimately provide higher spatial resolution, and that the neuronal responses can be measured simultaneously using fiber photometry, an optical calcium imaging technique that does not suffer from electrical interference with the device. Furthermore, the crystals used for the transducers are lithium niobate which can be driven at higher powers and produces less heat. Most importantly, the material is thin and light weight, permitting design of a device capable of being used while attached to the head of an awake, behaving mouse. Simultaneous fiber photometry imaging and ultrasound stimulation reveals that this device, too, is capable of evoking neuronal activity above certain parameter thresholds, suggesting that by sensitizing neurons to ultrasound below those thresholds, neural circuits can be manipulated sonogenetically in a freely-moving mouse.

Introduction

One of the challenges in neuroscience involves concurrently recording and modulating the brain activity of an awake, behaving, freely moving animals. Several recording techniques have been miniaturized: two-photon calcium imaging can now be done in a freely moving animal using miniscope gradient index (GRIN) lenses and *in vivo* electrophysiology recording devices can be implanted in the mouse brain via microelectrode arrays (MEA). Both work in freely moving animals and have been used in conjunction with neuromodulatory tools such as optogenetics and chemogenetics [208, 209]. While GRIN lenses are less invasive to brain tissue and MEAs are less bulky in weight, neither is sufficiently compact to also leave room for ultrasound stimulation, which must be done, ideally, through the exposed, un-occluded skull of the animal. Fiber photometry, a fiber optic fluorescence imaging technique, makes it possible to record bulk calcium activity from neurons *in vivo*, particularly from neurons in deeper brain regions. The cannula which carries light from the brain to the microscope can be implanted in the brain of the mouse without obstructing the entire skull, leaving enough surface exposed through which to deliver ultrasound. Additionally, because the technique is an optical one, it is orthogonal to the mechanism of ultrasound propagation and avoids some of the challenges in simultaneous fiber photometry and optogenetics, such as isolating fluorescence excitation and emission overlap.

Previous studies have successfully stimulated brain circuits *in vivo* using off-the-shelf lead zirconate transducers, whose size and weight requires the animal to be either anesthetized or immobilized [131, 132, 167, 210, 211]. These published works have used various techniques to measure neuronal activity, including electromyography, electrophysiology, and post-mortem histological analyses for neuronal activation and induced transcriptional changes. Furthermore, to facilitate greater transmission through mouse or rat skull, lower frequency US was used as low as

25 KHz and commonly below 1 MHz [210, 211]. Higher frequency US, however, allows for higher spatial resolution, and demonstrating its use in *in vivo* preparations, particularly in freely moving animals, would open the door to new technologies for transcranial US neuromodulation.

The purpose of this work is to validate the feasibility of recording fiber photometry data during US stimulation first using a larger ultrasound transducer in an immobilized animal, and then to validate a novel, custom designed transducer that could be (i) worn by a freely moving mouse, (ii) useable by multiple mice rather than surgically attached to one mouse, and (iii) sufficiently powerful to modify neuronal activity *in vivo* even without the presence of exogenous protein channels.

Materials and Methods

Experimental models

All animal procedures were performed in accordance with the regulations of the Salk Institute for Biological Studies IACUC. 8- to 12-week old mice were used for most experiments. Mice were group housed and maintained in a temperature and humidity-controlled room on a 12:12 h light/dark cycle. All animals were provided with food and water ad libitum. All tests were conducted during the light cycle.

Wild-type C57BL/6J mice were obtained from the Jackson Laboratory. *Chat*$^{ires\text{-}Cre}$ mice were obtained from Jackson Laboratory and were maintained in a homozygous breeding scheme.

Viral Injections and Implants

Intracranial injections were performed in a surgery work area under asceptic conditions. Mice were anesthetized via 5% isoflurane induction and held at 1% isoflurane (Somnosuite Kent Scientific) throughout surgery on a heating pad and stereotactic frame. After shaving and sterilization, a midline incision into skin to expose the skull was made, and the skull leveled.

For cannula and headplate implantation, the skull was dried and primed with OptiBond primer (KerrDental). A small craniotomy was made using a surgical drill at the appropriate coordinates. Injections into dorsal striatum were made using a Nanoject III (Drummond Scientific) via glass micropipette loaded with virus. Virus was injected at 3 nL/s with 1 s pause until total volume was injected. The micropipette was withdrawn 10 minutes after full volume of virus was injected, after which a 200 μm fiber optic cannula (Neurophotometrics) was lowered into dorsal striatum 5 μm above the injection site. Using a minimal amount of light-curable dental cement,

the cannula was affixed in place to the skull to provide maximal exposed skull for subsequent ultrasound experiments.

For behavior experiments, a custom-designed head plate was also affixed to the skull using dental cement just ventral to the cannula leaving the central portion of skull exposed. Following surgery, the skin was either closed where possible via suture (AD Surgical) or VetBond (3M). Mice were injected with buprenorphine (1 mg/kg) and monitored for at least 3 days post-surgery.

Injections were performed unilaterally into dorsal striatum using coordinates +1.0 AP, -2.3 ML, -3.5 DV for vertical injections and +1.7 AP, -2.3 ML, -3.5 DV for injections at 15* on AP axis when leaving more room for headplate for a total of 300 nL. AAV9 hSyn.GCaMP6s.WPRE.SV40 (Addgene #100843-AAV9) was injected into WT mice and AAV9 Syn.Flex.GCaMP6s.WPRE.SV40 (Addgene #100845-AAV9) was injected into *Chat*$^{ires\text{-}Cre}$ mice.

Hydrophone measurements

Ultrasound pressure and temperature measurements were collected in *ex vivo* preparations at positions in the skull used in fiber photometry recordings. A Precision Acoustics Fiber-Optic Hydrophone connected to a Tektronix TBS 1052B Oscilloscope was used to record pressure measurements and input current/voltage was measured via TCP0020 (Tektronix) and TPP0201 (Tektronix) probes, respectively. After sacrifice, the head of a 10-week-old mouse was prepared by removing the dermis and exposing the skull and removing the top palate of the mouse to expose the brain. The head was placed inverted (ventral side up) on the appropriate device and the hydrophone lowered into the brain using a micromanipulator stage (ThorLabs, PT3) for sub-millimeter control. Coordinates were measured from optic chiasm, the most identifiable feature on

exposed ventral brain. For head-device transducer measurements, a custom headplate was also implanted on the mouse head prior to sacrifice to replicate device distance and position for awake, behaving studies.

Fiber photometry recordings

A commercially available fiber photometry system Neurophotometrics FP3002 was used to measure calcium activity *in vivo*. Briefly, recordings were done by alternating 473 nm and 415 nm excitation light at 80 Hz, for a total of 40 Hz recordings in calcium dependent GCaMP6s and isosbestic (calcium independent) channels, respectively. Excitation power was adjusted to provide 50 uW of light at the tip of the patch cord, calibrated with a fiber optic power meter (ThorLabs, PM20A).

For anesthetized recordings with the larger device, mice were anesthetized and held at 1% isoflurane (SomnoSuite), adjusted as needed to maintain sedation on the stereotactic frame without abolishing all measurable brain activity. The skin over the skull was removed and the transducer coupled to the skull with ultrasound gel.

For awake, behaving recordings, the mouse was anesthetized briefly to allow for careful attachment of fiber optic cable. After the head mounted device was attached via magnets and coupled with ultrasound gel, the mouse was allowed to wake up in its home cage and ultrasound stimulations were delivered interspersed with “sham” control pulses.

Rotor Rod

Mouse locomotor behavior with head mounted transducer was evaluated on a Rotor-Rod (SD Instruments). Mice were allowed a single day of training at a constant speed of 3 revolutions

per minute to acclimate to the Rotor Rod system. The next day, mice were placed on a rod starting at 0 revolutions per and gradually increasing to 30 revolutions per minute over a five-minute period. Each mouse ran 5 trials and average latency to fall was collected. Head-mounted device locomotor inhibition was tested by running mice implanted with custom headplate and connected to head-mounted device similar to fiber photometry recordings. No ultrasound was applied during ambulation testing.

Open Field

Mouse locomotor behavior with head mounted transducer was evaluated in Open Field Test with IR actimeter (Panlab) to track mouse motion. Naïve mice were allowed to explore open field for 45 minutes and ambulation was compared to mice implanted with custom head plate and connected to head-mounted ultrasound device connected by magnets and coupled with ultrasound gel. No ultrasound was applied during ambulation testing. Total distance travelled and average velocity throughout open field time was collected.

Immunofluorescence

Immunofluorescence was collected from free-floating 50μm sections after extended (3 day) fixation in 4% paraformaldehyde or 10% formalin for better visualization of cannula lesion. Sections were blocked at room temperature for 1 hour in blocking buffer (0.2% Triton-X and 10% donkey serum in 1x phosphate buffered saline (PBS). Up to three of the following primary antibodies were then applied for incubation in blocking buffer overnight at 4°C: chicken or rabbit polyclonal GFP (1:250 Aves GFP-1020 or ThermoFisher A6455, respectively) for labelling GCaMP6s positive neurons, goat polyclonal ChAT (1:250 EMD Millipore, AB144P) for labelling

cholinergic neurons, chicken polyclonal Parvalbumin (1:250 Encor Biotech, CPCA-PvalB) for labeling PV-interneurons. Following primary antibody incubation, sections were washed three times for 10 minutes each in PBS to reduce non-specific antibody binding effects. Secondary antibodies conjugated to fluorophores 488, 594, or 647 raised in donkey or goat (1:500) were applied for three hours at room temperature in blocking buffer. Nuclei were stained with DAPI (1:1000 ThermoFisher D1306) before washing sections three times in PBS for ten minutes each. Sections were mounted on slides coverslipped with ProLong Gold Antifade Mountant (ThermoFisher P10144) and allowed to dry for 24 hours before confocal imaging (Zeiss LSM 880).

Analysis

All fiber photometry data was processed in Matlab by averaging traces in a peri-stimulus manner and compared within recording sessions. Statistical tests were performed in GraphPad Prism 9 using Ratio paired t-test.

Results

In order to test the efficacy of higher frequency ultrasound transmission through mouse skull, fiber optic hydrophone measurements were acquired from *ex vivo* preparations of 10-week old mice. After euthanasia, the decapitated head was prepared by placing the skull on the 1 x 1 cm transducer coupled with ultrasound gel and removing the hard palate to allow access to the brain (**Fig 2.1A**). Peak negative pressures were first measured at optic chiasm, the most ventral exposed surface as a function of amplifier gain (**Fig 2.1B**). Peak negative pressures reached upwards of 2.0 MPa, indicating that transmission of ~7 MHz ultrasound from the larger lithium niobate transducer was capable of permeating through intact mouse skull. Hydrophone measurements at different depths through lateral and posterior portions of the brain (**Fig 2.1C-G**) showed almost linear but somewhat variable relationships, with maximum pressures of ~0.75 MPa in striatum where subsequent recordings were conducted.

Similar recordings were conducted using the head-mounted custom-built transducer, including the custom designed headplate used to hold the transducer in place (**Fig 2.1H**). Peak negative pressures of ~0.5 MPa were measured in striatum. Temperature changes at power inputs used showed some increase at maximum pressures were < 0.1°C, consistent with modeling calculations and returned to baseline in < 20 seconds for subsequent trials. Temperature changes were slightly greater for longer burst durations (**Fig 2.1K**) as predicted but did not exceed 0.1°C in any conditions. Laser doppler vibrometer scans (**Fig 2.1L**) were used to determine the resonant frequency of the transducer (6.56 MHz) at which all experiments were conducted.

Figure 2.1 | Fiber optic hydrophone measurements in *ex vivo* preparations of mouse heads reveal substantial ultrasound transmission through intact skull. (**A**) Schematic of 1.5 x 1.5 cm device measurements. (**B**) Pressure measurements in optic chaism at longest distance from transducer face increase with increasing amplifier gain. (**C**) Schematic of measurement locations on ventral surface of mouse brain. (**D-G**) Ultrasound pressures at different distances from transducer face. (**H**) Schematic and location of hydrophone measurements for small, head mounted transducer. (**I**) Temperature increases were minimal during 500 ms ultrasound pulses. (**J**) Maximum transcranial pressures were 0.5 MPa in striatum. (**K**) Temperature changes were minimal for 100-500 ms pulses of ultrasound. (**L**) Laser doppler vibrometry shows maximum displacement across the transducer face at 6.56 MHz.

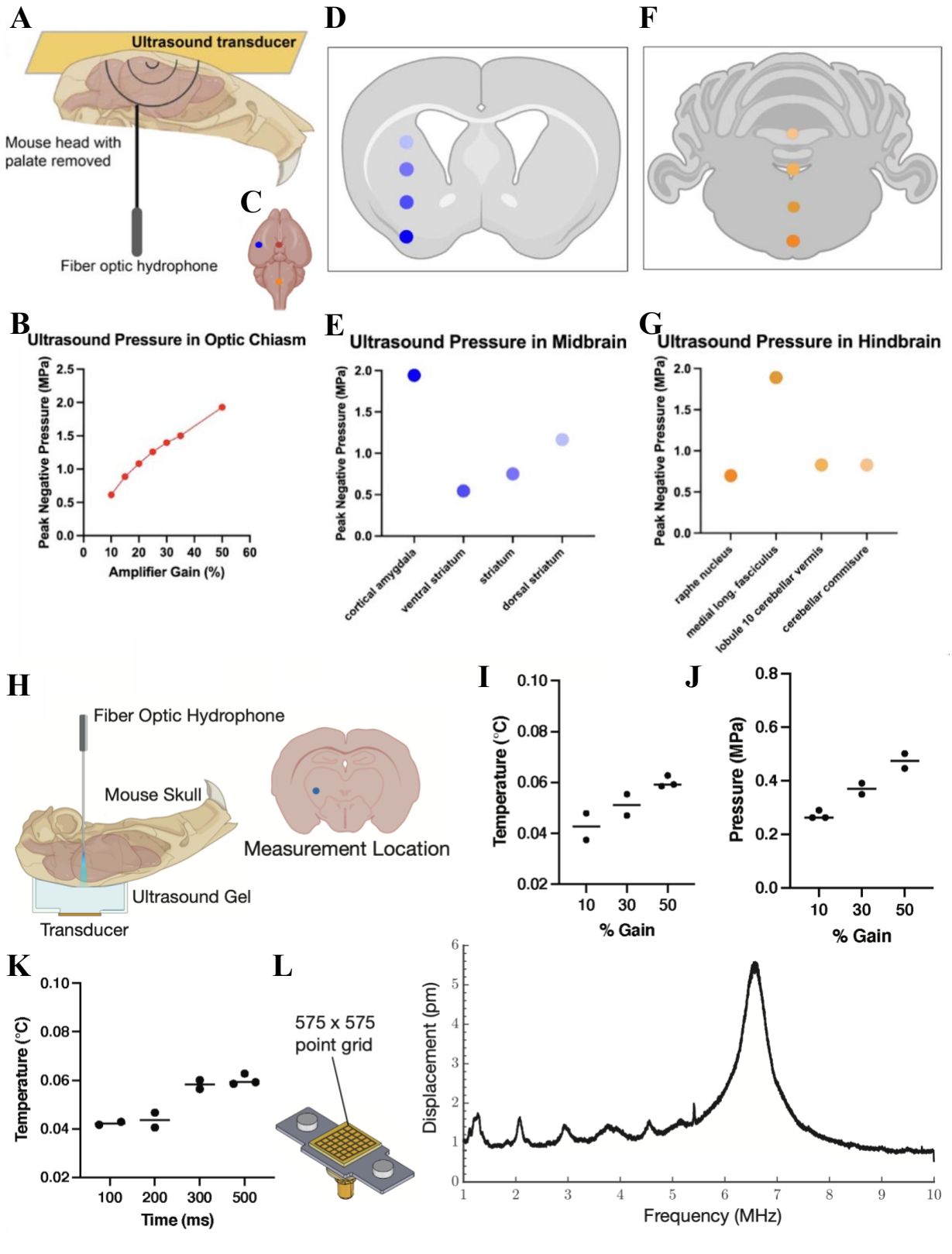
A
Ultrasound transducer
Mouse head with palate removed
Fiber optic hydrophone
C
D
F
B
Ultrasound Pressure in Optic Chiasm
Peak Negative Pressure (MPa)
Amplifier Gain (%)
E
Ultrasound Pressure in Midbrain
cortical amygdala
ventral striatum
striatum
dorsal striatum
G
Ultrasound Pressure in Hindbrain
raphe nucleus
medial long. fasciculus
lobule 10 cerebellar vermis
cerebellar commisure
H
Fiber Optic Hydrophone
Mouse Skull
Measurement Location
Ultrasound Gel
Transducer
I
Temperature (°C)
% Gain
J
Pressure (MPa)
% Gain
K
Temperature (°C)
Time (ms)
L
575 x 575 point grid
Displacement (pm)
Frequency (MHz)

Ultrasound-evoked calcium activity was analyzed by aligning GCaMP6s (473 nm) signal to the onset of ultrasound pulses (or sham controls) akin to a peri-stimulus time histogram. Prior to alignment, the full 473 nm trace was corrected for photobleaching by fitting the putatively static isosbestic 415 nm trace with a biexponential curve (**Fig 2.2A**). After confirming an interspersed distribution of ultrasound and sham-ultrasound pulses (**Fig 2.2B**), the full trace was filtered at 2 Hz with a low pass filter (**Fig 2.2C**) to eliminate high frequency noise. For a single action potential, GCaMP6s fluorescence has been shown to decay to baseline after >2 seconds [212], and spectrographic and fast-Fourier transform revealed that the majority of both higher-power spontaneous and evoked signal resided in the lower frequencies. Following alignment of 15-second windows to the onset of stimulus, each trace was normalized via z-score to the 5-second average of the calcium activity recorded prior to stimulus onset (**Fig 2.2D, Fig 2.2E**). The isosbestic signal was similarly normalized and checked for movement artefact (**Fig 2.2D, Fig 2.2E**), and the maximum fluorescence change was calculated in the 3 second window following stimulus delivery (**Fig 2.2F**).

Figure 2.2 | **Sample fiber photometry trace with analysis pipeline.** (**A**) 473 nm (top) and 415 nm (middle) recording from one epoch. Bottom trace shows 473 nm trace corrected using biexponential fit of 415 nm isosbestic trace. (**B**) Stimulation (red) and "sham" stimulation (green) controls plotted along calcium imaging trace, showing interspersed trials. (**C**) Low pass filter (2 Hz, bottom) of full corrected 473 nm trace. (**D**) Full 473 nm trace (top) aligned to stimulus or "sham" stimulus onset. Activity present in 473 but not 415 nm trace indicates calcium activity rather than motion artefact. (**E**) Normalization of traces from (D) using z-score averaged to 5 second window prior to stimulus onset. (**F**) 3 second window after stimulus used to determine maximum fluorescence change.

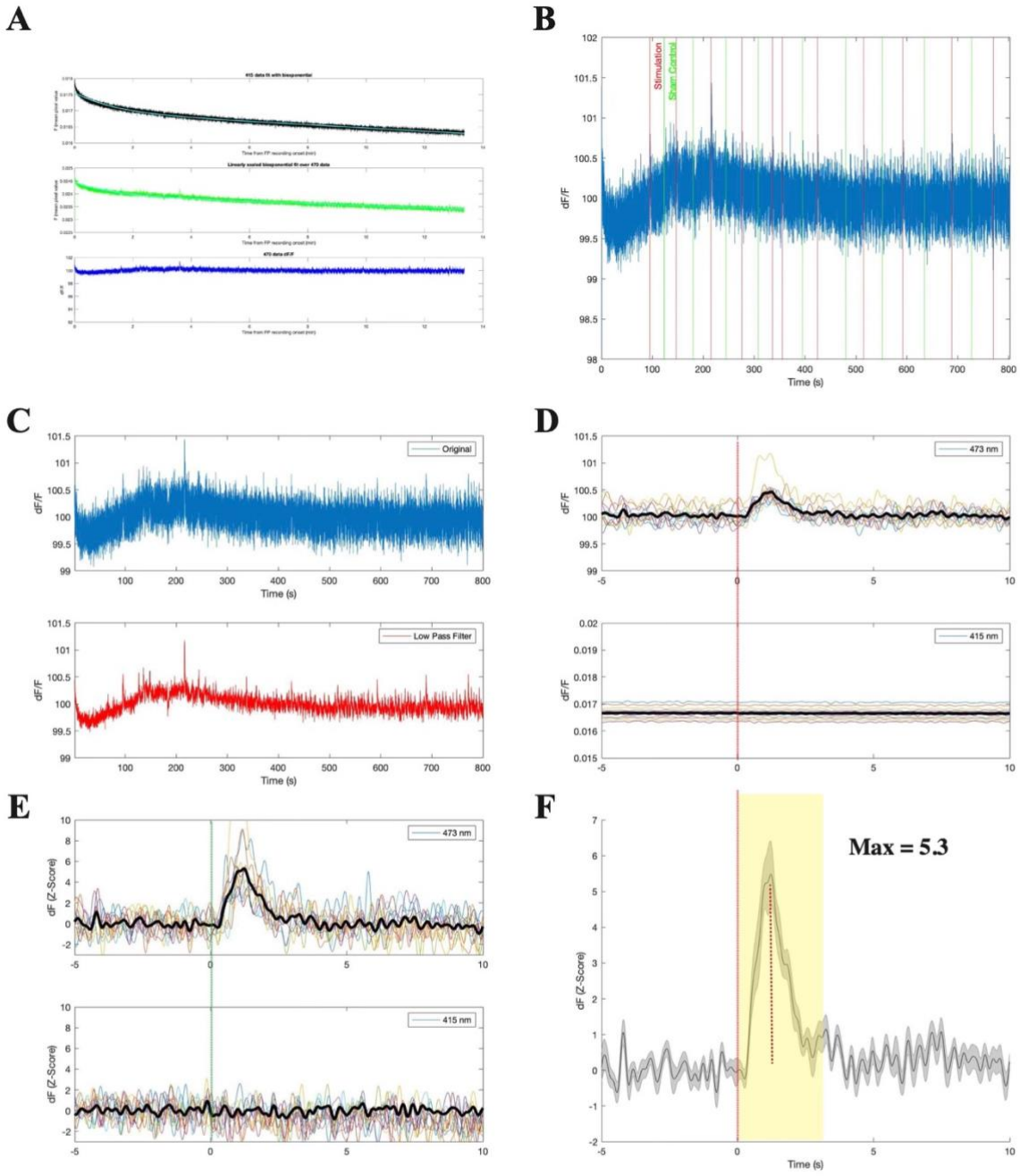
A
B
Stimulation
Sham Control
dF/F
Time (s)
C
Original
Low Pass Filter
dF/F
Time (s)
D
473 nm
415 nm
dF/F
E
473 nm
415 nm
dF (Z-Score)
F
Max = 5.3
dF (Z-Score)
Time (s)

Fiber photometry recordings were used to first confirm whether calcium activity *in vivo* could be evoked and measured simultaneously with transcranial ultrasound stimulation. Several objectives were targeted simultaneously in this study: to test whether a larger ultrasound device (~ 1.5 x 1.5 cm) could be used simultaneously with fiber photometry recordings, as well as to measure ultrasound-evoked calcium activity in deeper brain regions inaccessible to two-photon imaging. Dorsal striatum (DS) was chosen as the target brain region due to its stereotaxic location which permitted a fiber optic cannula implant that would not occlude the entire skull, as well as for its larger volume to target and its implication in many functions including habit formation, addiction, reward assessment and decision making [213, 214]. Previous studies have shown ultrasound-evoked neuronal activity in both cortex and hippocampus [167] but not necessarily in more ventral regions.

To broadly survey the wide range of cell types in striatum, 10-week-old C57Bl6 wild type (WT) mice were stereotactically injected in DS with an AAV9 Syn-driven genetically encoded calcium indicator GCaMP6s (AAV9-Syn-GCaMP6s-WPRE-SV40). A fiber optic cannula (200 mm) was then implanted directly over the injection site with minimal dental cement in order to leave a majority of the skull accessible for ultrasound transmission.

To allow for animal recovery and GCaMP6s expression, US-evoked bulk calcium activity was assessed in implanted mice two to four weeks post-surgery. Prior to stimulation, calcium activity signal was first confirmed by the presence of spontaneous events in the 473 nm but not the isosbestic 415 nm channel. Because the larger ultrasound device was too large to affix to the head of the animal, mice were anesthetized with 1% isoflurane and the transducer placed over the exposed skull coupled with ultrasound gel; ultrasound pulses were delivered interspersed with

sham controls (amplifier output turned off) and traces were compared only within single recording sessions to avoid confounds between anesthetic states [215].

All mice showed increased time-locked calcium activity to the maximum parameters delivered by the transducer, 500 ms and 0.7 MPa pressure (**Fig 2.3A-E**). The peak calcium activity was significantly increased in the 3-second window after ultrasound as compared to sham controls in which only the amplifier output was turned off (**Fig 2.3F**).

Once consistent US responses were established at maximized parameters, mice were stimulated with decreased pulse durations and amplitudes to test whether a lower threshold set of parameters could still evoke neuronal activity. At half maximum amplitude (0.35 MPa), ultrasound evoked responses were more variable across mice. The peak fluorescence after stimulation was higher in the stimulation condition than sham although this difference failed to reach significance, potentially suggesting a half-maximum activation point (**Fig 2.3G-L**). Similarly, the animals in which 300 ms pulses were tested showed increased calcium signal after stimulation, but with variability too high to reach significance (**Fig 2.3M-P**).

Average fluorescence traces showed variability across trials in several mice (**Fig 2.3A, Fig 2.3J, Fig 2.3N**) compared to others (**Fig 2.3O, Fig 2.3E**), as well as multi-phasic activity in some conditions (**Fig 2.3A, Fig 2.3H, Fig 2.3M**). While this variability could potentially be reduced by increasing the number of trials delivered, it could also be a result of recording calcium activity from a mixed population of neurons, including dopaminergic D1/D2 cells as well as their local inhibitory counterparts (PV, ChAT, SOM). Histological analysis post sacrifice revealed GCaMP6s expression in a heterogeneous population of neurons, with 1.1% of GCaMP6s-expressing cells surveyed being ChAT positive and 6.8% of cells surveyed being PV positive (**Fig 2.3Q-U**). Proportionally, this suggests that a majority of GCaMP-expressing neurons recorded were D1/D2

medium spiny neurons since these make up ~95% of the neurons in striatum [216]. Since there is interconnectedness between local neurons, this could contribute to the variable responses across mice and trials [217]. Additionally, slight changes in the position of the device relative to the skull and cannula throughout the course of 30-minute recordings could have some effect on the variability of responses.

Together these results suggest that the lithium niobate device similar to the one used in two-photon imaging experiments (data not shown) is capable of evoking ultrasound responses in intact, deeper brain regions at ~7 MHz through intact skull, consistent with prior findings which used similar frequencies [218].

Figure 2.3 | Simultaneous fiber photometry recordings and ultrasound stimulation in WT mice with larger ultrasound transducer. (**A-E**) Average traces of ultrasound on (red) versus sham control (gray) for five mice; 500 ms 0.7 MPa. (**F**) Maximum fluorescence change is significantly greater following ultrasound stimulation compared to sham controls. (**G-K**) Average traces of ultrasound on (red) versus sham control (gray) for five mice; 500 ms 0.35 MPa. (**L**) Maximum fluorescence change is greater following ultrasound stimulation compared to sham controls but fails to reach significance. (**M-O**) Average traces of ultrasound on (red) versus sham control (gray) for three mice; 300 ms 0.7MPa. (**P**) Maximum fluorescence change is greater following ultrasound stimulation compared to sham controls but fails to reach significance. (**Q**) Quantification of neurons expressing GCaMP6s. GCaMP6s+/ChAT+ neurons make up the least portion of the population, followed by GCaMP6s+/PV+ neurons. The remaining neurons are presumably D1/D2 medium spiny neurons based on neuronal subtype distributions in striatum. (**R-U**) Sample immunohistochemistry from WT animal co-stained with PV and ChAT antibodies, lesion at top of image from fiber photometry cannula implant.

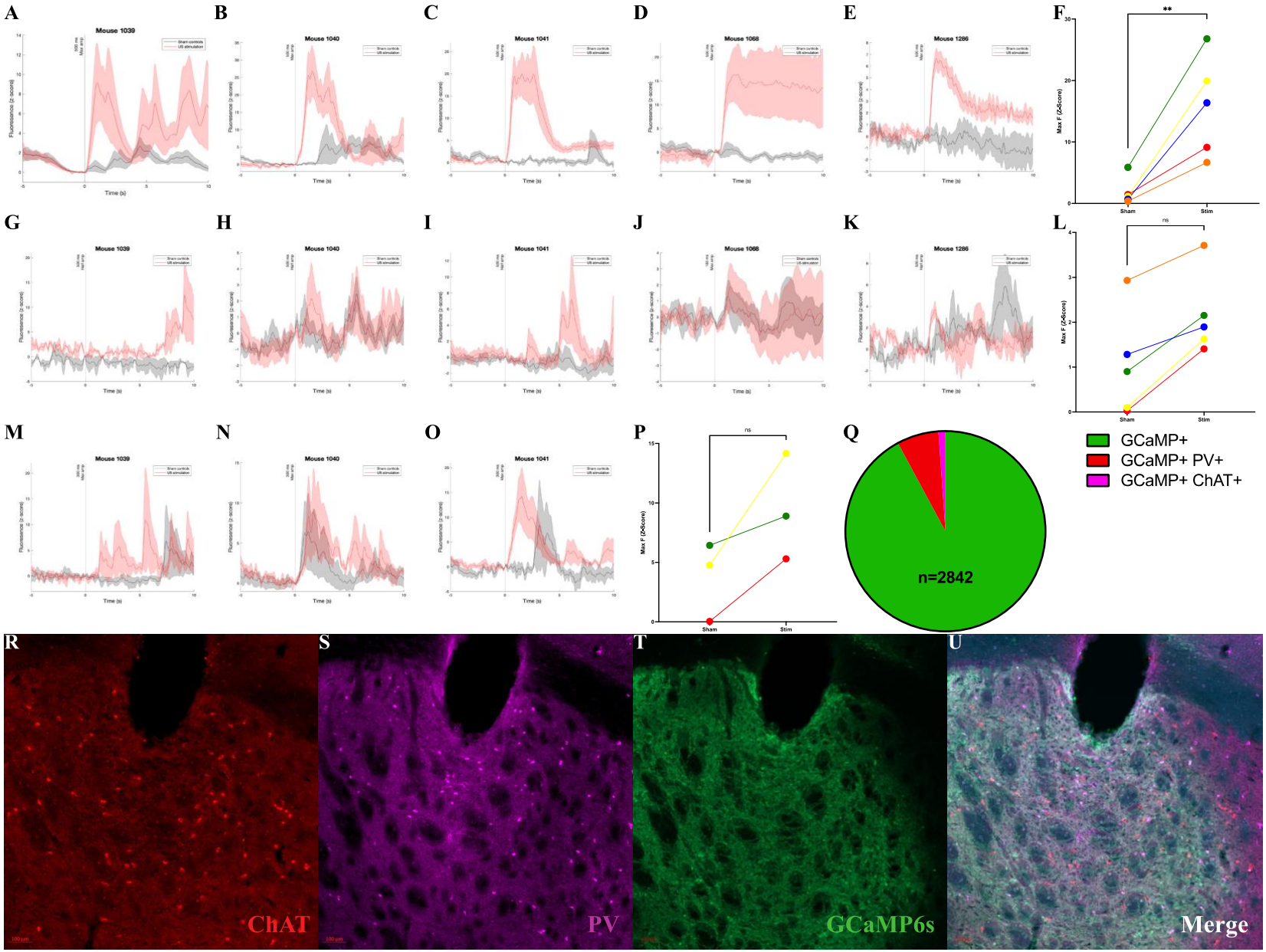
A
Mouse 1039
B
Mouse 1040
C
Mouse 1041
D
Mouse 1068
E
Mouse 1286
F
**
Max F (Δ-Score)
Sham
Stim
G
Mouse 1039
H
Mouse 1040
I
Mouse 1041
J
Mouse 1068
K
Mouse 1286
L
ns
Max F (Δ-Score)
Sham
Stim
M
Mouse 1039
N
Mouse 1040
O
Mouse 1041
P
ns
Max F (Δ-Score)
Sham
Stim
Q
n=2842
GCaMP+
GCaMP+ PV+
GCaMP+ ChAT+
R
ChAT
S
PV
T
GCaMP6s
U
Merge

To test whether a sparser population of neurons could be stimulated with ultrasound, cholinergic cells in the striatum were targeted using *Chat*$^{ires\text{-}Cre}$ (ChAT-Cre) mice. Cholinergic neurons in striatum are interesting due to their role in regulating motor movements [219] and histological analysis showed that these neurons are indeed sparse and capable of expressing GCaMP6s (**Fig 2.3T**). These neurons make up about 2% of neurons in dorsal striatum and provide dense local cholinergic innervation [220].

ChAT-Cre mice were prepared similarly to WT mice, but with GCaMP6s expression limited to cholinergic neurons using Cre-dependent AAV9 (**Fig 2.4Q-T**). Animals were held under 1% isoflurane when possible and subjected to parameters similar to those used in WT studies.

Under maximum ultrasound conditions (500 ms, 0.7 MPa), mice showed ultrasound-evoked responses whose maximum fluorescence was significantly greater after ultrasound stimulation compared to sham controls (**Fig 2.4A-E**). A similar trend was observed in half-maximum amplitude stimulation (2.500 ms, 0.35 MPa), although individual average traces (**Fig 2.4F**, **Fig 2.4I**) revealed that these results may have been skewed by a particularly responsive and a particularly unresponsive mouse (**Fig 2.4J**). All mice showed responses at 300ms, with significant increases in fluorescence time locked to ultrasound stimulation (**Fig 2.4K-P**).

Interestingly, responses in all conditions were less variable than those in WT animals. Cholinergic interneurons in striatum appear to exert control very densely in their local anatomical field [220], suggesting that they may exert less control over each other. Together, these results indicate that ~7 MHz ultrasound can evoke calcium activity in a sparse subset of striatum neurons, validating stimulation-observation paradigm for further exploration of US neuronal stimulation *in vivo*.

Figure 2.4 | Simultaneous fiber photometry recordings and ultrasound stimulation in ChAT-Cre mice with larger ultrasound transducer. (**A-D**) Average traces of ultrasound on (red) versus sham control (gray) for four mice; 500 ms 0.7 MPa. (**E**) Maximum fluorescence change is significantly greater following ultrasound stimulation compared to sham controls. (**F-I**) Average traces of ultrasound on (red) versus sham control (gray) for four mice; 500 ms 0.35 MPa. (**J**) Maximum fluorescence change is significantly greater following ultrasound stimulation compared to sham controls. (**K-O**) Average traces of ultrasound on (red) versus sham control (gray) for five mice; 300 ms 0.7MPa. (**P**) Maximum fluorescence change is significantly greater following ultrasound stimulation compared to sham controls. (**Q-T**) Histological confirmation that GCaMP6s expression was restricted to ChAT+ cells, black portion at top middle of image as result of lesion from fiber optic cannula implant.

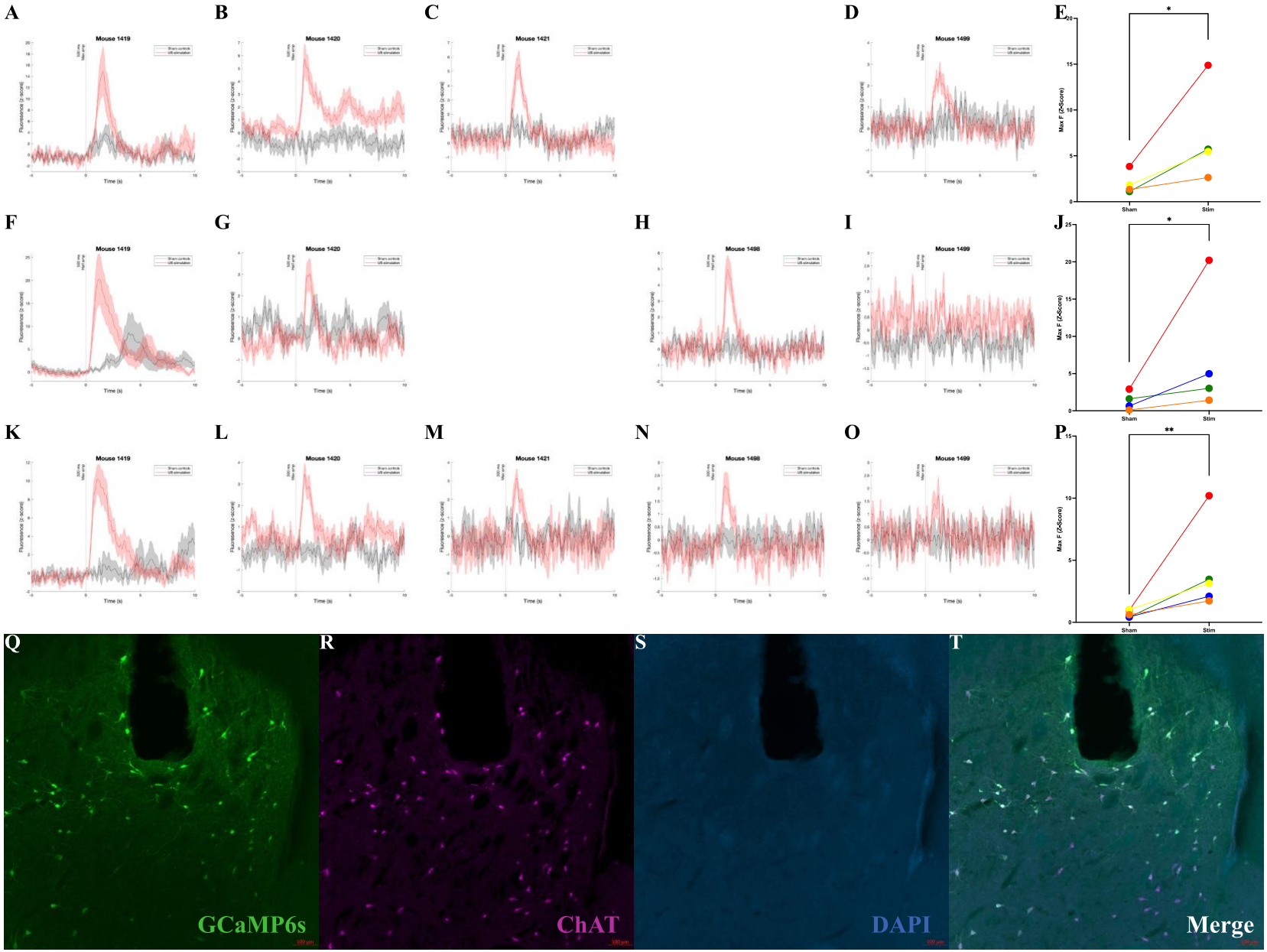
A
B
C
D
E
Mouse 1419
Mouse 1420
Mouse 1421
Mouse 1499
Sham controls
US stimulation
Time (s)
Max F (Z-Score)
Sham
Stim
*
F
G
H
I
J
Mouse 1419
Mouse 1420
Mouse 1498
Mouse 1499
*
K
L
M
N
O
P
Mouse 1419
Mouse 1420
Mouse 1421
Mouse 1498
Mouse 1499
**
Q
R
S
T
GCaMP6s
ChAT
DAPI
Merge

Since ChAT-Cre mice showed more consistent ultrasound responses both within and across mice, the same genotype was chosen to test the efficacy of a custom designed, head-mountable ultrasound transducer in stimulating neurons *in vivo* in freely-moving animals. ChAT-Cre mice were injected with GCaMP6s and implanted with a fiber optic cannula as before, but this time a custom design headplate designed to hold the ultrasound transducer in place was implanted just caudal to the cannula.

After brief anesthesia to affix the fiber optic cable, mice were allowed to wake up in their home cage for simultaneous ultrasound stimulation and fiber photometry recording (**Fig 2.5A**). Of the animals tested, at least three animals showed a consistent response to ultrasound pulses (500 ms, 0.5 MPa) compared to sham control counterparts (**Fig 2.5E-G**). One mouse showed no response to US stimulation, while another showed an indication of a response that failed to reach significance (**Fig 2.5H-I)**. The peak fluorescence following US pulses compared to sham controls was significantly greater across the group (**Fig 2.5J**). It was noticed that despite being attached by magnets, the angle of the device relative to the head plate, and thus the skull, did occasionally appear to shift, indicating the need for improved affixation methods and potentially contributing to variability between trials. However, no trials were run when the device was not connected to the head of the animal.

Behavioral assay showed that attachment of the device did not result in any observable motor defects, both in an open field as well as during rotor rod testing. In the open field assay, control mice (naïve animals) did not exhibit any increase in the total distance ambulated, nor in average velocity throughout the entire testing period (**Fig 2.5K**), nor during the first 5 minutes of testing after first introduction to the assay (**Fig 2.5L**). Similarly, when tested on the rotor rod, mice which were outfitted with both a headplate and the ultrasound device did not show any

impairment in their ability to stay on the rotor rod as measured by time-to-fall (**Fig 2.5M**). During ultrasound testing, mice were able to freely move and explore for up to 20 minutes at a time, despite having to be periodically "untangled" as their fiber optic and device wires crossed.

Overall, these data suggest that a 7 MHz lithium niobate transducer small enough to be worn on the head by adult mice is capable of evoking neuronal activity in brain regions as deep as striatum; it is feasible that this transducer could be used in the future for behavioral testing as well as other sonogenetic applications for manipulating and dissecting neural circuits.

Figure 2.5 | Simultaneous fiber photometry recordings and ultrasound stimulation in awake, freely-moving ChAT-Cre mice with head-mounted transducer. (**A**) Schematic of experiment, mouse is connected to both ultrasound device (input from signal generator and amplifier) as well as fiber photometry microscope. (**B**) Schematic of fiber implant and histological confirmation of GCaMP6s expression restricted to ChAT+ cells. Red box highlights 10x tile image, yellow boxes highlight 20x tile images. (**C-D**) Sample trace shows increased activity following ultrasound stimulation in 473 nm trace but not 415 nm isosbestic recording, indicating calcium concentration change and not movement artefact. (**E-I**) Average traces of ultrasound on (red) versus sham control (gray) for five mice; 500 ms 0.5MPa. (**J**) Maximum fluorescence change is significantly greater following ultrasound stimulation compared to sham controls. (**K**) Total distance traveled and average velocity over 45 minutes in an open field assay shows mice are not inhibited by headplate and ultrasound device. (**L**) During the first 5 minutes in an open field assay, mice with a headplate and ultrasound device (red) show similar distance traveled and average velocity compared to naïve controls (gray). (**M**) Mice with a headplate and ultrasound device (red) are able to stay on the rotor rod as long as, or longer, than naïve control counterparts (gray).

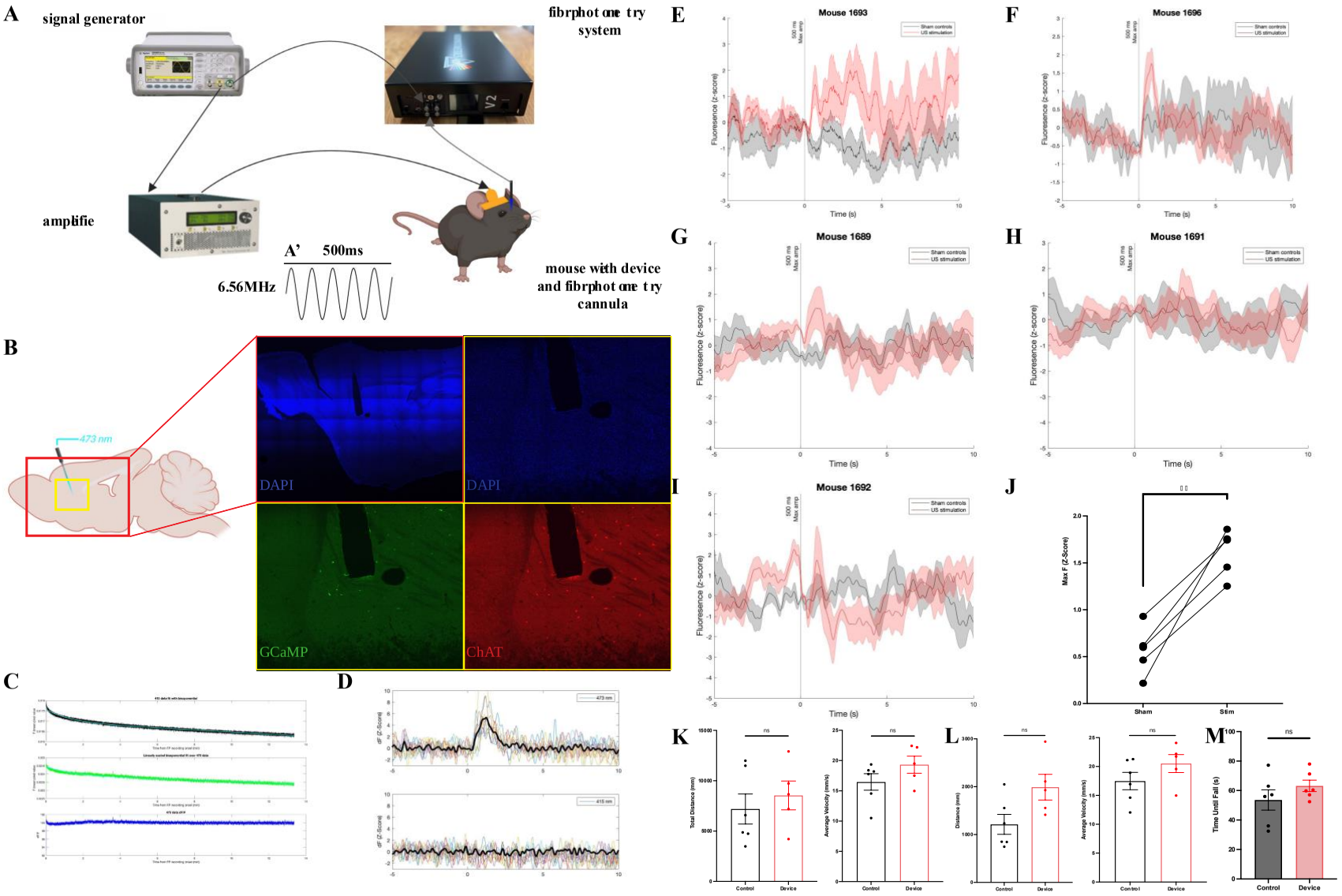
A
signal generator
fibrphot one try system
amplifie
A'
500ms
6.56MHz
mouse with device and fibrphot one try cannula
B
473 nm
DAPI
DAPI
GCaMP
ChAT
C
D
473 nm
415 nm
E
Mouse 1693
F
Mouse 1696
G
Mouse 1689
H
Mouse 1691
I
Mouse 1692
Sham controls
US stimulation
Fluorescence (z-score)
Time (s)
J
Max F (Z-Score)
Sham
Stim
K
L
M
ns
Control
Device
Total Distance (mm)
Average Velocity (mm/s)
Distance (mm)
Time Until Fall (s)

Discussion

To date, previous studies of *in vivo*, transcranial neuronal stimulation in mice have fallen short of stimulating and recording the altered activity of neurons in awake, behaving mice. Numerous previous studies have examined the effects of ultrasound in nervous tissue across a spectrum of biological models, from neuronal cultures and slice preparations to primates and humans. For the most part, *in vivo* transcranial US stimulation has been restricted to either anesthetized or immobilized mice [130-132]. Additionally, these studies have examined physiological effects of US neuronal stimulation via EMG, electrophysiology, and even evoked motor responses but not direct calcium imaging of targeted brain regions in awake, behaving mice. In other words, the experiments and results described in this study are one of the first of their kind, evoking neuronal activation via ultrasound stimulation and simultaneously monitoring the neuronal effects directly in freely-moving animals.

In addition to being one of the first results of its kind regarding freely-moving US neuronal stimulation and observation, the US frequencies used in these studies are higher than the majority of those done in the past few decades, which have, for the most part, used frequencies below 1 MHz – US considered in the lower frequency ultrasound range [221]. While lower frequency ultrasound can provide greater tissue penetration and decreased absorption, it also means sacrificing spatial resolution in future studies, since the wavelength of propagation correlates inversely with frequency. Previous *in vivo* studies of mice have used frequencies of 25 KHz, 35 KHz, 50 KHz [130, 131], and some as high as 1.9 and 2.9 MHz [132] with limited success, but none in the literature have used >5 MHz frequencies *in vivo*, particularly in freely moving animals. However, hippocampal slices stimulated with 7.5 MHz ultrasound showed increased spike frequency, consistent with observations *in vivo* [218]. This is an exciting development suggesting

that with proper engineering, novel ultrasound devices that operate in higher frequency ranges can be built to target and modulate neuronal activity in mice, and perhaps in humans.

Thermal effects of ultrasound have been points of contention as long as ultrasound has been used in biological tissue. The FDA sets upper boundaries on safe levels of ultrasound based in part on a thermal index (TI) to avoid excessive heating of tissue [222]. However, the predominant US effects observed in these studies are likely mechanical, given that calculated and fiber optic measurements of temperature changes were < 0.1°C (Fig 1). Further dissection of mechanical effects would be needed to fully understand the effects of 6.56 MHz US *in vivo*.

Further investigations would also reveal the nature of both heterogenous and cholinergic-isolated stimulation effects of US *in vivo*. It has been shown that striatum, and ChAT+ neurons in particular, receive extensive inputs via cortical innervation [223]. These effects could be dissected in multiple ways, including simultaneous fiber photometry recordings from multiple regions including cortex and striatum [224], as well as pharmacological or optogenetic silencing of cortical brain regions during US ensonification. Furthermore, calcium indicators with faster dynamics and greater dynamic ranges could help elucidate the latency between US pulses and calcium activity in target neurons [225]. Although previous studies have shown elevated levels of BDNF- or cfos-based activation in stimulated regions [167], more intricate dissection of activated neurons could reveal insights into activation mechanisms. For example, repeating US stimulation experiments in a TRAP2 mouse strain injected with Cre-dependent fluorescent markers during tamoxifen exposure could label active cells in the stimulation time window, and dissection of stimulated tissue with fluorescence-activated cell sorting could reveal differences in expression levels of candidate mechanosensitive channels versus inactive neurons.

It has been suggested by several studies that the neuronal effects in non-cortical regions of transcranial stimulation are secondary effects of either auditory cortex activation or those via a cochlear pathway [144, 145]. These findings are concerning regarding the ability of ultrasound to directly modulate neuronal activity by mechanical mechanisms rather than secondary synaptic effects, and must be addressed for future ultrasound neuromodulation studies. As a further control, mice whose auditory pathways can be selectively ablated such as Pout45^{DTR} could be used to isolate direct versus indirect effects. However, it is also not clear whether this auditory mechanism would apply to the significantly higher frequencies of ultrasound used here (~7 MHz in present studies compared to 250 KHz and 500 KHz in auditory cortex/cochlear studies), especially given that the lower frequencies are closer to the range of ultrasound produced by mouse vocalizations (upwards of 100 KHz [226]).

While the custom-designed transducer used in these studies is a useful proof-of-concept for using higher frequency ultrasound for neuromodulation in mice (and perhaps other animals), it does not represent the best case scenario for wearable transcranial ultrasound transducers. Phased array probes used in medical imaging [227] and multiple, constructively interfering transducers both indicate methods of improving targeting spatially precise regions of the brain with intense but safe levels of ultrasound. Diffusers attached to the face of the transducer have been shown to increase the uniformity of the generated ultrasound field [228], suggesting that if particular neurons are sensitized to ultrasound, ensonifying the whole brain while still only targeting a specific population of neurons could be possible.

Novel technology must be assessed for safety, the present study not excluded. The mechanical index of US stimulation did not exceed 0.78 (0.2 for head-mounted transducers), well below the FDA established safe mechanical index of 1.9 thought to cause cavitation and tissue

damage. Still, further studies would help elucidate whether neurons exposed to repeated US stimulation at various display signs of degradation or even apoptosis. Previous studies have used BDNF as an activation marker and caspase-3 as an apoptotic marker to assess longer term effects of US stimulation [130, 229] – these markers would be useful in the present study with more significant and numerous stimulations to assess whether some viability threshold exists in both the US parameter space and in repeated exposure. Although both thermal and cavitation effects are believed to be minimal in these studies, since the true mechanism of US activation is not known, cell health must be assessed empirically.

The human skull has a substantially different architecture than that of a mouse, with acoustic impedances that make higher-frequency US transmission more difficult [230]. This does not exclude the possibility that novel technologies will emerge which make transcranial US stimulation at higher frequencies possible, including the development of impedance matching metamaterials [231] which could help overcome scattering and absorbance at the skull surface. Still, the acoustic properties, and many of the neuronal ones, of mouse and human brain are similar enough to suggest that higher frequency US stimulation could be a useful technique for neuromodulation. Together with piezoelectric materials which make powerful devices lightweight enough to be worn on the head of a freely-moving mouse, these finding represent an exciting step towards ultrasound neuromodulatory driven dissection of neural circuits with minimal invasiveness.

DISCUSSION AND CONCLUSIONS

Prior investigations into ultrasound-based neuromodulation and ultrasound mechanosensation have produced substantial insights, but significant challenges remain in turning ultrasound into a widespread neuromodulation tool. The findings and developments described in this dissertation represent steps towards improved understanding of mechanosensitive protein-mediated ultrasound sensation as well as novel technology that could become a useful tool in neuroscience and perhaps medical research.

The first portion of studies in this dissertation described the biological actuators of ultrasound transduction- protein channels capable of turning ultrasonic acoustic radiation forces into neuronal signals and behavior. Specifically, findings suggested that multiple protein channels in the nematode *C. elegans* were responsible for ultrasound transduction and behavioral responses [232], and appear to be engaged in the sensation and transduction under different parameters. This means that even in a single organism, mechanical sensing and ultrasound-based modulation of neuronal activity could have both multiple biological components as well as different components engaged under different US conditions, complicating the already complex hypotheses underlying US neuromodulation.

The second portion of this dissertation focused on US neuromodulation in mammals. A novel, custom-designed US transducer made of lithium niobate and small enough to be worn on the head of a mouse was tested for its power output and ability to trigger neuronal responses in mice whose neuronal properties had not otherwise been altered for mechano-sensitivity. Fiber photometry measurements paired with ultrasound stimulation revealed time-locked activity that, despite needing more follow up studies, suggests that higher frequency US is capable of evoking neuronal activity and can do so in an awake, behaving mouse. This finding is exciting because it

opens the door to sonogenetic applications *in vivo* without the need for cannula implantations and the animals do not have to be anesthetized or otherwise immobilized.

Together, these findings represent advances on both fronts of building a single-component sonogenetic tool: new understanding of mechanosensitive protein channels and overcoming prior technological limitations.

Mechanisms of Ultrasonic Neuromodulation

There are numerous hypotheses about the mechanisms of ultrasound neuromodulation including thermal and cavitation effects, microstreaming, membrane permeabilization, and transduction through mechanosensitive protein channels, but a definitive explanation remains elusive. More informative experiments can be performed in preparations in neuronal and tissue culture, where pharmacology, genetic manipulation, and acoustic field modeling are more tractable and measurements can be made using both electrophysiology and imaging [127-129, 233]. However, the conclusions drawn from these studies are difficult to extend to those *in vivo* due to the increasingly complex nature of the system and its interaction with ultrasound. For example, neuronal activity was evoked in hippocampus slices stimulated with 44 KHz ultrasound for just 22.7 μs [129], but follow-up experiments *in vivo* required stimulation with 25, 35, and 50 KHz US at longer timescales (up to 0.57 ms) [130]. That the original parameters did not translate directly from culture to intact brain is suggestive of a lack of full understanding of US mechanism of action and perhaps the need for additional research and sonogenetic tools. Still other *in vivo* follow up studies used even longer durations and other frequencies to achieve noticeable effects [131]. Similarly, Chinese hamster ovary (CHO) cells transfected with Piezo1, but not those transfected with sodium channel Nav1.2 were activated by 43 MHz ultrasound [234]. Despite being an

interesting finding, it is unlikely such high frequency stimulation would necessarily translate to *in vivo* results, nor has this same result been shown in mammalian neurons.

As discussed in the Introduction section, thermal and cavitation effects were originally thought to be the main sources of US driven neuromodulation. However, researchers interested in isolating more nuanced mechanisms take care to use US conditions that minimize or altogether avoid the parameters necessary to cause these effects. *C. elegans* experiments described in this dissertation used microbubbles in order to use US cavitation as an amplifier for US stimulation, but this was done in order to maintain a consistent story with previous experiments [235] and some experiments showed significant reversals and behavior in response to US without microbubbles as well (Fig 2). All mouse experiments were done without the presence of exogenous agents such as microbubbles, suggesting that the endogenous interaction between the US field and intact brain was sufficient to cause neuronal activation.

For many experiments in the literature, particularly in the last few decades, the mechanical index and thermal index are below the threshold to account entirely for neuromodulatory effects. Other effects from acoustic radiation forces propagation through tissue could explain observed neuromodulatory US effects: as US waves pass through tissue, radiation torque and acoustic streaming forces capable of moving small ions and molecules can cause streaming around cell membranes due to small impedance mismatches [104, 236]. All of these forces combined, including stable cavitation, microturbulence and shear stresses could change the permeability of cell membranes themselves, or cause small fluctuations in area leading to capacitance changes that could affect membrane polarization [237]. Alternatively, protein channels in the membrane whose gating depends either on the forces in the lipid bilayer or via anchors in the cytoarchitecture and extracellular matrix could sense local displacements and either open or exhibit altered kinetics

[238]. The complexities of the skull cavity as well as higher-order mechanical properties of ultrasound make it difficult to model the system for predictive purposes [239], and empirical results and parameters vary across studies. One of the goals of the mouse studies described in this dissertation were to characterize the parameters at which neuronal activity could be evoked endogenously with custom-built transducers for future work to express sensitizing mechanosensitive proteins in genetically targeted neurons for activation at sub-threshold amplitudes and durations.

These hurdles towards a complete mechanistic picture of US neuromodulation, together with the observation that physiological effects have lower boundaries in US studies motivate the need for a sensitizing molecule that can confer ultrasound sensitivity to otherwise insensitive neurons.

Safety Considerations

As described in the introduction, the widespread use and supervision by the FDA indicate that under proper conditions many ultrasound applications in biology in medicine are safe. However, this does not necessarily account for the novel research of the last few decades concerning specifically US neuromodulation.

Diagnostic imaging regulated by the FDA uses frequencies ~1-20 MHz, suggesting that the higher frequencies used in both *C. elegans* and mouse studies could be evaluated under the auspices of the FDA's regulations. While the health of worms and mice was evaluated "by eye" after stimulation and full ambulation was confirmed, this does not necessarily account for potentially hidden or longer-term effects. More studies would need to be done to evaluate the health of individual neurons after stimulation across a spectrum of parameters and durations, including histological analysis of tissues post-mortem. Additionally, analysis of glia in the

surrounding tissue, as well as blood brain barrier, and skull would need to be evaluated to empirically determine the safety limits of higher-frequency ultrasound stimulation that produce neuromodulatory effects.

Analysis of central nervous tissues exposed to ultrasound in numerous neuromodulation studies showed no signs of damage. In hippocampal slices, even 36-48 hours of ultrasound exposure (stimulation ever 8 minutes) did not change the structure of membranes, blood brain barrier, or synaptic morphology [129], and *in vivo* stimulations at higher intensities (300 mW/cm^2) also did not alter subsequent performance in rotorod or wire-hanging tasks, nor increased numbers of apoptotic neurons or glia [130]. Other US neuromodulation studies of mice and rats also revealed little to no damage using hematoxylin and eosin staining, as well as DNA fragmentation (TUNEL) histological assessments post-mortem [240-242].

For ethical reasons, intentional damaging of tissue, particularly when not in the scope of the goals of the study, should be avoided. Incidental damage has been reported on a few occasions and can also provide valuable insights into dangerous US parameters. A study in rats found that 0.35 MHz, I_{SPTA} = 22.4 W/cm^2 caused local bleeding in one of the subjects tested [243], and in sheep repeated stimulations with 250 KHz US at 1 second intervals eventually caused micro-hemorrhages that were avoided when the interval was increased to 5 seconds, although no ambulatory issues post stimulation were observed [244]. These findings are rare but valuable, as they indicate the need for more intelligent US parameter design, as well as the possibility that individual variability could play a role in both neuromodulatory effects and safety thresholds between subjects. Comparing the after-effects of US exposure in both nematodes and mice on an individual basis could also provide insights into whether certain genes and protein expression levels across individuals confer particular resistance to higher intensity ultrasound stimulation.

These assessments as a whole do not suggest that any and all ultrasound neuromodulation is safe, but rather that there are many regions of the ultrasound parameter space that can produce neuromodulatory effects while being safe, as was the case for dozens of transcranial and peripheral US neuromodulation studies [221]. Since post-stimulation histological assessment in human subjects is not viable, sensitizing neurons to even lower pressures and durations of stimulation in the future can ensure that no tissue damage occurs.

Technical Challenges

Ultrasound technology has evolved since the discovery of piezoelectric materials over a century ago and is widely used in industry and medicine. Tradeoffs are made in transducer design between power, weight, and sturdiness of materials, and clever transducer arrangements such as phased arrays can be used to improve imaging conditions. The shape of the face of the transducer also has effects on US delivery- transducers with focal points and lines use constructive and destructive interference for better targeting, while those with flat faces produce more uniform US fields.

The US transducers used in the majority of *in vivo* studies thus far, including those described previously in the introduction, have used commercial, lead zirconate titonate (PZT) transducers, exploiting their ease-of-access and relative affordability. Furthermore, these transducers are attractive because they are commercially made and precisely machined, so that variability between transducers is likely minimal. PZT transducers were used in this dissertation's *C. elegans* portion for historical reasons and consistency as well [235, 245].

Lithium niobate transducers were used in the *in vivo* mouse portion of this dissertation for their powerful output while still being lightweight- this permitted manufacture of a device small and light enough to be attached to the head of a freely-moving animal. Furthermore, the

temperature changes at the face of the lithium niobate transducers was reduced and the absence of lead makes it safer to work with. The crystal structure also permits more power to be delivered to the device without damaging it as compared to lead zirconate titonate. Further research will likely produce even more powerful, lightweight devices that can be driven at higher powers, produce less heat, output different frequencies, and perhaps one day be driven wirelessly.

Accurate measurements of ultrasound fields and thermal changes present another technical challenge for *in vivo* applications. Determining empirically what pressures are being delivered to the brain of an intact animal requires at least some portion of the animal remain intact. *Ex vivo* preparations of mouse heads with brain exposed inside of skull do permit some measurements be made using needle or fiberoptic hydrophones. This is a concession, however, since the properties and integrity of the tissue change post-mortem, and while paraformaldehyde fixation could provide some structural integrity, these measurements would still only be approximations of those made *in vivo*. *In vivo* measurements were attempted for this dissertation (data not shown) by using stereotactic coordinates, but turned out to be prohibitively difficult and highly risky in terms of potential damage to the fragile hydrophone tip. Modeling of acoustic and thermal properties provides insights and guiding principles for the impacts of different US parameters on brain tissue, but accurate measurements with high temporal and spatial resolution, especially across the entire brain, remain elusive.

Clinical Prospects of Sonogenetics

Mechanosensitive channels for sensitizing mammalian neurons would ideally come from non-mammalian species, similar to those used for optogenetics applications. Although this could present challenges in protein trafficking and expression, confounding factors such as off-target

effects would potentially be avoided. Indications in recent studies suggest that sensitizing neurons and possibly other cell types by expressing exogenous proteins on their surface is possible.

One interesting method for finding potential ultrasound-sensitizing protein channel candidates is by screening species for ultrasound sensitivity across the phylogenetic tree. For example, many marine creatures are known to use and sense ultrasound to navigate their underwater surroundings, and behavioral responses to various frequencies of ultrasound could suggest the presence of genes encoding ultrasound-sensitive proteins which could then be expressed in mammalian cells. Early experiments in this space were performed during this dissertation (data not shown) and have provided some candidate genes of interest.

Piezo1, which has received much attention since its discovery in 2010 [246] has been tested for ultrasound sensitivity by several groups. Stimulation of cultured human umbilical vein endothelial cells with 0.2 W 1 MHz ultrasound induced influx of calcium ions into the cells, with reduced influx after Piezo1 knockdown [247]. Piezo1 transfection into Chinese hamster ovary cells also increased their sensitivity to ultrasound at 43 MHz at 50 or 90 W/cm^2 [234]. In primary cultured rat hippocampal neurons, expression of a mutant of the *E. coli* channel MscL elicited action potentials when the cells were exposed to 0.25 – 0.45 MPa, 30 MHz US [248]. MscL also mediated ultrasound responses in retinal pigment epithelium cells transfected with the channel (as well as its G22S mutant) when integrin-bound microbubbles were used to apply shear forces to the cytoskeleton of the cells, suggesting that the cytoarchitecture of cells plays an important role in mechanosensation [249]. These findings are promising but fall short of an *in vivo* manipulation of neurons with ultrasound stimulation.

*hs*TRPA1, a member of the transient receptor potential (TRP) family, was shown to sensitize HEK293 cells in culture to 7 MHz ultrasound. In these studies, mouse neuronal cultures

also exhibited increased activity in response to 7 MHz US stimulation after infection with *hs*TRPA1, suggesting that this channel could be used *in vivo* in mice to sensitize neurons to US below the endogenous-activation threshold. Indeed, mice infected with *hs*TRPA1 showed elevated EMG responses in forelimbs as well as elevated levels of *c-fos* in infected/stimulated areas as compared to control counterparts [250]. These studies marked the first methods for sonogenetic control of mammalian neurons *in vivo*, but more work remains to make sonogenetics a powerful circuit dissection tool.

Clinical applications of US technology, and eventually sonogenetic technology, are promising. Human studies in transcranial US stimulation demonstrate its ability to be focused onto target tissue, and while the mechanisms of neuronal activation and its excitatory versus inhibitory effects are still under review, physiological effects are demonstrable in human M1, V1, S1, S2, and even thalamus [136, 251-253]. Evaluations of specifically the human skull by pioneers in human transcranial ultrasound studies suggest that there is movement towards exploring US neuromodulation in more detail [254], and a review of 35 studies with 677 subjects total suggests that although transcranial ultrasound stimulation is in its early phases, mild symptoms (scalp heating, neck pain, anxiety, etc.) were mild (2.4%) in a variety of cohorts that included healthy subjects as well as those with dementia, epilepsy, traumatic brain injury, and depression [255]. In fact, some clinical trials are already underway in treating anxiety and depression using focused transcranial ultrasound, indicating that this technology is on the verge of being accepted alongside electrical and magnetic non-invasive neuromodulation methods in clinical applications [256]. Combined with potential manipulations to sensitize genetically targeted neurons in a sonogenetic manner, in the future these methods could provide effective, non-invasive neurological relief.

REFERENCES

1. Brunet, T. and D. Arendt, *From damage response to action potentials: early evolution of neural and contractile modules in stem eukaryotes.* Philosophical Transactions of the Royal Society B: Biological Sciences, 2016. **371**(1685): p. 20150043.

2. Sousa, A.M.M., K.A. Meyer, G. Santpere, F.O. Gulden, and N. Sestan, *Evolution of the Human Nervous System Function, Structure, and Development.* Cell, 2017. **170**(2): p. 226-247.

3. Marder, E., *Neuromodulation of Neuronal Circuits: Back to the Future.* Neuron, 2012. **76**(1): p. 1-11.

4. Hari, R., L. Parkkonen, and C. Nangini, *The brain in time: insights from neuromagnetic recordings.* Ann N Y Acad Sci, 2010. **1191**: p. 89-109.

5. Papo, D., *Time scales in cognitive neuroscience.* Front Physiol, 2013. **4**: p. 86.

6. Hari, R. and L. Parkkonen, *The brain timewise: how timing shapes and supports brain function.* Philos Trans R Soc Lond B Biol Sci, 2015. **370**(1668).

7. Golesorkhi, M., J. Gomez-Pilar, F. Zilio, N. Berberian, A. Wolff, M.C.E. Yagoub, and G. Northoff, *The brain and its time: intrinsic neural timescales are key for input processing.* Communications Biology, 2021. **4**(1): p. 970.

8. Wang, B., W. Ke, J. Guang, G. Chen, L. Yin, S. Deng, Q. He, Y. Liu, T. He, R. Zheng, Y. Jiang, X. Zhang, T. Li, G. Luan, H.D. Lu, M. Zhang, X. Zhang, and Y. Shu, *Firing Frequency Maxima of Fast-Spiking Neurons in Human, Monkey, and Mouse Neocortex.* Frontiers in Cellular Neuroscience, 2016. **10**.

9. Abraham, W.C., O.D. Jones, and D.L. Glanzman, *Is plasticity of synapses the mechanism of long-term memory storage?* npj Science of Learning, 2019. **4**(1): p. 9.

10. Bliss, T.V. and T. Lomo, *Long-lasting potentiation of synaptic transmission in the dentate area of the anaesthetized rabbit following stimulation of the perforant path.* J Physiol, 1973. **232**(2): p. 331-56.

11. Baillet, S., *Magnetoencephalography for brain electrophysiology and imaging.* Nature Neuroscience, 2017. **20**(3): p. 327-339.

12. Soikkeli, R., J. Partanen, H. Soininen, A. Pääkkönen, and P. Riekkinen, Sr., *Slowing of EEG in Parkinson's disease.* Electroencephalogr Clin Neurophysiol, 1991. **79**(3): p. 159-65.

13. López-Sanz, D., N. Serrano, and F. Maestú, *The Role of Magnetoencephalography in the Early Stages of Alzheimer's Disease.* Front Neurosci, 2018. **12**: p. 572.

14. O'Reilly, C., J.D. Lewis, and M. Elsabbagh, *Is functional brain connectivity atypical in autism? A systematic review of EEG and MEG studies.* PLoS One, 2017. **12**(5): p. e0175870.

15. Wulff, K., D.J. Dijk, B. Middleton, R.G. Foster, and E.M. Joyce, *Sleep and circadian rhythm disruption in schizophrenia.* Br J Psychiatry, 2012. **200**(4): p. 308-16.

16. Johansson, A.S., B. Owe-Larsson, J. Hetta, and G.B. Lundkvist, *Altered circadian clock gene expression in patients with schizophrenia.* Schizophr Res, 2016. **174**(1-3): p. 17-23.

17. Peters, C.R. and A. Lock, *Handbook of human symbolic evolution*. 1999: Blackwell.

18. Cavanagh, J.B., *The problems of neurons with long axons.* Lancet, 1984. **1**(8389): p. 1284-7.

19. Dahl, M.J., M. Mather, S. Düzel, N.C. Bodammer, U. Lindenberger, S. Kühn, and M. Werkle-Bergner, *Rostral locus coeruleus integrity is associated with better memory performance in older adults.* Nat Hum Behav, 2019. **3**(11): p. 1203-1214.

20. Herculano-Houzel, S., *The human brain in numbers: a linearly scaled-up primate brain.* Frontiers in Human Neuroscience, 2009. **3**.

21. Cragg, B.G., *The density of synapses and neurons in normal, mentally defective ageing human brains.* Brain, 1975. **98**(1): p. 81-90.

22. Gabbiani, F. and S.J. Cox, *CHAPTER 12 - Synaptic Transmission and Quantal Release*, in *Mathematics for Neuroscientists*, F. Gabbiani and S.J. Cox, Editors. 2010, Academic Press: London. p. 175-191.

23. Izadi, A., K. Ondek, A. Schedlbauer, I. Keselman, K. Shahlaie, and G. Gurkoff, *Clinically indicated electrical stimulation strategies to treat patients with medically refractory epilepsy.* Epilepsia Open, 2018. **3**(Suppl Suppl 2): p. 198-209.

24. Llinás, R.R., *The contribution of Santiago Ramón y Cajal to functional neuroscience.* Nat Rev Neurosci, 2003. **4**(1): p. 77-80.

25. Watkins, J.C. and D.E. Jane, *The glutamate story.* Br J Pharmacol, 2006. **147 Suppl 1**(Suppl 1): p. S100-8.

26. Spiering, M.J., *The discovery of GABA in the brain.* J Biol Chem, 2018. **293**(49): p. 19159-19160.

27. Childs, G., *History of Immunohistochemistry*. 2014. p. 3775-3796.

28. Molyneaux, B.J., P. Arlotta, J.R.L. Menezes, and J.D. Macklis, *Neuronal subtype specification in the cerebral cortex.* Nature Reviews Neuroscience, 2007. **8**(6): p. 427-437.

29. Mukamel, E.A. and J. Ngai, *Perspectives on defining cell types in the brain.* Curr Opin Neurobiol, 2019. **56**: p. 61-68.

30. Paulus, W., *Transcranial electrical stimulation (tES – tDCS; tRNS, tACS) methods.* Neuropsychological Rehabilitation, 2011. **21**(5): p. 602-617.

31. Siebner, H.R., *IS 26. Transcranial magnetic stimulation (TMS) and functional magnetic resonance imaging (fMRI).* Clinical Neurophysiology, 2013. **124**(10): p. e47.

32. Amon, A. and F. Alesch, *Systems for deep brain stimulation: review of technical features.* Journal of Neural Transmission, 2017. **124**(9): p. 1083-1091.

33. Joshi, J., M. Rubart, and W. Zhu, *Optogenetics: Background, Methodological Advances and Potential Applications for Cardiovascular Research and Medicine.* Frontiers in Bioengineering and Biotechnology, 2020. **7**.

34. Lozano, A.M., N. Lipsman, H. Bergman, P. Brown, S. Chabardes, J.W. Chang, K. Matthews, C.C. McIntyre, T.E. Schlaepfer, M. Schulder, Y. Temel, J. Volkmann, and J.K. Krauss, *Deep brain stimulation: current challenges and future directions.* Nature Reviews Neurology, 2019. **15**(3): p. 148-160.

35. Laitinen, L.V., A.T. Bergenheim, and M.I. Hariz, *Ventroposterolateral pallidotomy can abolish all parkinsonian symptoms.* Stereotact Funct Neurosurg, 1992. **58**(1-4): p. 14-21.

36. Anderson, V.C., K.J. Burchiel, P. Hogarth, J. Favre, and J.P. Hammerstad, *Pallidal vs subthalamic nucleus deep brain stimulation in Parkinson disease.* Arch Neurol, 2005. **62**(4): p. 554-60.

37. Au, K.L.K., J.K. Wong, T. Tsuboi, R.S. Eisinger, K. Moore, J. Lemos Melo Lobo Jofili Lopes, M.T. Holland, V.M. Holanda, Z. Peng-Chen, A. Patterson, K.D. Foote, A. Ramirez-Zamora, M.S. Okun, and L. Almeida, *Globus Pallidus Internus (GPi) Deep*

Brain Stimulation for Parkinson's Disease: Expert Review and Commentary. Neurol Ther, 2021. **10**(1): p. 7-30.

38. McIntyre, C.C., M. Savasta, L. Kerkerian-Le Goff, and J.L. Vitek, *Uncovering the mechanism(s) of action of deep brain stimulation: activation, inhibition, or both.* Clinical Neurophysiology, 2004. **115**(6): p. 1239-1248.

39. Chiken, S. and A. Nambu, *Mechanism of Deep Brain Stimulation: Inhibition, Excitation, or Disruption?* Neuroscientist, 2016. **22**(3): p. 313-22.

40. Dostrovsky, J.O. and A.M. Lozano, *Mechanisms of deep brain stimulation.* Mov Disord, 2002. **17 Suppl 3**: p. S63-8.

41. Basil, B., J. Mahmud, M. Mathews, C. Rodriguez, and B. Adetunji, *Is there evidence for effectiveness of transcranial magnetic stimulation in the treatment of psychiatric disorders?* Psychiatry (Edgmont), 2005. **2**(11): p. 64-9.

42. Deng, Z.D., S.H. Lisanby, and A.V. Peterchev, *Coil design considerations for deep transcranial magnetic stimulation.* Clin Neurophysiol, 2014. **125**(6): p. 1202-12.

43. Harel, E.V., L. Rabany, L. Deutsch, Y. Bloch, A. Zangen, and Y. Levkovitz, *H-coil repetitive transcranial magnetic stimulation for treatment resistant major depressive disorder: An 18-week continuation safety and feasibility study.* World J Biol Psychiatry, 2014. **15**(4): p. 298-306.

44. Zibman, S., G.S. Pell, N. Barnea-Ygael, Y. Roth, and A. Zangen, *Application of transcranial magnetic stimulation for major depression: Coil design and neuroanatomical variability considerations.* European Neuropsychopharmacology, 2021. **45**: p. 73-88.

45. Rossi, S., A. Antal, S. Bestmann, M. Bikson, C. Brewer, J. Brockmöller, L.L. Carpenter, M. Cincotta, R. Chen, J.D. Daskalakis, V. Di Lazzaro, M.D. Fox, M.S. George, D. Gilbert, V.K. Kimiskidis, G. Koch, R.J. Ilmoniemi, J.P. Lefaucheur, L. Leocani, S.H. Lisanby, C. Miniussi, F. Padberg, A. Pascual-Leone, W. Paulus, A.V. Peterchev, A. Quartarone, A. Rotenberg, J. Rothwell, P.M. Rossini, E. Santarnecchi, M.M. Shafi, H.R. Siebner, Y. Ugawa, E.M. Wassermann, A. Zangen, U. Ziemann, and M. Hallett, *Safety and recommendations for TMS use in healthy subjects and patient populations, with updates on training, ethical and regulatory issues: Expert Guidelines.* Clin Neurophysiol, 2021. **132**(1): p. 269-306.

46. Chervyakov, A.V., A.Y. Chernyavsky, D.O. Sinitsyn, and M.A. Piradov, *Possible Mechanisms Underlying the Therapeutic Effects of Transcranial Magnetic Stimulation.* Front Hum Neurosci, 2015. **9**: p. 303.

47. Klomjai, W., R. Katz, and A. Lackmy-Vallée, *Basic principles of transcranial magnetic stimulation (TMS) and repetitive TMS (rTMS).* Ann Phys Rehabil Med, 2015. **58**(4): p. 208-213.

48. Zhou, S. and Y. Yu, *Synaptic E-I Balance Underlies Efficient Neural Coding.* Frontiers in Neuroscience, 2018. **12**.

49. English, D.F., S. McKenzie, T. Evans, K. Kim, E. Yoon, and G. Buzsáki, *Pyramidal Cell-Interneuron Circuit Architecture and Dynamics in Hippocampal Networks.* Neuron, 2017. **96**(2): p. 505-520.e7.

50. Luan, S., I. Williams, K. Nikolic, and T.G. Constandinou, *Neuromodulation: present and emerging methods.* Front Neuroeng, 2014. **7**: p. 27.

51. Boyden, E.S., F. Zhang, E. Bamberg, G. Nagel, and K. Deisseroth, *Millisecond-timescale, genetically targeted optical control of neural activity.* Nat Neurosci, 2005. **8**(9): p. 1263-8.

52. Mager, T., D. Lopez de la Morena, V. Senn, J. Schlotte, A. D´Errico, K. Feldbauer, C. Wrobel, S. Jung, K. Bodensiek, V. Rankovic, L. Browne, A. Huet, J. Jüttner, P.G. Wood, J.J. Letzkus, T. Moser, and E. Bamberg, *High frequency neural spiking and auditory signaling by ultrafast red-shifted optogenetics.* Nature Communications, 2018. **9**(1): p. 1750.

53. Savanthrapadian, S., T. Meyer, C. Elgueta, S.A. Booker, I. Vida, and M. Bartos, *Synaptic properties of SOM- and CCK-expressing cells in dentate gyrus interneuron networks.* J Neurosci, 2014. **34**(24): p. 8197-209.

54. Gunaydin, L.A., O. Yizhar, A. Berndt, V.S. Sohal, K. Deisseroth, and P. Hegemann, *Ultrafast optogenetic control.* Nat Neurosci, 2010. **13**(3): p. 387-92.

55. Shemesh, O.A., D. Tanese, V. Zampini, C. Linghu, K. Piatkevich, E. Ronzitti, E. Papagiakoumou, E.S. Boyden, and V. Emiliani, *Temporally precise single-cell-resolution optogenetics.* Nature Neuroscience, 2017. **20**(12): p. 1796-1806.

56. Menegas, W., K. Akiti, R. Amo, N. Uchida, and M. Watabe-Uchida, *Dopamine neurons projecting to the posterior striatum reinforce avoidance of threatening stimuli.* Nature Neuroscience, 2018. **21**(10): p. 1421-1430.

57. Jayaprakash, N., Z. Wang, B. Hoeynck, N. Krueger, A. Kramer, E. Balle, D.S. Wheeler, R.A. Wheeler, and M.G. Blackmore, *Optogenetic Interrogation of Functional Synapse Formation by Corticospinal Tract Axons in the Injured Spinal Cord.* J Neurosci, 2016. **36**(21): p. 5877-90.

58. Hamada, S., M. Nagase, T. Yoshizawa, A. Hagiwara, Y. Isomura, A.M. Watabe, and T. Ohtsuka, *An engineered channelrhodopsin optimized for axon terminal activation and circuit mapping.* Communications Biology, 2021. **4**(1): p. 461.

59. Zell, V., T. Steinkellner, N.G. Hollon, S.M. Warlow, E. Souter, L. Faget, A.C. Hunker, X. Jin, L.S. Zweifel, and T.S. Hnasko, *VTA Glutamate Neuron Activity Drives Positive Reinforcement Absent Dopamine Co-release.* Neuron, 2020. **107**(5): p. 864-873.e4.

60. Flytzanis, N.C., C.N. Bedbrook, H. Chiu, M.K. Engqvist, C. Xiao, K.Y. Chan, P.W. Sternberg, F.H. Arnold, and V. Gradinaru, *Archaerhodopsin variants with enhanced voltage-sensitive fluorescence in mammalian and Caenorhabditis elegans neurons.* Nat Commun, 2014. **5**: p. 4894.

61. Zhang, C., S. Yang, T. Flossmann, S. Gao, O.W. Witte, G. Nagel, K. Holthoff, and K. Kirmse, *Optimized photo-stimulation of halorhodopsin for long-term neuronal inhibition.* BMC Biology, 2019. **17**(1): p. 95.

62. Chen, S.X., A.N. Kim, A.J. Peters, and T. Komiyama, *Subtype-specific plasticity of inhibitory circuits in motor cortex during motor learning.* Nature neuroscience, 2015. **18**(8): p. 1109-1115.

63. Senova, S., I. Scisniak, C.-C. Chiang, I. Doignon, S. Palfi, A. Chaillet, C. Martin, and F. Pain, *Experimental assessment of the safety and potential efficacy of high irradiance photostimulation of brain tissues.* Scientific Reports, 2017. **7**(1): p. 43997.

64. Tyssowski, K.M. and J.M. Gray, *Blue Light Increases Neuronal Activity-Regulated Gene Expression in the Absence of Optogenetic Proteins.* eNeuro, 2019. **6**(5).

65. *An historical account of pharmacology to the twentieth century.* Medical History, 1977. **21**(3): p. 329-329.

66. Coward, P., H.G. Wada, M.S. Falk, S.D. Chan, F. Meng, H. Akil, and B.R. Conklin, *Controlling signaling with a specifically designed Gi-coupled receptor.* Proc Natl Acad Sci U S A, 1998. **95**(1): p. 352-7.

67. Strader, C.D., T. Gaffney, E.E. Sugg, M.R. Candelore, R. Keys, A.A. Patchett, and R.A. Dixon, *Allele-specific activation of genetically engineered receptors.* J Biol Chem, 1991. **266**(1): p. 5-8.

68. Sweger, E.J., K.B. Casper, K. Scearce-Levie, B.R. Conklin, and K.D. McCarthy, *Development of hydrocephalus in mice expressing the G(i)-coupled GPCR Ro1 RASSL receptor in astrocytes.* J Neurosci, 2007. **27**(9): p. 2309-17.

69. Wang, Y., P. Xue, M. Cao, T. Yu, S.T. Lane, and H. Zhao, *Directed Evolution: Methodologies and Applications.* Chemical Reviews, 2021. **121**(20): p. 12384-12444.

70. Dong, S., S.C. Rogan, and B.L. Roth, *Directed molecular evolution of DREADDs: a generic approach to creating next-generation RASSLs.* Nat Protoc, 2010. **5**(3): p. 561-73.

71. Pei, Y., S.C. Rogan, F. Yan, and B.L. Roth, *Engineered GPCRs as tools to modulate signal transduction.* Physiology (Bethesda), 2008. **23**: p. 313-21.

72. Armbruster, B.N., X. Li, M.H. Pausch, S. Herlitze, and B.L. Roth, *Evolving the lock to fit the key to create a family of G protein-coupled receptors potently activated by an inert ligand.* Proc Natl Acad Sci U S A, 2007. **104**(12): p. 5163-8.

73. Wang, W., B. Rein, F. Zhang, T. Tan, P. Zhong, L. Qin, and Z. Yan, *Chemogenetic Activation of Prefrontal Cortex Rescues Synaptic and Behavioral Deficits in a Mouse Model of 16p11.2 Deletion Syndrome.* The Journal of Neuroscience, 2018. **38**(26): p. 5939.

74. Kakava-Georgiadou, N., M.M. Zwartkruis, C. Bullich-Vilarrubias, M.C.M. Luijendijk, K.M. Garner, G. van der Plasse, and R.A.H. Adan, *An Intersectional Approach to Target Neural Circuits With Cell- and Projection-Type Specificity: Validation in the Mesolimbic Dopamine System.* Frontiers in Molecular Neuroscience, 2019. **12**.

75. Alexander, G.M., S.C. Rogan, A.I. Abbas, B.N. Armbruster, Y. Pei, J.A. Allen, R.J. Nonneman, J. Hartmann, S.S. Moy, M.A. Nicolelis, J.O. McNamara, and B.L. Roth, *Remote control of neuronal activity in transgenic mice expressing evolved G protein-coupled receptors.* Neuron, 2009. **63**(1): p. 27-39.

76. Smith, K.S., D.J. Bucci, B.W. Luikart, and S.V. Mahler, *DREADDS: Use and application in behavioral neuroscience.* Behav Neurosci, 2016. **130**(2): p. 137-55.

77. MacLaren, D.A., R.W. Browne, J.K. Shaw, S. Krishnan Radhakrishnan, P. Khare, R.A. España, and S.D. Clark, *Clozapine N-Oxide Administration Produces Behavioral Effects in Long-Evans Rats: Implications for Designing DREADD Experiments.* eNeuro, 2016. **3**(5).

78. Martinez, V.K., F. Saldana-Morales, J.J. Sun, P.J. Zhu, M. Costa-Mattioli, and R.S. Ray, *Off-Target Effects of Clozapine-N-Oxide on the Chemosensory Reflex Are Masked by High Stress Levels.* Frontiers in Physiology, 2019. **10**.

79. Inc, E. *Ultrasound in medicine and biology*. 2022; Available from: https://www.umbjournal.org/.

80. Grinnell, A.D., *Early milestones in the understanding of echolocation in bats.* J Comp Physiol A Neuroethol Sens Neural Behav Physiol, 2018. **204**(6): p. 519-536.

81. Kellog, W.N., *Ultrasonic hearing in the porpoise, Tursiops truncatus.* J Comp Physiol Psychol, 1953. **46**(6): p. 446-50.

82. Maloney, S.E., K.C. Chandler, C. Anastasaki, M.A. Rieger, D.H. Gutmann, and J.D. Dougherty, *Characterization of early communicative behavior in mouse models of neurofibromatosis type 1.* Autism Res, 2018. **11**(1): p. 44-58.

83. Curie, P. and J. Curie, *Développement par compression de l'électricité polaire dans les cristaux hémièdres à faces inclinées.* Bulletin de Minéralogie, 1880: p. 90-93.

84. Lippmann, G., *Principe de la conservation de l'électricité, ou second principe de la théorie des phénomènes électriques.* Journal de Physique Théorique et Appliquée, 1881. **10**(1): p. 381-394.

85. Curie, J. and P. Curie, *Contractions et dilatations produites par des tensions électriques dans les cristaux hémièdres à faces inclinées.* Compt. Rend, 1881. **93**: p. 1137-1140.

86. Serway, R.A. and R.J. Beichner, *Physics for Scientists and Engineers: Volume 1 Chapters 1-22*. 1999: Harcourt.

87. Duck, F.A., *Chapter 4 - Acoustic Properties of Tissue at Ultrasonic Frequencies*, in *Physical Properties of Tissues*, F.A. Duck, Editor. 1990, Academic Press: London. p. 73-135.

88. Connor, C.W., G.T. Clement, and K. Hynynen, *A unified model for the speed of sound in cranial bone based on genetic algorithm optimization.* Physics in Medicine and Biology, 2002. **47**(22): p. 3925-3944.

89. Lucas, V.S., R.S. Burk, S. Creehan, and M.J. Grap, *Utility of high-frequency ultrasound: moving beyond the surface to detect changes in skin integrity.* Plast Surg Nurs, 2014. **34**(1): p. 34-8.

90. Wells, P.N.T., *Absorption and dispersion of ultrasound in biological tissue.* Ultrasound in Medicine & Biology, 1975. **1**(4): p. 369-376.

91. Haar, G.t., *Ultrasonic imaging: safety considerations*. Interface Focus, 2011. **1**(4): p. 686-697.

92. Santoro, M.G., *Heat shock factors and the control of the stress response.* Biochemical Pharmacology, 2000. **59**(1): p. 55-63.

93. Gu, Z.T., H. Wang, L. Li, Y.S. Liu, X.B. Deng, S.F. Huo, F.F. Yuan, Z.F. Liu, H.S. Tong, and L. Su, *Heat stress induces apoptosis through transcription-independent p53-mediated mitochondrial pathways in human umbilical vein endothelial cell.* Sci Rep, 2014. **4**: p. 4469.

94. Ziskin, M.C. and J. Morrissey, *Thermal thresholds for teratogenicity, reproduction, and development.* International Journal of Hyperthermia, 2011. **27**(4): p. 374-387.

95. Duck, F.A., *Physical properties of tissues: a comprehensive reference book*. 2013: Academic press.

96. Starritt, H.C. and F.A. Duck, *CHAPTER 4 - Safety*, in *Clinical Ultrasound (Third Edition)*, P.L. Allan, G.M. Baxter, and M.J. Weston, Editors. 2011, Churchill Livingstone: Edinburgh. p. 51-60.

97. Starritt, H.C. and F.A. Duck, *4CHAPTER.* Clinical Ultrasound, 2-Volume Set E-Book: Expert Consult: Online and Print, 2011. **2**: p. 51.

98. Ashokkumar, M., *The characterization of acoustic cavitation bubbles – An overview.* Ultrasonics Sonochemistry, 2011. **18**(4): p. 864-872.

99. Tung, Y.S., F. Vlachos, J.A. Feshitan, M.A. Borden, and E.E. Konofagou, *The mechanism of interaction between focused ultrasound and microbubbles in blood-brain barrier opening in mice.* J Acoust Soc Am, 2011. **130**(5): p. 3059-67.

100. Fan, Z., R.E. Kumon, and C.X. Deng, *Mechanisms of microbubble-facilitated sonoporation for drug and gene delivery.* Ther Deliv, 2014. **5**(4): p. 467-86.

101. Nyborg, W.L., *Ultrasonic microstreaming and related phenomena.* Br J Cancer Suppl, 1982. **5**: p. 156-60.

102. Loch, E.G., A.B. Fischer, and E. Kuwert, *Effect of diagnostic and therapeutic intensities of ultrasonics on normal and malignant human cells in vitro.* American Journal of Obstetrics and Gynecology, 1971. **110**(4): p. 457-460.

103. Webster, D.F., J.B. Pond, M. Dyson, and W. Harvey, *The role of cavitation in the in vitro stimulation of protein synthesis in human fibroblasts by ultrasound.* Ultrasound in Medicine & Biology, 1978. **4**(4): p. 343-351.

104. Johns, L.D., *Nonthermal effects of therapeutic ultrasound: the frequency resonance hypothesis.* J Athl Train, 2002. **37**(3): p. 293-9.

105. Szabo, T.L., *Diagnostic ultrasound imaging: inside out*. 2004: Academic press.

106. Şen, T., O. Tüfekçioğlu, and Y. Koza, *Mechanical index.* Anatol J Cardiol, 2015. **15**(4): p. 334-6.

107. Apfel, R.E. and C.K. Holland, *Gauging the likelihood of cavitation from short-pulse, low-duty cycle diagnostic ultrasound.* Ultrasound in Medicine & Biology, 1991. **17**(2): p. 179-185.

108. Schneider-Kolsky, M.E., Z. Ayobi, P. Lombardo, D. Brown, B. Kedang, and M.E. Gibbs, *Ultrasound exposure of the foetal chick brain: effects on learning and memory.* International Journal of Developmental Neuroscience, 2009. **27**(7): p. 677-683.

109. Medicine, A.I.o.U.i., *Who's Afraid of a Hundred Milliwatts per Square Centimeter (100 mW/cm2, SPTA).* Laurel, MD: American Institute of Ultrasound in Medicine, 1978.

110. Abramowicz, J.S., *Benefits and risks of ultrasound in pregnancy.* Seminars in Perinatology, 2013. **37**(5): p. 295-300.

111. Carovac, A., F. Smajlovic, and D. Junuzovic, *Application of ultrasound in medicine.* Acta Inform Med, 2011. **19**(3): p. 168-71.

112. Hewick, S.A., A.C. Fairhead, J.C. Culy, and H.R. Atta, *A comparison of 10 MHz and 20 MHz ultrasound probes in imaging the eye and orbit.* Br J Ophthalmol, 2004. **88**(4): p. 551-5.

113. Jacobson, J.A., S. Lancaster, A. Prasad, M.T. van Holsbeeck, J.G. Craig, and P. Kolowich, *Full-thickness and partial-thickness supraspinatus tendon tears: value of US signs in diagnosis.* Radiology, 2004. **230**(1): p. 234-42.

114. Syrop, I., Y. Fukushima, K. Mullins, S. Raiser, R. Lawley, L. Bosshardt, A. Finlay, J. Ray, and M. Fredericson, *Comparison of Ultrasonography to MRI in the Diagnosis of Lower Extremity Bone Stress Injuries.* Journal of Ultrasound in Medicine, 2022. **n/a**(n/a).

115. Hung, E.H., J.F. Griffith, A.W. Ng, R.K. Lee, D.T. Lau, and J.C. Leung, *Ultrasound of musculoskeletal soft-tissue tumors superficial to the investing fascia.* AJR Am J Roentgenol, 2014. **202**(6): p. W532-40.

116. Leighton, T.G. and R.O. Cleveland, *Lithotripsy.* Proc Inst Mech Eng H, 2010. **224**(2): p. 317-42.

117. Zhou, Y.F., *High intensity focused ultrasound in clinical tumor ablation.* World J Clin Oncol, 2011. **2**(1): p. 8-27.

118. Cosgrove, D., *Ultrasound contrast agents: An overview.* European Journal of Radiology, 2006. **60**(3): p. 324-330.

119. Harvey, E.N., *THE EFFECT OF HIGH FREQUENCY SOUND WAVES ON HEART MUSCLE AND OTHER IRRITABLE TISSUES.* American Journal of Physiology-Legacy Content, 1929. **91**(1): p. 284-290.

120. Harvey, E.N., E.B. Harvey, and A.L. Loomis, *Further Observations on the Effect of High Frequency Sound Waves on Living Matter.* Biological Bulletin, 1928. **55**(6): p. 459-469.

121. Fry, W.J., V.J. Wulff, D. Tucker, and F.J. Fry, *Physical Factors Involved in Ultrasonically Induced Changes in Living Systems: I. Identification of Non-Temperature Effects.* The Journal of the Acoustical Society of America, 1950. **22**(6): p. 867-876.

122. Young, R.R. and E. Henneman, *Functional effects of focused ultrasound on mammalian nerves.* Science, 1961. **134**(3489): p. 1521-2.

123. Fry, W.J., *Intense ultrasound; a new tool for neurological research.* J Ment Sci, 1954. **100**(418): p. 85-96.

124. Fry, W.J., *Ultrasound in neurology.* Neurology, 1956. **6**(10): p. 693-704.

125. Fry, W.J., *Use of intense ultrasound in neurological research.* Am J Phys Med, 1958. **37**(3): p. 143-7.

126. Foster, K.R. and M.L. Wiederhold, *Auditory responses in cats produced by pulsed ultrasound.* J Acoust Soc Am, 1978. **63**(4): p. 1199-205.

127. Rinaldi, P.C., J.P. Jones, F. Reines, and L.R. Price, *Modification by focused ultrasound pulses of electrically evoked responses from an in vitro hippocampal preparation.* Brain Res, 1991. **558**(1): p. 36-42.

128. Bachtold, M.R., P.C. Rinaldi, J.P. Jones, F. Reines, and L.R. Price, *Focused ultrasound modifications of neural circuit activity in a mammalian brain.* Ultrasound Med Biol, 1998. **24**(4): p. 557-65.

129. Tyler, W.J., Y. Tufail, M. Finsterwald, M.L. Tauchmann, E.J. Olson, and C. Majestic, *Remote excitation of neuronal circuits using low-intensity, low-frequency ultrasound.* PLoS One, 2008. **3**(10): p. e3511.

130. Tufail, Y., A. Matyushov, N. Baldwin, M.L. Tauchmann, J. Georges, A. Yoshihiro, S.I.H. Tillery, and W.J. Tyler, *Transcranial Pulsed Ultrasound Stimulates Intact Brain Circuits.* Neuron, 2010. **66**(5): p. 681-694.

131. King, R.L., J.R. Brown, W.T. Newsome, and K.B. Pauly, *Effective parameters for ultrasound-induced in vivo neurostimulation.* Ultrasound Med Biol, 2013. **39**(2): p. 312-31.

132. Ye, P.P., J.R. Brown, and K.B. Pauly, *Frequency Dependence of Ultrasound Neurostimulation in the Mouse Brain.* Ultrasound Med Biol, 2016. **42**(7): p. 1512-30.

133. Legon, W., A. Rowlands, A. Opitz, T.F. Sato, and W.J. Tyler, *Pulsed ultrasound differentially stimulates somatosensory circuits in humans as indicated by EEG and FMRI.* PLoS One, 2012. **7**(12): p. e51177.

134. Lee, W., H. Kim, S. Lee, S.-S. Yoo, and Y.A. Chung, *Creation of various skin sensations using pulsed focused ultrasound: Evidence for functional neuromodulation.* International Journal of Imaging Systems and Technology, 2014. **24**(2): p. 167-174.

135. Legon, W., L. Ai, P. Bansal, and J.K. Mueller, *Neuromodulation with single-element transcranial focused ultrasound in human thalamus.* Human Brain Mapping, 2018. **39**(5): p. 1995-2006.

136. Legon, W., P. Bansal, R. Tyshynsky, L. Ai, and J.K. Mueller, *Transcranial focused ultrasound neuromodulation of the human primary motor cortex.* Scientific Reports, 2018. **8**(1): p. 10007.

137. Pasquinelli, C., L.G. Hanson, H.R. Siebner, H.J. Lee, and A. Thielscher, *Safety of transcranial focused ultrasound stimulation: A systematic review of the state of knowledge from both human and animal studies.* Brain Stimul, 2019. **12**(6): p. 1367-1380.

138. Buzatu, S., *The temperature-induced changes in membrane potential.* Riv Biol, 2009. **102**(2): p. 199-217.

139. Wang, Y., W. Wang, Z. Li, S. Hao, and B. Wang, *A novel perspective on neuron study: damaging and promoting effects in different neurons induced by mechanical stress.* Biomech Model Mechanobiol, 2016. **15**(5): p. 1019-27.

140. Nyborg, W.L. and R.B. Steele, *Temperature elevation in a beam of ultrasound.* Ultrasound in Medicine & Biology, 1983. **9**(6): p. 611-620.

141. Borrelli, M.J., K.I. Bailey, and F. Dunn, *Early ultrasonic effects upon mammalian CNS structures (chemical synapses).* J Acoust Soc Am, 1981. **69**(5): p. 1514-6.

142. Prieto, M.L., O. Ömer, B.T. Khuri-Yakub, and M.C. Maduke, *Dynamic response of model lipid membranes to ultrasonic radiation force.* PLoS One, 2013. **8**(10): p. e77115.

143. Vasan, A., J. Orosco, U. Magaram, M. Duque, C. Weiss, Y. Tufail, S.H. Chalasani, and J. Friend, *Ultrasound Mediated Cellular Deflection Results in Cellular Depolarization.* Adv Sci (Weinh), 2022. **9**(2): p. e2101950.

144. Guo, H., M. Hamilton, S.J. Offutt, C.D. Gloeckner, T. Li, Y. Kim, W. Legon, J.K. Alford, and H.H. Lim, *Ultrasound Produces Extensive Brain Activation via a Cochlear Pathway.* Neuron, 2018. **98**(5): p. 1020-1030.e4.

145. Sato, T., M.G. Shapiro, and D.Y. Tsao, *Ultrasonic Neuromodulation Causes Widespread Cortical Activation via an Indirect Auditory Mechanism.* Neuron, 2018. **98**(5): p. 1031-1041.e5.

146. Haswell, E.S., R. Phillips, and D.C. Rees, *Mechanosensitive channels: what can they do and how do they do it?* Structure, 2011. **19**(10): p. 1356-69.

147. Liu, H., J. Hu, Q. Zheng, X. Feng, F. Zhan, X. Wang, G. Xu, and F. Hua, *Piezo1 Channels as Force Sensors in Mechanical Force-Related Chronic Inflammation.* Front Immunol, 2022. **13**: p. 816149.

148. Zhao, Q., H. Zhou, S. Chi, Y. Wang, J. Wang, J. Geng, K. Wu, W. Liu, T. Zhang, M.Q. Dong, J. Wang, X. Li, and B. Xiao, *Structure and mechanogating mechanism of the Piezo1 channel.* Nature, 2018. **554**(7693): p. 487-492.

149. Saotome, K., S.E. Murthy, J.M. Kefauver, T. Whitwam, A. Patapoutian, and A.B. Ward, *Structure of the mechanically activated ion channel Piezo1.* Nature, 2018. **554**(7693): p. 481-486.

150. Martinac, B., M. Buechner, A.H. Delcour, J. Adler, and C. Kung, *Pressure-sensitive ion channel in Escherichia coli.* Proc Natl Acad Sci U S A, 1987. **84**(8): p. 2297-301.

151. Sukharev, S.I., P. Blount, B. Martinac, F.R. Blattner, and C. Kung, *A large-conductance mechanosensitive channel in E. coli encoded by mscL alone.* Nature, 1994. **368**(6468): p. 265-8.

152. Sukharev, S.I., B. Martinac, V.Y. Arshavsky, and C. Kung, *Two types of mechanosensitive channels in the Escherichia coli cell envelope: solubilization and functional reconstitution.* Biophys J, 1993. **65**(1): p. 177-83.

153. Walker, R.G., A.T. Willingham, and C.S. Zuker, *A Drosophila mechanosensory transduction channel.* Science, 2000. **287**(5461): p. 2229-34.

154. Zhang, W., L.E. Cheng, M. Kittelmann, J. Li, M. Petkovic, T. Cheng, P. Jin, Z. Guo, M.C. Göpfert, L.Y. Jan, and Y.N. Jan, *Ankyrin Repeats Convey Force to Gate the NOMPC Mechanotransduction Channel.* Cell, 2015. **162**(6): p. 1391-403.

155. Kang, L., J. Gao, W.R. Schafer, Z. Xie, and X.Z. Xu, *C. elegans TRP family protein TRP-4 is a pore-forming subunit of a native mechanotransduction channel.* Neuron, 2010. **67**(3): p. 381-91.

156. Morris, C.E., *Voltage-gated channel mechanosensitivity: fact or friction?* Front Physiol, 2011. **2**: p. 25.

157. Schmidt, D., J. del Mármol, and R. MacKinnon, *Mechanistic basis for low threshold mechanosensitivity in voltage-dependent K+ channels.* Proceedings of the National Academy of Sciences, 2012. **109**(26): p. 10352-10357.

158. Administration, U.S.F.D. *Ultrasound Imaging*. 2020 09/28/2020 [cited 2022; Available from: https://www.fda.gov/radiation-emitting-products/medical-imaging/ultrasound-imaging#facilities.

159. Clement, G.T. and K. Hynynen, *A non-invasive method for focusing ultrasound through the human skull.* Phys Med Biol, 2002. **47**(8): p. 1219-36.

160. Kim, S., Y. Jo, G. Kook, C. Pasquinelli, H. Kim, K. Kim, H.-S. Hoe, Y. Choe, H. Rhim, A. Thielscher, J. Kim, and H.J. Lee, *Transcranial focused ultrasound stimulation with high spatial resolution.* Brain Stimulation, 2021. **14**(2): p. 290-300.

161. Faria, P., M. Hallett, and P.C. Miranda, *A finite element analysis of the effect of electrode area and inter-electrode distance on the spatial distribution of the current density in tDCS.* J Neural Eng, 2011. **8**(6): p. 066017.

162. Deng, Z.D., S.H. Lisanby, and A.V. Peterchev, *Electric field depth-focality tradeoff in transcranial magnetic stimulation: simulation comparison of 50 coil designs.* Brain Stimul, 2013. **6**(1): p. 1-13.

163. Schüz, A. and G. Palm, *Density of neurons and synapses in the cerebral cortex of the mouse.* Journal of Comparative Neurology, 1989. **286**(4): p. 442-455.

164. Hoffman Benjamin, U., Y. Baba, A. Lee Stephen, C.-K. Tong, E. Konofagou Elisa, and A. Lumpkin Ellen, *Focused ultrasound excites action potentials in mammalian peripheral neurons in part through the mechanically gated ion channel PIEZO2.* Proceedings of the National Academy of Sciences, 2022. **119**(21): p. e2115821119.

165. Legon, W., T.F. Sato, A. Opitz, J. Mueller, A. Barbour, A. Williams, and W.J. Tyler, *Transcranial focused ultrasound modulates the activity of primary somatosensory cortex in humans.* Nat Neurosci, 2014. **17**(2): p. 322-9.

166. Legon, W., P. Bansal, R. Tyshynsky, L. Ai, and J.K. Mueller, *Transcranial focused ultrasound neuromodulation of the human primary motor cortex.* Sci Rep, 2018. **8**(1): p. 10007.

167. Tufail, Y., A. Matyushov, N. Baldwin, M.L. Tauchmann, J. Georges, A. Yoshihiro, S.I. Tillery, and W.J. Tyler, *Transcranial pulsed ultrasound stimulates intact brain circuits.* Neuron, 2010. **66**(5): p. 681-94.

168. Yoo, S.-S., A. Bystritsky, J.-H. Lee, Y. Zhang, K. Fischer, B.-K. Min, N.J. McDannold, A. Pascual-Leone, and F.A. Jolesz, *Focused ultrasound modulates region-specific brain activity.* Neuroimage, 2011. **56**(3): p. 1267-1275.

169. Kim, H., S.J. Taghados, K. Fischer, L.-S. Maeng, S. Park, and S.-S. Yoo, *Noninvasive transcranial stimulation of rat abducens nerve by focused ultrasound.* Ultrasound in medicine & biology, 2012. **38**(9): p. 1568-1575.

170. Downs, M.E., S.A. Lee, G. Yang, S. Kim, Q. Wang, and E.E. Konofagou, *Non-invasive peripheral nerve stimulation via focused ultrasound in vivo.* Physics in Medicine & Biology, 2018. **63**(3): p. 035011.

171. Fry, F., H. Ades, and W. Fry, *Production of reversible changes in the central nervous system by ultrasound.* Science, 1958. **127**(3289): p. 83-84.

172. Kim, H., M.Y. Park, S.D. Lee, W. Lee, A. Chiu, and S.-S. Yoo, *Suppression of EEG visual-evoked potentials in rats via neuromodulatory focused ultrasound.* Neuroreport, 2015. **26**(4): p. 211.

173. Collins, M.N. and K.A. Mesce, *Focused Ultrasound Neuromodulation and the Confounds of Intracellular Electrophysiological Investigation.* eneuro, 2020. **7**(4): p. ENEURO.0213-20.2020.

174. Darrow, D.P., P. O'Brien, T.J. Richner, T.I. Netoff, and E.S. Ebbini, *Reversible neuroinhibition by focused ultrasound is mediated by a thermal mechanism.* Brain stimulation, 2019. **12**(6): p. 1439-1447.

175. Lele, P., *Effects of focused ultrasonic radiation on peripheral nerve, with observations on local heating.* Experimental Neurology, 1963. **8**(1): p. 47-83.

176. Colucci, V., G. Strichartz, F. Jolesz, N. Vykhodtseva, and K. Hynynen, *Focused ultrasound effects on nerve action potential in vitro.* Ultrasound in medicine & biology, 2009. **35**(10): p. 1737-1747.

177. Plaksin, M., S. Shoham, and E. Kimmel, *Intramembrane cavitation as a predictive bio-piezoelectric mechanism for ultrasonic brain stimulation.* Physical review X, 2014. **4**(1): p. 011004.

178. Menz, M.D., P. Ye, K. Firouzi, A. Nikoozadeh, K.B. Pauly, P. Khuri-Yakub, and S.A. Baccus, *Radiation force as a physical mechanism for ultrasonic neurostimulation of the ex vivo retina.* Journal of Neuroscience, 2019. **39**(32): p. 6251-6264.

179. Wright, C.J., S.R. Haqshenas, J. Rothwell, and N. Saffari, *Unmyelinated peripheral nerves can be stimulated in vitro using pulsed ultrasound.* Ultrasound in medicine & biology, 2017. **43**(10): p. 2269-2283.

180. Bachtold, M.R., P.C. Rinaldi, J.P. Jones, F. Reines, and L.R. Price, *Focused ultrasound modifications of neural circuit activity in a mammalian brain.* Ultrasound in medicine & biology, 1998. **24**(4): p. 557-565.

181. Oh, S.J., J.M. Lee, H.B. Kim, J. Lee, S. Han, J.Y. Bae, G.S. Hong, W. Koh, J. Kwon, E.S. Hwang, D.H. Woo, I. Youn, I.J. Cho, Y.C. Bae, S. Lee, J.W. Shim, J.H. Park, and C.J. Lee, *Ultrasonic Neuromodulation via Astrocytic TRPA1.* Curr Biol, 2019. **29**(20): p. 3386-3401 e8.

182. Sato, T., M.G. Shapiro, and D.Y. Tsao, *Ultrasonic Neuromodulation Causes Widespread Cortical Activation via an Indirect Auditory Mechanism.* Neuron, 2018. **98**(5): p. 1031-1041 e5.

183. Guo, H., M. Hamilton, 2nd, S.J. Offutt, C.D. Gloeckner, T. Li, Y. Kim, W. Legon, J.K. Alford, and H.H. Lim, *Ultrasound Produces Extensive Brain Activation via a Cochlear Pathway.* Neuron, 2018. **98**(5): p. 1020-1030 e4.

184. Ibsen, S., A. Tong, C. Schutt, S. Esener, and S.H. Chalasani, *Sonogenetics is a non-invasive approach to activating neurons in Caenorhabditis elegans.* Nat Commun, 2015. **6**: p. 8264.

185. Kubanek, J., P. Shukla, A. Das, S.A. Baccus, and M.B. Goodman, *Ultrasound Elicits Behavioral Responses through Mechanical Effects on Neurons and Ion Channels in a Simple Nervous System.* J Neurosci, 2018. **38**(12): p. 3081-3091.

186. Yoo, S.H., P. Croce, R.W. Margolin, S.D. Lee, and W. Lee, *Pulsed focused ultrasound changes nerve conduction of earthworm giant axonal fibers.* Neuroreport, 2017. **28**(4): p. 229-233.

187. Yoo, S., D.R. Mittelstein, R.C. Hurt, J.J. Lacroix, and M.G. Shapiro, *Focused ultrasound excites neurons via mechanosensitive calcium accumulation and ion channel amplification.* bioRxiv, 2020.

188. Qiu, Z., J. Guo, S. Kala, J. Zhu, Q. Xian, W. Qiu, G. Li, T. Zhu, L. Meng, R. Zhang, H.C. Chan, H. Zheng, and L. Sun, *The Mechanosensitive Ion Channel Piezo1 Significantly Mediates In Vitro Ultrasonic Stimulation of Neurons.* iScience, 2019. **21**: p. 448-457.

189. Prieto, M.L., K. Firouzi, B.T. Khuri-Yakub, and M. Maduke, *Activation of Piezo1 but Not NaV1.2 Channels by Ultrasound at 43 MHz.* Ultrasound Med Biol, 2018. **44**(6): p. 1217-1232.

190. White, J.G., E. Southgate, J.N. Thomson, and S. Brenner, *The structure of the nervous system of the nematode Caenorhabditis elegans.* Philos Trans R Soc Lond B Biol Sci, 1986. **314**(1165): p. 1-340.

191. Varshney, L.R., B.L. Chen, E. Paniagua, D.H. Hall, and D.B. Chklovskii, *Structural properties of the Caenorhabditis elegans neuronal network.* PLoS Comput Biol, 2011. **7**(2): p. e1001066.

192. de Bono, M. and A.V. Maricq, *Neuronal substrates of complex behaviors in C. elegans.* Annu Rev Neurosci, 2005. **28**: p. 451-501.

193. Li, W., Z. Feng, P.W. Sternberg, and X.Z. Xu, *A C. elegans stretch receptor neuron revealed by a mechanosensitive TRP channel homologue.* Nature, 2006. **440**(7084): p. 684-7.

194. Beard, P.C., A.M. Hurrell, and T.N. Mills, *Characterization of a polymer film optical fiber hydrophone for use in the range 1 to 20 MHz: A comparison with PVDF needle and membrane hydrophones.* IEEE Transactions on ultrasonics, ferroelectrics, and frequency control, 2000. **47**(1): p. 256-264.

195. ; Available from: https://www.acoustics.co.uk/wp-content/uploads/2022/03/Fibre-Optic-Hydrophone-System-V2-FOHSV2-TDS-V1-0222.pdf.

196. Gray, J.M., J.J. Hill, and C.I. Bargmann, *A circuit for navigation in Caenorhabditis elegans.* Proc Natl Acad Sci U S A, 2005. **102**(9): p. 3184-91.

197. Wakabayashi, T., I. Kitagawa, and R. Shingai, *Neurons regulating the duration of forward locomotion in Caenorhabditis elegans.* Neurosci Res, 2004. **50**(1): p. 103-11.

198. Inglis, P.N., G. Ou, M.R. Leroux, and J.M. Scholey, *The sensory cilia of Caenorhabditis elegans.* WormBook, 2007: p. 1-22.

199. Hilliard, M.A., C. Bergamasco, S. Arbucci, R.H. Plasterk, and P. Bazzicalupo, *Worms taste bitter: ASH neurons, QUI-1, GPA-3 and ODR-3 mediate quinine avoidance in Caenorhabditis elegans.* Embo J, 2004. **23**(5): p. 1101-11.

200. Chalasani, S.H., N. Chronis, M. Tsunozaki, J.M. Gray, D. Ramot, M.B. Goodman, and C.I. Bargmann, *Dissecting a circuit for olfactory behaviour in Caenorhabditis elegans.* Nature, 2007. **450**(7166): p. 63-70.

201. O'Hagan, R., M. Chalfie, and M.B. Goodman, *The MEC-4 DEG/ENaC channel of Caenorhabditis elegans touch receptor neurons transduces mechanical signals.* Nat Neurosci, 2005. **8**(1): p. 43-50.

202. Cueva, J.G., A. Mulholland, and M.B. Goodman, *Nanoscale organization of the MEC-4 DEG/ENaC sensory mechanotransduction channel in Caenorhabditis elegans touch receptor neurons.* J Neurosci, 2007. **27**(51): p. 14089-98.

203. Zhou, W., J. Wang, K. Wang, B. Huang, L. Niu, F. Li, F. Cai, Y. Chen, X. Liu, and X. Zhang, *Ultrasound neuro-modulation chip: activation of sensory neurons in Caenorhabditis elegans by surface acoustic waves.* Lab on a Chip, 2017. **17**(10): p. 1725-1731.

204. Zhou, W., X. Wang, K. Wang, U. Farooq, L. Kang, L. Niu, and L. Meng, *Ultrasound activation of mechanosensory ion channels in Caenorhabditis elegans.* IEEE Transactions on Ultrasonics, Ferroelectrics, and Frequency Control, 2021.

205. Ye, J., S. Tang, L. Meng, X. Li, X. Wen, S. Chen, L. Niu, X. Li, W. Qiu, H. Hu, M. Jiang, S. Shang, Q. Shu, H. Zheng, S. Duan, and Y. Li, *Ultrasonic Control of Neural Activity through Activation of the Mechanosensitive Channel MscL.* Nano Lett, 2018. **18**(7): p. 4148-4155.

206. Huang, Y.S., C.H. Fan, N. Hsu, N.H. Chiu, C.Y. Wu, C.Y. Chang, B.H. Wu, S.R. Hong, Y.C. Chang, A. Yan-Tang Wu, V. Guo, Y.C. Chiang, W.C. Hsu, L. Chen, C. Pin-Kuang Lai, C.K. Yeh, and Y.C. Lin, *Sonogenetic Modulation of Cellular Activities Using an Engineered Auditory-Sensing Protein.* Nano Lett, 2020. **20**(2): p. 1089-1100.

207. Kubanek, J., J. Shi, J. Marsh, D. Chen, C. Deng, and J. Cui, *Ultrasound modulates ion channel currents.* Sci Rep, 2016. **6**: p. 24170.

208. Stamatakis, A.M., M.J. Schachter, S. Gulati, K.T. Zitelli, S. Malanowski, A. Tajik, C. Fritz, M. Trulson, and S.L. Otte, *Simultaneous Optogenetics and Cellular Resolution Calcium Imaging During Active Behavior Using a Miniaturized Microscope.* Frontiers in Neuroscience, 2018. **12**.

209. Deffains, M., T.H. Nguyen, H. Orignac, N. Biendon, S. Dovero, E. Bezard, and T. Boraud, *In vivo electrophysiological validation of DREADD-based modulation of pallidal neurons in the non-human primate.* Eur J Neurosci, 2021. **53**(7): p. 2192-2204.

210. Liu, Y., G. Wang, C. Cao, G. Zhang, E.B. Tanzi, Y. Zhang, W. Zhou, and Y. Li, *Neuromodulation Effect of Very Low Intensity Transcranial Ultrasound Stimulation on Multiple Nuclei in Rat Brain.* Frontiers in Aging Neuroscience, 2021. **13**.

211. Niu, X., K. Yu, and B. He, *Transcranial focused ultrasound induces sustained synaptic plasticity in rat hippocampus.* Brain Stimulation, 2022. **15**(2): p. 352-359.

212. Chen, T.W., T.J. Wardill, Y. Sun, S.R. Pulver, S.L. Renninger, A. Baohan, E.R. Schreiter, R.A. Kerr, M.B. Orger, V. Jayaraman, L.L. Looger, K. Svoboda, and D.S. Kim, *Ultrasensitive fluorescent proteins for imaging neuronal activity.* Nature, 2013. **499**(7458): p. 295-300.

213. Lipton, D.M., B.J. Gonzales, and A. Citri, *Dorsal Striatal Circuits for Habits, Compulsions and Addictions.* Frontiers in Systems Neuroscience, 2019. **13**.

214. Balleine, B.W., M.R. Delgado, and O. Hikosaka, *The Role of the Dorsal Striatum in Reward and Decision-Making.* The Journal of Neuroscience, 2007. **27**(31): p. 8161-8165.

215. Ou, M., W. Zhao, J. Liu, P. Liang, H. Huang, H. Yu, T. Zhu, and C. Zhou, *The General Anesthetic Isoflurane Bilaterally Modulates Neuronal Excitability.* iScience, 2020. **23**(1): p. 100760.

216. Yager, L.M., A.F. Garcia, A.M. Wunsch, and S.M. Ferguson, *The ins and outs of the striatum: role in drug addiction.* Neuroscience, 2015. **301**: p. 529-541.

217. Burke, D.A., H.G. Rotstein, and V.A. Alvarez, *Striatal Local Circuitry: A New Framework for Lateral Inhibition.* Neuron, 2017. **96**(2): p. 267-284.

218. Khraiche, M.L., W.B. Phillips, N. Jackson, and J. Muthuswamy, *Ultrasound induced increase in excitability of single neurons.* Annu Int Conf IEEE Eng Med Biol Soc, 2008. **2008**: p. 4246-9.

219. Xu, M., A. Kobets, J.-C. Du, J. Lennington, L. Li, M. Banasr, R.S. Duman, F.M. Vaccarino, R.J. DiLeone, and C. Pittenger, *Targeted ablation of cholinergic interneurons*

in the dorsolateral striatum produces behavioral manifestations of Tourette syndrome. Proceedings of the National Academy of Sciences, 2015. **112**(3): p. 893-898.

220. Zhou, F.M., C.J. Wilson, and J.A. Dani, *Cholinergic interneuron characteristics and nicotinic properties in the striatum.* J Neurobiol, 2002. **53**(4): p. 590-605.

221. Blackmore, J., S. Shrivastava, J. Sallet, C.R. Butler, and R.O. Cleveland, *Ultrasound Neuromodulation: A Review of Results, Mechanisms and Safety.* Ultrasound Med Biol, 2019. **45**(7): p. 1509-1536.

222. Allan, P.L., G.M. Baxter, and M.J. Weston, *Clinical Ultrasound, 2-Volume Set E-Book: Expert Consult: Online and Print*. 2011: Elsevier Health Sciences.

223. Klug, J.R., M.D. Engelhardt, C.N. Cadman, H. Li, J.B. Smith, S. Ayala, E.W. Williams, H. Hoffman, and X. Jin, *Differential inputs to striatal cholinergic and parvalbumin interneurons imply functional distinctions.* eLife, 2018. **7**: p. e35657.

224. Sych, Y., M. Chernysheva, L.T. Sumanovski, and F. Helmchen, *High-density multi-fiber photometry for studying large-scale brain circuit dynamics.* Nature Methods, 2019. **16**(6): p. 553-560.

225. Zhang, Y., M. Rózsa, Y. Liang, D. Bushey, Z. Wei, J. Zheng, D. Reep, G.J. Broussard, A. Tsang, G. Tsegaye, S. Narayan, C.J. Obara, J.-X. Lim, R. Patel, R. Zhang, M.B. Ahrens, G.C. Turner, S.S.H. Wang, W.L. Korff, E.R. Schreiter, K. Svoboda, J.P. Hasseman, I. Kolb, and L.L. Looger, *Fast and sensitive GCaMP calcium indicators for imaging neural populations.* bioRxiv, 2021: p. 2021.11.08.467793.

226. Grimsley, J.M., S. Sheth, N. Vallabh, C.A. Grimsley, J. Bhattal, M. Latsko, A. Jasnow, and J.J. Wenstrup, *Contextual Modulation of Vocal Behavior in Mouse: Newly Identified 12 kHz "Mid-Frequency" Vocalization Emitted during Restraint.* Front Behav Neurosci, 2016. **10**: p. 38.

227. Bushberg, J.T. and J.M. Boone, *The essential physics of medical imaging*. 2011: Lippincott Williams & Wilkins.

228. Vasan, A., F. Allein, M. Duque, U. Magaram, N. Boechler, S.H. Chalasani, and J. Friend, *Microscale Concert Hall Acoustics to Produce Uniform Ultrasound Stimulation for Targeted Sonogenetics in hsTRPA1-Transfected Cells.* Advanced NanoBiomed Research, 2022. **2**(5): p. 2100135.

229. Tyler, W.J., M. Alonso, C.R. Bramham, and L.D. Pozzo-Miller, *From acquisition to consolidation: on the role of brain-derived neurotrophic factor signaling in hippocampal-dependent learning.* Learn Mem, 2002. **9**(5): p. 224-37.

230. Fry, F.J. and J.E. Barger, *Acoustical properties of the human skull.* J Acoust Soc Am, 1978. **63**(5): p. 1576-90.

231. Ding, Y., E.C. Statharas, K. Yao, and M. Hong, *A broadband acoustic metamaterial with impedance matching layer of gradient index.* Applied Physics Letters, 2017. **110**(24): p. 241903.

232. Magaram, U., C. Weiss, A. Vasan, K.C. Reddy, J. Friend, and S.H. Chalasani, *Two pathways are required for ultrasound-evoked behavioral changes in Caenorhabditis elegans.* PLOS ONE, 2022. **17**(5): p. e0267698.

233. Choi, J.B., S.H. Lim, K.W. Cho, D.H. Kim, D.P. Jang, and I.Y. Kim. *The effect of focused ultrasonic stimulation on the activity of hippocampal neurons in multi-channel electrode*. in *2013 6th International IEEE/EMBS Conference on Neural Engineering (NER)*. 2013.

234. Prieto, M.L., K. Firouzi, B.T. Khuri-Yakub, and M. Maduke, *Activation of Piezo1 but Not Na(V)1.2 Channels by Ultrasound at 43 MHz.* Ultrasound Med Biol, 2018. **44**(6): p. 1217-1232.

235. Ibsen, S., A. Tong, C. Schutt, S. Esener, and S.H. Chalasani, *Sonogenetics is a non-invasive approach to activating neurons in Caenorhabditis elegans.* Nature Communications, 2015. **6**(1): p. 8264.

236. Dalecki, D., *Mechanical bioeffects of ultrasound.* Annu Rev Biomed Eng, 2004. **6**: p. 229-48.

237. Tyler, W.J., *Noninvasive neuromodulation with ultrasound? A continuum mechanics hypothesis.* Neuroscientist, 2011. **17**(1): p. 25-36.

238. Morris, C.E. and P.F. Juranka, *Nav channel mechanosensitivity: activation and inactivation accelerate reversibly with stretch.* Biophys J, 2007. **93**(3): p. 822-33.

239. Leighton, T.G., *What is ultrasound?* Prog Biophys Mol Biol, 2007. **93**(1-3): p. 3-83.

240. Dallapiazza, R.F., K.F. Timbie, S. Holmberg, J. Gatesman, M.B. Lopes, R.J. Price, G.W. Miller, and W.J. Elias, *Noninvasive neuromodulation and thalamic mapping with low-intensity focused ultrasound.* J Neurosurg, 2018. **128**(3): p. 875-884.

241. Mehić, E., J.M. Xu, C.J. Caler, N.K. Coulson, C.T. Moritz, and P.D. Mourad, *Increased anatomical specificity of neuromodulation via modulated focused ultrasound.* PLoS One, 2014. **9**(2): p. e86939.

242. Min, B.-K., P.S. Yang, M. Bohlke, S. Park, D. R.Vago, T.J. Maher, and S.-S. Yoo, *Focused ultrasound modulates the level of cortical neurotransmitters: Potential as a new functional brain mapping technique.* International Journal of Imaging Systems and Technology, 2011. **21**(2): p. 232-240.

243. Kim, H., A. Chiu, S.D. Lee, K. Fischer, and S.S. Yoo, *Focused ultrasound-mediated non-invasive brain stimulation: examination of sonication parameters.* Brain Stimul, 2014. **7**(5): p. 748-56.

244. Lee, W., S.D. Lee, M.Y. Park, L. Foley, E. Purcell-Estabrook, H. Kim, K. Fischer, L.S. Maeng, and S.S. Yoo, *Image-Guided Focused Ultrasound-Mediated Regional Brain Stimulation in Sheep.* Ultrasound Med Biol, 2016. **42**(2): p. 459-70.

245. Kubanek, J., P. Shukla, A. Das, S.A. Baccus, and M.B. Goodman, *Ultrasound Elicits Behavioral Responses through Mechanical Effects on Neurons and Ion Channels in a Simple Nervous System.* The Journal of Neuroscience, 2018. **38**(12): p. 3081.

246. Coste, B., J. Mathur, M. Schmidt, T.J. Earley, S. Ranade, M.J. Petrus, A.E. Dubin, and A. Patapoutian, *Piezo1 and Piezo2 are essential components of distinct mechanically activated cation channels.* Science, 2010. **330**(6000): p. 55-60.

247. Zhang, L., X. Liu, L. Gao, Y. Ji, L. Wang, C. Zhang, L. Dai, J. Liu, and Z. Ji, *Activation of Piezo1 by ultrasonic stimulation and its effect on the permeability of human umbilical vein endothelial cells.* Biomedicine & Pharmacotherapy, 2020. **131**: p. 110796.

248. Ye, J., S. Tang, L. Meng, X. Li, X. Wen, S. Chen, L. Niu, X. Li, W. Qiu, H. Hu, M. Jiang, S. Shang, Q. shu, H. Zheng, S. Duan, and Y. Li, *Ultrasonic Control of Neural Activity through Activation of the Mechanosensitive Channel MscL.* Nano Letters, 2018. **18**(7): p. 4148-4155.

249. Heureaux, J., D. Chen, V.L. Murray, C.X. Deng, and A.P. Liu, *Activation of a bacterial mechanosensitive channel in mammalian cells by cytoskeletal stress.* Cell Mol Bioeng, 2014. **7**(3): p. 307-319.

250. Duque, M., C.A. Lee-Kubli, Y. Tufail, U. Magaram, J. Patel, A. Chakraborty, J. Mendoza Lopez, E. Edsinger, A. Vasan, R. Shiao, C. Weiss, J. Friend, and S.H. Chalasani, *Sonogenetic control of mammalian cells using exogenous Transient Receptor Potential A1 channels.* Nature Communications, 2022. **13**(1): p. 600.

251. Legon, W., L. Ai, P. Bansal, and J.K. Mueller, *Neuromodulation with single-element transcranial focused ultrasound in human thalamus.* Hum Brain Mapp, 2018. **39**(5): p. 1995-2006.

252. Lee, W., H.C. Kim, Y. Jung, Y.A. Chung, I.U. Song, J.H. Lee, and S.S. Yoo, *Transcranial focused ultrasound stimulation of human primary visual cortex.* Sci Rep, 2016. **6**: p. 34026.

253. Ai, L., P. Bansal, J.K. Mueller, and W. Legon, *Effects of transcranial focused ultrasound on human primary motor cortex using 7T fMRI: a pilot study.* BMC Neurosci, 2018. **19**(1): p. 56.

254. Mueller, J.K., L. Ai, P. Bansal, and W. Legon, *Numerical evaluation of the skull for human neuromodulation with transcranial focused ultrasound.* Journal of Neural Engineering, 2017. **14**(6): p. 066012.

255. Sarica, C., J.-F. Nankoo, A. Fomenko, T.C. Grippe, K. Yamamoto, N. Samuel, V. Milano, A. Vetkas, G. Darmani, M.N. Cizmeci, A.M. Lozano, and R. Chen, *Human Studies of Transcranial Ultrasound neuromodulation: A systematic review of effectiveness and safety.* Brain Stimulation, 2022. **15**(3): p. 737-746.

256. Tsai, S.-J., *Transcranial focused ultrasound as a possible treatment for major depression.* Medical Hypotheses, 2015. **84**(4): p. 381-383.